

2009

The Effects of Elasticity in the Foundation on the Flutter of a Metallic High Aspect Ratio Wing

Horacio Esteban Sepic Kriskovich

Embry-Riddle Aeronautical University - Daytona Beach

Follow this and additional works at: <https://commons.erau.edu/db-theses>



Part of the [Aerospace Engineering Commons](#)

Scholarly Commons Citation

Kriskovich, Horacio Esteban Sepic, "The Effects of Elasticity in the Foundation on the Flutter of a Metallic High Aspect Ratio Wing" (2009). *Theses - Daytona Beach*. 107.

<https://commons.erau.edu/db-theses/107>

This thesis is brought to you for free and open access by Embry-Riddle Aeronautical University – Daytona Beach at ERAU Scholarly Commons. It has been accepted for inclusion in the Theses - Daytona Beach collection by an authorized administrator of ERAU Scholarly Commons. For more information, please contact commons@erau.edu.

**The Effects of Elasticity in the Foundation on the Flutter of a Metallic High
Aspect Ratio Wing**

by

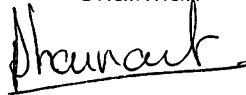
Horacio Esteban Sepic Kriskovich

This thesis was prepared under the direction of the candidate's thesis committee chairman, Dr. Habib Eslami, Department of Aerospace Engineering, and has been approved by members of the thesis committee. It was submitted to the Department of Aerospace Engineering and was accepted in partial fulfillment of the requirements for the degree of Master of Science in Aerospace Engineering.

THESIS COMMITTEE



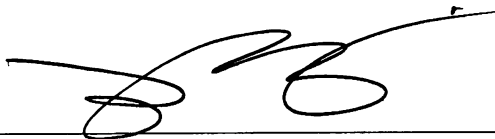
Dr. Habib Eslami
Chairman



Dr. Jean-Michell Dhainaut
Member



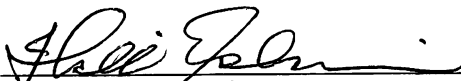
Dr. James Ladesic
Member



Dr. Yi Zhao
Graduate Program Coordinator, Aerospace Engineering

2/29/2010

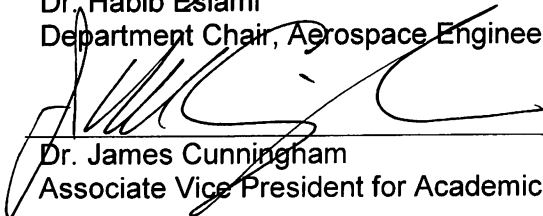
Date



Dr. Habib Eslami
Department Chair, Aerospace Engineering

2-26-2010

Date



Dr. James Cunningham
Associate Vice President for Academics

3/3/10

Date

UMI Number: EP31982

INFORMATION TO USERS

The quality of this reproduction is dependent upon the quality of the copy submitted. Broken or indistinct print, colored or poor quality illustrations and photographs, print bleed-through, substandard margins, and improper alignment can adversely affect reproduction.

In the unlikely event that the author did not send a complete manuscript and there are missing pages, these will be noted. Also, if unauthorized copyright material had to be removed, a note will indicate the deletion.

UMI[®]

UMI Microform EP31982
Copyright 2011 by ProQuest LLC
All rights reserved. This microform edition is protected against
unauthorized copying under Title 17, United States Code.

ProQuest LLC
789 East Eisenhower Parkway
P.O. Box 1346
Ann Arbor, MI 48106-1346

ACKNOWLEDGEMENTS

First of all, I would like to thank God for the life I have, and my family for its unconditional support during these years, for encouraging me always to take a step further and never miss my goals. I would also like to appreciate the support and guidance of my advisor, Dr. Habib Eslami, throughout my career at ERAU, and for always giving me a hand when most needed. Of course my special thanks go also to Dr. James Ladesic for proposing this project and Dr. Jean-Michell Dhainaut for his background in the topic and guidance through this work.

ABSTRACT

Author: Horacio Esteban Sepic Kriskovich
Title: The Effects of Elasticity in the Foundation on the Flutter of a Metallic High Aspect Ratio Wing
Institution: Embry-Riddle Aeronautical University
Degree: Master of Science in Aerospace Engineering
Year: 2009

The goal of this thesis is to study the flutter characteristics of a metallic high-aspect ratio wing, with linearly varying chord across the semis-span, and a simulated elastic foundation. The general planform of the wing is similar to the one found in a High-Altitude Long-Endurance Uninhabited Aerial Surveillance Vehicle (HALE USAV).

The problem is studied using a simplified aerodynamic loading based on thin-airfoil theory, which is then combined with a Lagrangian formulation to solve the system as stationary. The wing has no control surfaces or external stores, and is modeled as a uniform beam with known mechanical properties, being attached to a combination of torsion springs at the root to reproduce the elastic foundation.

The analysis of the problem includes the development of a Matlab code, which permits different root conditions to be defined, and computes the flutter speed and frequency, outputting information in the form of plots and data lists, making the analysis easy to follow.

TABLE OF CONTENTS

ACKNOWLEDGEMENTS.....	iii
ABSTRACT	iv
1. INTRODUCTION	1
2. THE STUDY MODEL	4
2.1. The Wing Model.....	9
3. FORMULATION OF EQUATIONS OF MOTION.....	19
3.1. Aerodynamic Forces.....	20
3.2. Kinetic Energy.....	22
3.3. Potential Energy	23
3.4. Lagrange's Equation.....	24
3.5. The Flutter Problem	26
3.6. The Divergence Problem.....	27
3.7. Correction for Compressibility Effects: Theodorsen's Curve	30
4. FREE VIBRATION ANALYSIS	32
4.1. Rayleigh-Ritz Method (RRM).....	32
4.1.1. The Bending Problem (BF_RRM).....	33
4.1.2. The Torsion Problem (RRM_TF).....	35
4.2. Finite Element Method (FEM).....	37
4.2.1. The Bending Problem (BF_FEM)	38
4.2.2. The Torsion Problem (TF_FEM).....	39
4.3. Validation of Free Vibration Model (RRM-FEM-NASTRAN).....	41
5. METHOD OF RESOLUTION.....	42
5.1. Program Flow and Subroutines	42
6. PROGRAM VALIDATION: THE GOLAND'S WING	44
6.1. Data Input File	44
6.2. Validation	45
7. ELASTIC FOUNDATION MODEL	46
7.1. Contribution Using FEM (FEM_EF).....	46
7.1.1. The Bending Problem (FEM_EF_BF).....	46

7.1.2. The Torsion Problem (FEM_EF_TF).....	48
7.2. Validation of the Model (FEM_EF & FEM).....	49
8. RESULTS	51
8.1. Case I: Effects of Elastic Foundation in Torsion	51
8.2. Case II: Effects of Elastic Foundation in Bending.....	54
8.3. Case III: Effects of Flight Altitude.....	57
9. ANALYSIS	60
9.1. Case I: Effects of Elastic Foundation in Torsion	60
9.2. Case II: Effects of Elastic Foundation in Bending.....	65
9.3. Case III: Effects of Flight Altitude.....	70
10. CONCLUSIONS	74
11. REFERENCES	77
APPENDIX	A1
A1. DATA INPUT FILE SAMPLE.....	A2
A2. STUDY CASES PROGRAM OUTPUT.....	A3
A3. VALIDATION OF FREE VIBRATION MODEL OUTPUT	A17
A4. MATLAB CODE.....	A22

LIST OF FIGURES

Figure 2A: A view of the HALE USAV	5
Figure 2B: The conceptual HALE USAV CATIA model.....	5
Figure 2C: Airfoil lift and polar curves [12].....	7
Figure 2.1a: Airfoil coordinates [12].....	9
Figure 2.1b: Half-wing general drawing.....	10
Figure 2.1c: Isometric view.....	10
Figure 2.1d: Wing's coordinate system from CATIA and spanwise stations	11
Figure 2.1e: Chord and unbalance distribution (a and b)	15
Figure 2.1f: Cross-sectional area distribution	15
Figure 2.1g: Mass per unit length distribution.....	16
Figure 2.1h: Location of EA, CG and AC.....	16
Figure 2.1i: Inertial and torsional constant distribution	17
Figure 2.1j: Rigidity distribution	17
Figure 3a: Wing's planform and coordinate system	19
Figure 3.1a: Streamwise AOA [2]	20
Figure 3.1b: Airfoil cross-section and aerodynamic forces diagram.....	21
Figure 3.5a: Flutter boundary for a two-mode analysis [2]	27
Figure 3.7a: Theodorsen's curve.....	31
Figure 4.2.1a: Beam element for bending analysis with FEM	38
Figure 4.2.2a: Rod element for torsion analysis with FEM	40
Figure 5.1a: Information flow within the Matlab code	43
Figure 7.1.1a: First beam element and its elastic contribution	47
Figure 7.1.2a: First rod element and its elastic contribution	48
Figure 8.1a: Frequency vs. dynamic pressure	52
Figure 8.1b: Frequency vs. speed	52
Figure 8.1c: Frequency vs. KTAS.....	53
Figure 8.1d: Frequency vs. Mach number.....	53
Figure 8.2a: Frequency vs. dynamic pressure	55
Figure 8.2b: Frequency vs. speed.....	55
Figure 8.2c: Frequency vs. KTAS.....	56
Figure 8.2d: Frequency vs. Mach number.....	56
Figure 8.3a: Frequency vs. dynamic pressure	58

Figure 8.3b: Frequency vs. speed	58
Figure 8.3c: Frequency vs. KTAS.....	59
Figure 8.3d: Frequency vs. Mach number	59
Figure 9.1a: Effect on flutter and torsion frequencies	61
Figure 9.1b: Effect on flutter and divergence dynamic pressure	61
Figure 9.1c: Effect on flutter and divergence speed	62
Figure 9.1d: Effect on flutter and divergence Mach number.....	62
Figure 9.1e: Effect on flutter reduced frequency	63
Figure 9.2a: Effect on flutter and torsion frequencies	66
Figure 9.2b: Effect on flutter and divergence dynamic pressure	66
Figure 9.2c: Effect on flutter and divergence speed	67
Figure 9.2d: Effect on flutter and divergence Mach number.....	67
Figure 9.2e: Effect on flutter reduced frequency	68
Figure 9.3a: Effect on flutter frequency	71
Figure 9.3b: Effect on flutter and divergence dynamic pressure	71
Figure 9.3c: Effect on flutter and divergence speed	72
Figure 9.3d: Effect on flutter and divergence Mach number.....	72
Figure 9.3e: Effect on flutter reduced frequency	73
Figure A.3a: NASTRAN model already meshed and constrained	A18
Figure A.3b: NASTRAN model first vibration mode (pure bending)	A18
Figure A.3c: NASTRAN model first vibration mode (top view)	A19
Figure A.3d: NASTRAN model first vibration mode (front view).....	A19
Figure A.3e: NASTRAN model first torsion mode approximation (mode 7)	A20
Figure A.3f: NASTRAN model first torsion mode approximation (top view)	A20
Figure A.3g: NASTRAN model first torsion mode approximation (front view)	A21

LIST OF TABLES

Table 2.1-1: Wing's general data.....	13
Table 2.1-2: Cross-sectional properties.....	14
Table 3.7-1: Theodorsen's experimental data.....	31
Table 4.3-1: Free vibration model validation.....	41
Table 6.2-1: Code validation with the Goland's wing.....	45
Table 7.2-1: Elastic foundation validation.....	50
Table 7.2-2: Modified elastic foundation validation.....	50
Table 9.1-1: Case I results.....	60
Table 9.2-1: Case II results.....	65
Table 9.3-1: Case III results.....	70

LIST OF ABBREVIATIONS

DBE2: beam element to simulate elastic foundations.
CATIA: Computer Aided Three-dimensional Interactive Application (software).
3D: three dimensions.
CNC: Computer Numerical Controlled.
ERAU: Embry-Riddle Aeronautical University.
HALE: High-Altitude Long-Endurance.
USAV: Uninhabited Surveillance Aerial Vehicle.
US: United States.
USAF: United States Air Force.
Max: maximum.
KTAS: True Air Speed in knots.
MGC: Mean Geometric Chord.
MTOW: Maximum Take-Off Weight.
MFW: Maximum Fuel Weight.
AR: Aspect Ratio.
MAC: Mean Aerodynamic Chord.
NACA: National Advisory Committee for Aeronautics.
AOA: Angle Of Attack.
NASTRAN: NASA Structural Analysis (software).
EA: Elastic Axis.
AC: Aerodynamic Center.
CG: Center of Gravity.
RM: Rayleigh's Method.
RRM: Rayleigh-Ritz Method.
Matlab: Matrix Laboratory (software).
BF_RRM: Bending Frequency by RRM.
TF_RRM: Torsion Frequency by RRM.
FEM: Finite Element Method.
PDE: Partial Differential Equation.
DOF: Degree Of Freedom.
BF_FEM: Bending Frequency by FEM.
TF_FEM: Torsion Frequency by FEM.

SL: Sea Level.

FL: Flight Level.

ISA: International Standard Atmosphere.

FEM_EF: FEM with Elastic Foundation.

BF_FEM_EF: Bending Frequency by FEM with Elastic Foundation.

TF_FEM_EF: Torsion Frequency by FEM with Elastic Foundation.

MEMS: Micro Electronic Measuring Sensor.

AIAA: American Institute for Aeronautics and Astronautics.

1. INTRODUCTION

The study and understanding of the flutter characteristics of a wing is extremely important during the aircraft design process. This structural dynamics phenomenon is responsible for limiting the flight speed due to its unstable nature, and represents a potentially catastrophic condition if not taken properly into account.

Flutter is understood as the harmonic oscillations of a structural member as a result of its interaction with the surrounding fluid stream. In the case of wing flutter, the wing is subjected to aerodynamic loads as it moves into the airstream, and the critical condition appears when harmonic oscillations for bending and torsion are coupled with no damping. At this particular point, any increase in the airspeed will introduce an increase in the amplitude of oscillations, making the structure unstable and leading to the risks which this represents. When the airspeed has met this point, the structure is said to reach its critical flutter speed.

The flutter phenomenon related to aircraft structures has been studied for many years, for almost all different types of wing configurations and airspeed regimes such as subsonic incompressible flow (sailplanes, general aviation aircraft, etc.), transonic compressible flow (high speed turboprops, jet liners, propeller and turbo machinery blades, etc.), supersonic compressible flow with the effects of temperature (jet fighters and jet liners, missiles, etc.), and hypersonic compressible flow with heat interaction for space reentry vehicles.

In the classical theoretical approach for the flutter of a cantilever wing, the wing's root boundary conditions are typically fixed constraints requiring all displacements and rotations at the boundary to be zero with no damping. These conditions make solution to the problem tractable and complete.

Using this classical approach and a simplified aerodynamic load, the flutter of a uniform cantilever wing was studied by the author of this report in a previous work [1] (using a similar model to the one developed by Dhainaut [2] to study the aeroelastic behavior of sweep wings) that was validated with results obtained by Goland [3] in his work on the flutter of a uniform wing.

For the case under consideration, a Lagrangian formulation is employed to formulate the equations of motion of the system according to the formulation used by the author [1] and Dhainaut [2]. In this report, a Matlab code has been developed to calculate the flutter boundary for the problem based on the previous works of Dhainaut [2] and the author [1], which has the ability to introduce the effects of an elastic foundation by combining torsion springs located at the root of the wing, as well as analyzing the problem with an ideal clamp.

The idea of studying the aeroelastic behavior of a wing with elastic foundation is not new, as the work done by De Baets, Battoo and Mavris [4] studying the root flexibility effects on the aeroelastic characteristics of a uniform high-aspect ratio composite wingbox, simulating the elastic root with a beam element (DBE2).

As part of this work, a similar idea has been taken into account to simulate the root flexibility for the actual problem by employing a combination of torsion springs located at the wing's elastic axis, instead of a beam. However, the case under study corresponds to a metallic high-aspect ratio wing, with linearly varying chord (due to the wing's taper ratio) and, therefore, all mass, mechanical and geometrical properties vary along the semi-span, which adds to the complexity of the problem.

The Matlab code developed for this work enables the user to analyze the problem using either clamped or elastic roots, which allows validation of classical clamped cases. For the elastic foundation however, the available sources to this type of problems are limited, and in the particular case of root flexibility on a subsonic metallic high-aspect ratio

wing, with varying properties along the semi-span, there is no reference available to the best of the author's knowledge.

For this reason, the construction of a wind tunnel model would be an enormous tool to obtain data that made validation possible, in a similar way that Dhainaut, Desmond and Gangadharan [5] validated their results for a uniform model wing in a low-speed wind tunnel.

A scaled model for this purpose could be easily modeled in CATIA and machined with the Komo 3D CNC router at the ERAU Manufacturing Laboratory. Also the Wind Tunnel Laboratory facility available at ERAU could be used to test the model, and considering that the university counts with different measuring devices, a similar task to the work done by De Marqui Junior, Rebolho, Belo and Marques [5], where the flutter parameters of a uniform wing model were identified during wind tunnel testing by using a combination of strain gages and accelerometers mounted in a flexible mounting structure, might be considered as a model instrumentation option.

The main purpose of this current work is to develop a preliminary design tool to study the flutter behavior of general-shaped subsonic wings and, if future work permits, validate this tool via comparison with a low-speed wind tunnel model.

2. THE STUDY MODEL

The proposed case of study has its application on the relatively new High-Altitude Long-Endurance Uninhabited Aerial Surveillance Vehicle (HALE USAV) RQ-4 Block 20 Global Hawk manufactured by Northrop-Grumman in the United States of America.

This aircraft's main role is surveillance, and it has been serving the US Armed Forces and Intelligence services since it was first deployed in the late 90's.

The Global Hawk has a low-mounted, high aspect ratio, linearly tapered cantilever wing, with a clean semi-span length of nearly 20 m, which serves as a high-surface, low-drag wing plan form ideal for high-altitude missions with extended periods of operation.

Although most of the general characteristics of this HALE USAV aircraft are known, for the purpose of this work a simplified model of this wing is introduced by the author with some particular characteristics to make the approach of the problem easier, thus a solid model is chosen reducing enormously the modeling task, and focusing strictly on the flutter problem.

Based on the previous data, the new conceptual aircraft was modeled in CATIA by the author, with the following characteristics:

Specifications: HALE USAV

Wingspan	131.2 ft (40 m)
Length	47.6 ft (14.5 m)
Height	15.4 ft (4.7 m)
Max Take-Off Weight (<i>MTOW</i>)	32,500 lb (14,736 Kg)
Max Fuel Weight (<i>MFW</i>)	14,500 lb (6,575 Kg)
Cruise Altitude (H_{cr})	32,800 ft (10.0 Km)
Cruise Velocity (V_{cr})	343 KTAS (635 Km/h)

Wing:

Wingspan (b_w)	131.2 ft (40 m)
Root Chord (c_r).....	8.20 ft (2.5 m)
Tip Chord (c_t)	2.95 ft (0.9 m)
Mean Geometric Chord (MGC)	5.58 ft (1.7 m)
Wing Surface (S_w)	732 ft ² (68 m ²)
Aspect Ratio (AR)	23.53
Tapper Ratio (λ).....	0.36
AC line sweep back angle (Δ_{AC}).....	6 ⁰

The following pictures correspond to this conceptual aircraft modeled in CATIA:

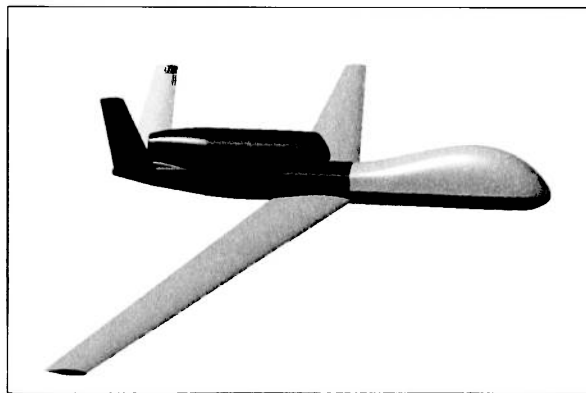


Figure 2a: A view of the HALE USAV.



Figure 2b: The conceptual HALE USAV CATIA model.

It was stated above that the first step is to consider an airfoil for the wing that allows meeting the operational requirements as close as possible for the design condition. In the case under consideration, the design condition is the cruise condition, that is

$$\begin{cases} S_w = 68m^2 \\ W_{cr} = MTOW - \frac{MFW}{2} = 11,448.5 \vec{K}g \\ V_{cr} = 634.6 Km/h = 176.3 m/s \\ H_{cr} = 10,000m \\ \rho_{cr} = 0.4127 Kg/m^3 \\ \mu_{cr} = 0.00001457 Ns/m^2 \end{cases} \quad (2-1)$$

In the expression 2-1, the new parameters introduced are W_{cr} (average cruise weight), ρ_{cr} (cruise air density, according to ISA [11] and [17]) and μ_{cr} (cruise air viscosity, from [11] and [17]). From basic Aerodynamics [7], the lift of an aircraft while flying level and steady can be expressed as

$$L = W_{cr} = \frac{\rho_{cr}}{2} V_{cr}^2 S_w C_{L-cr} \quad (2-2)$$

Substituting data from expression 2-1 into 2-2 and solving for the aircraft lift coefficient it yields

$$C_{L-cr} = \frac{2W_{cr} / S_w}{\rho_{cr} V_{cr}^2} = 0.2575 \quad (2-3)$$

Since the wing has a large aspect ratio (>23), the 3-D effects may be neglected, and the local lift coefficient (airfoil design lift coefficient) may be taken as the wing's lift coefficient (cruise lift coefficient for the aircraft), thus

$$C_{l-design} |_{airfoil} = C_{L-cr} = 0.2575 \quad (2-4)$$

The Mean Aerodynamic Chord (MAC) is defined as the follows [7]

$$MAC = \frac{2}{S_w} \int_0^{b/2} c(y)^2 dy \quad (2-5)$$

The new wing's chord distribution is expressed in meters as:

$$c(y) = 2.50 - 0.08y \quad (2-6)$$

Substituting expression 2-6 into 2-5, it yields:

$$MAC = 1.825m \quad (2-7)$$

Having calculated the airfoil lift coefficient, for simplicity a symmetric airfoil will be chosen, thus avoiding the introduction of the wing off set angle; the cruise Reynolds number at MAC is:

$$Re = \frac{\rho_{cr} V_{cr} MAC}{\mu_{cr}} = 9.114e^6 \quad (2-8)$$

With the design lift coefficient and the Reynolds number for the defined condition, the choice of the airfoil is narrowed to 6-series airfoil, since it presents a region where, for a particular lift coefficient, the drag coefficient is comparatively low (the so called laminar bucket). After a basic search through [12], the selected airfoil is the NACA 63₁-012, with the following characteristics:

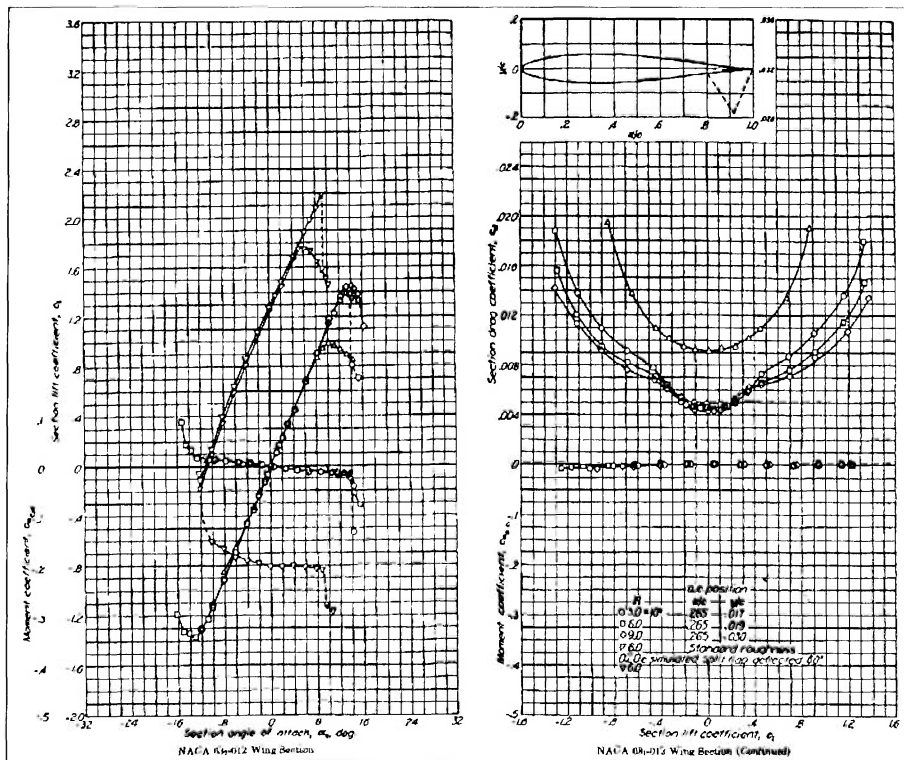


Figure 2c: Airfoil lift and polar curves [12].

From these curves, at the desired lift coefficient (C_l), drag coefficient (C_d), angle of attack (AOA), the ratio C_l/C_d , and the lift slope of the airfoil ($C_{l\alpha}$) are obtained:

$$\begin{array}{l}
 C_{l-cr} = 0.2575 @ AOA = 2.6^\circ \Rightarrow C_d \approx 0.006 \\
 C_{l-cr}/C_d \approx 42.92 \\
 C_{l\alpha} = 6.446 / rad
 \end{array}
 \tag{2-9}$$

From the previous expression, it can be seen that the drag coefficient is much smaller than the lift coefficient, and therefore, it can be neglected, leaving aerodynamic forces due to lift only. Additionally, according to the work done by Dhainaut, Desmond and Gangadharan [5], the aerodynamic moment is also neglected.

As the general geometry of the wing has been already introduced, the following step is to model the wing in CATIA, which will allow having a detailed 3-D model that will be later imported to NASTRAN to obtain the cross sectional properties and to validate the free vibration analysis.

2.1. The Wing Model

The airfoil's geometry from [12] was used to model the wing in CATIA; the following table gives the geometrical coordinates:

x (per cent c)	y (per cent c)	$(v/V)^2$	v/V	$\Delta u_a/V$
0	0	0	0	2.336
0.5	0.985	0.750	0.866	1.695
0.75	1.194	0.925	0.962	1.513
1.25	1.619	1.005	1.003	1.266
2.5	2.102	1.129	1.063	0.933
5.0	2.925	1.217	1.103	0.682
7.5	3.542	1.261	1.123	0.559
10	4.039	1.294	1.138	0.484
15	4.799	1.330	1.153	0.387
20	5.342	1.349	1.161	0.326
25	5.712	1.362	1.167	0.283
30	5.930	1.370	1.170	0.249
35	6.000	1.366	1.169	0.221
40	5.920	1.348	1.161	0.196
45	5.704	1.317	1.148	0.174
50	5.370	1.276	1.130	0.155
55	4.935	1.229	1.109	0.137
60	4.420	1.181	1.087	0.121
65	3.840	1.131	1.063	0.106
70	3.210	1.076	1.037	0.091
75	2.556	1.023	1.011	0.079
80	1.902	0.969	0.984	0.067
85	1.274	0.920	0.959	0.055
90	0.707	0.871	0.933	0.042
95	0.250	0.826	0.909	0.029
100	0	0.791	0.889	0

L.E. radius. 1.087 per cent c
NACA 63,-012 Basic Thickness Form

Figure 2.1a: Airfoil coordinates [12].

With this geometry an Excel file is created which is imported to CATIA to get the basic profile to make the solid model.

The CATIA model has the following characteristics:

Semi-span ($b_w/2$).....	20.00 m
Root Chord (c_r).....	2.50 m
Tip Chord (c_t)	0.90 m
Root maximum thickness (t_{r-max})	0.30 m
Tip maximum thickness (t_{t-max}).....	0.108 m
Mean Geometric Chord (MGC)	1.70 m
Mean Aerodynamic Chord (MAC).....	1.825 m

Aspect Ratio (AR)	23.53
Tapper Ratio (λ).....	0.36
AC line sweep back angle (Δ_{AC}).....	6°
LE line sweep back angle (Δ_{LE}).....	7.19°
TE line sweep back angle (Δ_{TE}).....	2.65°

The next two figures show the drawing and a general isometric view (both obtained from CATIA) respectively:

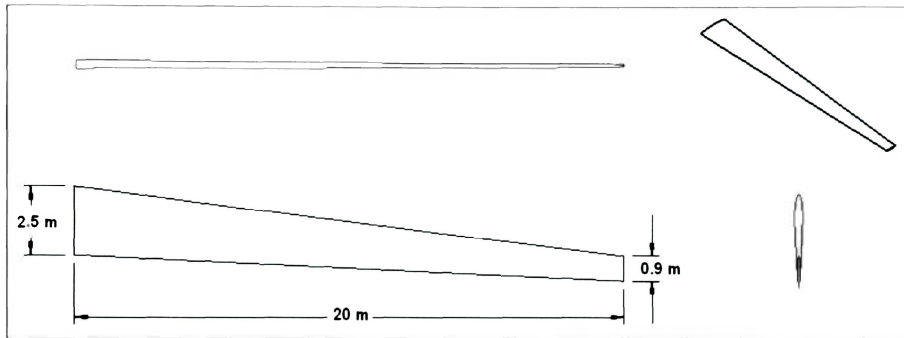


Figure 2.1b: Half-wing general drawing.

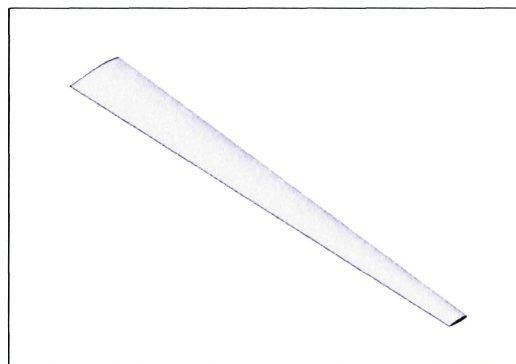


Figure 2.1c: Isometric view.

After the creation of the CATIA model, the semi-wing is divided into 5 stations upon which the cross-sectional properties will be computed from NASTRAN. Each station is created as a solid for the corresponding span-wise station, and saved as *igs* format files to be imported from NASTRAN. The location of these spanwise stations is detailed in table 2.1-2 (see following pages).

The coordinate system to create the model in CATIA is shown in the next figure:

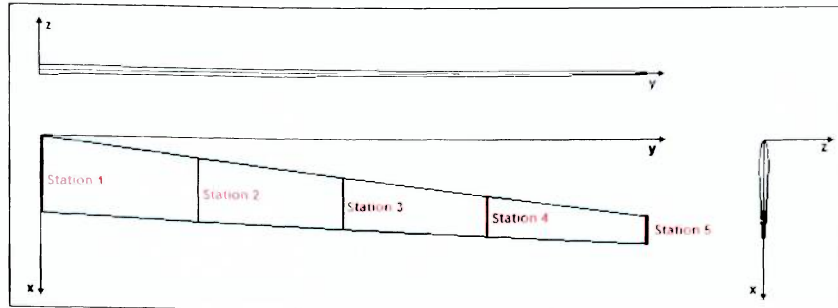


Figure 2.1d: Wing's coordinate system from CATIA and spanwise stations.

The accuracy of the computation of cross-sectional properties as function of the semi-span coordinate depends on the number of cross-sectional stations chosen. After a trial and error selection, the number of cross-sectional station was fixed to five, which provides enough accuracy to compute these varying properties, which at the most have the shape of a third grade polynomial function.

The geometric properties for each of the cross-sectional stations, as they are calculated from NASTRAN, are presented below (in the following data the suffixes y and z indicate local orientation for cross sectional elements, not being related to the global coordinate system of the wing. All units are SI system):

STATION 01

Orientation of Section Properties:

Origin:	X=	0.	Y=	0.	Z=	0.
Y Axis:	X=	1.	Y=	0.	Z=	0.
Z Axis:	X=	0.	Y=	0.	Z=	1.

Section Properties:

Area	A=	0.47161		
Centroid (from Origin):	Cy=	1.01991	Cz=	6.43838E-11
Moment of Inertia:	Iyy=	0.0023897	Izz=	0.1385
	Iyz=	0.		
Principal Moment of Inertia:	I1=	0.1385	I2=	0.0023897
Radius of Gyration:	Ry=	0.071183	Rz=	0.54191
Angle to Principal Axes:	Ang=	-8.44797E-9		
Polar Moment of Inertia:	Ip=	0.14089		
Shear Center (from Origin):	SCy=	0.88854	SCz=	-1.5298E-6
Shear Center (from Centroid):	SCy=	-0.13137	SCz=	-1.5298E-6
Shear Area:	Asy=	0.44148	Asz=	0.17417
Torsional Constant:	J=	0.0093632		
Warping Constant:	W=	0.00033995		

STATION 02

Orientation of Section Properties:

Origin: X= 0. Y= 0. Z= 0.
Y Axis: X= 1. Y= 0. Z= 0.
Z Axis: X= 0. Y= 0. Z= 1.

Section Properties:

Area A= 0.33277
Centroid (from Origin): Cy= 0.85672 Cz= -7.70955E-10
Moment of Inertia: Iyy= 0.0011897 Izz= 0.068953
Iyz= 1.67603E-10
Principal Moment of Inertia: I1= 0.068953 I2= 0.0011897
Radius of Gyration: Ry= 0.059794 Rz= 0.4552
Angle to Principal Axes: Ang= 1.4171E-7
Polar Moment of Inertia: Ip= 0.070143
Shear Center (from Origin): SCy= 0.74637 SCz= -1.2718E-6
Shear Center (from Centroid): SCy= -0.11035 SCz= -0.000001271
Shear Area: Asy= 0.31151 Asz= 0.12289
Torsional Constant: J= 0.0046616
Warping Constant: W= 0.00012015

STATION 03

Orientation of Section Properties:

Origin: X= 0. Y= 0. Z= 0.
Y Axis: X= 1. Y= 0. Z= 0.
Z Axis: X= 0. Y= 0. Z= 1.

Section Properties:

Area A= 0.21807
Centroid (from Origin): Cy= 0.69355 Cz= -2.13231E-9
Moment of Inertia: Iyy= 0.00051094 Izz= 0.029611
Iyz= 2.88207E-10
Principal Moment of Inertia: I1= 0.029611 I2= 0.00051094
Radius of Gyration: Ry= 0.048404 Rz= 0.36849
Angle to Principal Axes: Ang= 5.6746E-7
Polar Moment of Inertia: Ip= 0.030122
Shear Center (from Origin): SCy= 0.60422 SCz= 8.3335E-7
Shear Center (from Centroid): SCy= -0.089333 SCz= 8.3548E-7
Shear Area: Asy= 0.20414 Asz= 0.08054
Torsional Constant: J= 0.002002
Warping Constant: W= 0.000033602

STATION 04

Orientation of Section Properties:

Origin: X= 0. Y= 0. Z= 0.
Y Axis: X= 1. Y= 0. Z= 0.
Z Axis: X= 0. Y= 0. Z= 1.

Section Properties:

Area A= 0.12752
Centroid (from Origin): Cy= 0.53036 Cz= 4.57334E-11
Moment of Inertia: Iyy= 0.00017472 Izz= 0.010126
Iyz= 0.

Principal Moment of Inertia: I1= 0.010126 I2= 0.00017472
 Radius of Gyration: Ry= 0.037015 Rz= 0.28179
 Angle to Principal Axes: Ang= -8.2594E-9
 Polar Moment of Inertia: Ip= 0.010301
 Shear Center (from Origin): SCy= 0.46205 SCz= -9.11391E-7
 Shear Center (from Centroid): SCy= -0.068311 SCz= -9.11437E-7
 Shear Area: Asy= 0.11937 Asz= 0.047097
 Torsional Constant: J= 0.00068462
 Warping Constant: W= 0.0000067419

STATION 05

Orientation of Section Properties:

Origin: X= 0. Y= 0. Z= 0.
 Y Axis: X= 1. Y= 0. Z= 0.
 Z Axis: X= 0. Y= 0. Z= 1.

Section Properties:

Area A= 0.06112
 Centroid (from Origin): Cy= 0.36717 Cz= 1.55445E-9
 Moment of Inertia: Iyy= 0.000040136 Izz= 0.0023261
 Iyz= -1.32527E-12

Principal Moment of Inertia: I1= 0.0023261 I2= 0.000040136
 Radius of Gyration: Ry= 0.025626 Rz= 0.19508
 Angle to Principal Axes: Ang= -3.32169E-8
 Polar Moment of Inertia: Ip= 0.0023662
 Shear Center (from Origin): SCy= 0.31988 SCz= -6.15603E-7
 Shear Center (from Centroid): SCy= -0.047293 SCz= -6.17158E-7
 Shear Area: Asy= 0.057215 Asz= 0.022573
 Torsional Constant: J= 0.00015727
 Warping Constant: W= 0.0000007398

In this work, the study model of the wing consists of a solid piece of metal made out of aluminum 2024 T351, with the following characteristics:

Table 2.1-1: Wing's general data

c-root [m]	2.500
c-tip [m]	0.900
b/2 [m]	20.000
Material	Al 2024 T351
Density [kg/m ³]	2.765E+03
E [Pa]	7.385E+10
G [Pa]	2.870E+10
n	0.33
Airfoil	NACA 63,-012
AC [x/c]	0.265
CL-alpha [1/rad]	6.446

Based on table 2.1-1 and the data for the cross-sectional stations calculated from NASTRAN, the following tables are obtained:

Table 2.1-2: Cross-sectional properties

Station	1	2	3	4	5
y [m]	0	5	10	15	20
c [m]	2.50	2.10	1.70	1.30	0.90
A [m ²]	4.716E-01	3.328E-01	2.181E-01	1.275E-01	6.112E-02
m [kg/m]	1304.00	920.11	602.96	352.59	169.00
I _{xx} [m ⁴]	2.390E-03	1.190E-03	5.109E-04	1.747E-04	4.014E-05
I _p [m ⁴]	1.409E-01	7.014E-02	3.012E-02	1.030E-02	2.366E-03
J [m ⁴]	9.363E-03	4.662E-03	2.002E-03	6.846E-04	1.573E-04
C _x [m] LE	1.020E+00	8.567E-01	6.936E-01	5.304E-01	3.672E-01
SC _x [m] LE	8.885E-01	7.464E-01	6.042E-01	4.621E-01	3.199E-01
SC _x - C _x [m]	-1.314E-01	-1.104E-01	-8.933E-02	-6.831E-02	-4.729E-02
b=C _x - SC _x [m]	1.314E-01	1.104E-01	8.933E-02	6.831E-02	4.729E-02
X _{ac} [m] LE	6.625E-01	5.565E-01	4.505E-01	3.445E-01	2.385E-01
a=CS _x - X _{ac} [m]	2.260E-01	1.899E-01	1.537E-01	1.176E-01	8.138E-02
EI _{xx} [N*m ²]	1.765E+08	8.786E+07	3.773E+07	1.290E+07	2.964E+06
GJ [N*m ²]	2.687E+08	1.338E+08	5.746E+07	1.965E+07	4.514E+06
GJ/EI _{xx}	1.523	1.523	1.523	1.523	1.523

From table 2.1-2 it can be seen the semi-span varying properties: moments of inertia and torsion constant, chord, area and mass per unit length, location of EA, AC and CG, etc. With this data, the following plots are obtained from Excel, showing the distribution along the semi-span of all these properties:

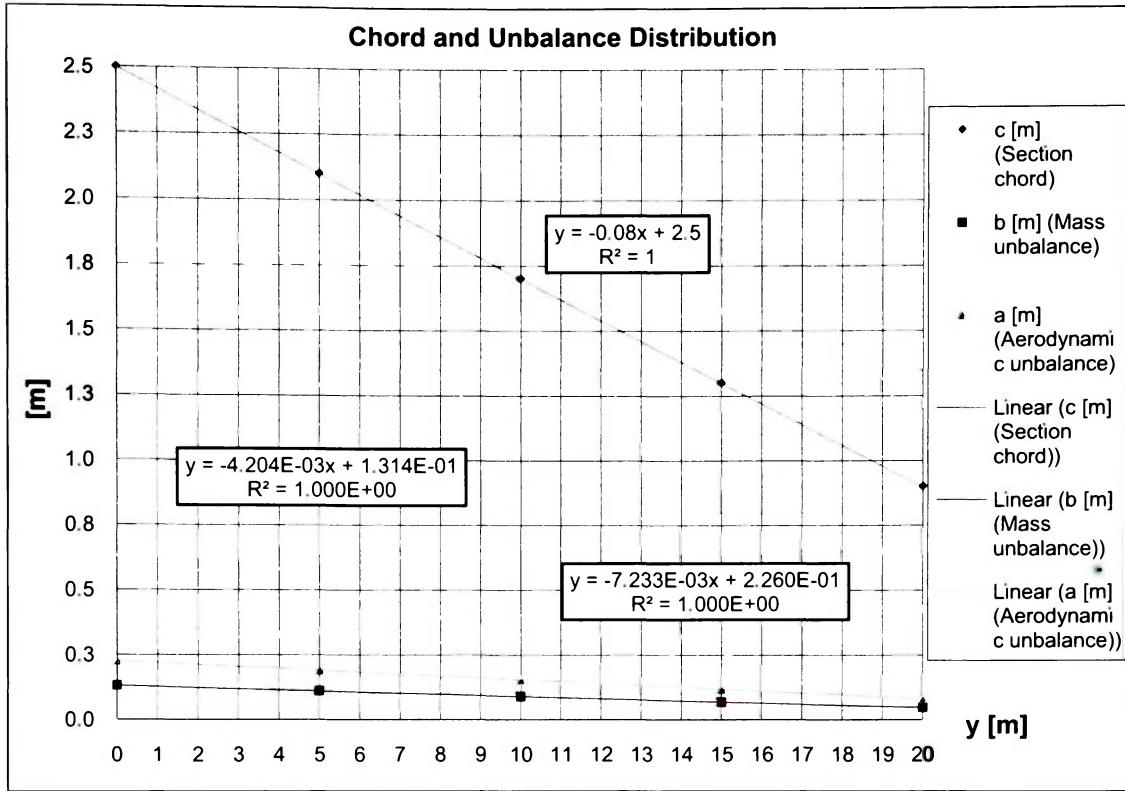


Figure 2.1e- Chord and unbalance distribution (a and b).

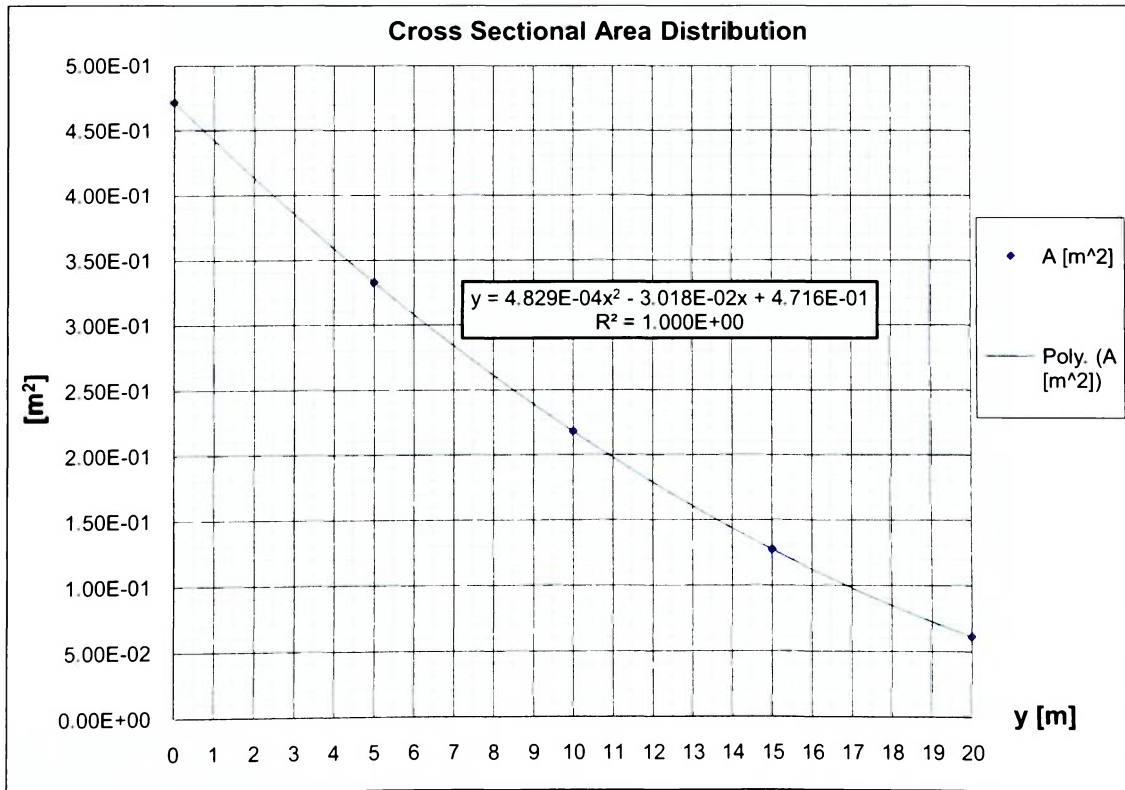


Figure 2.1f- Cross-sectional area distribution.

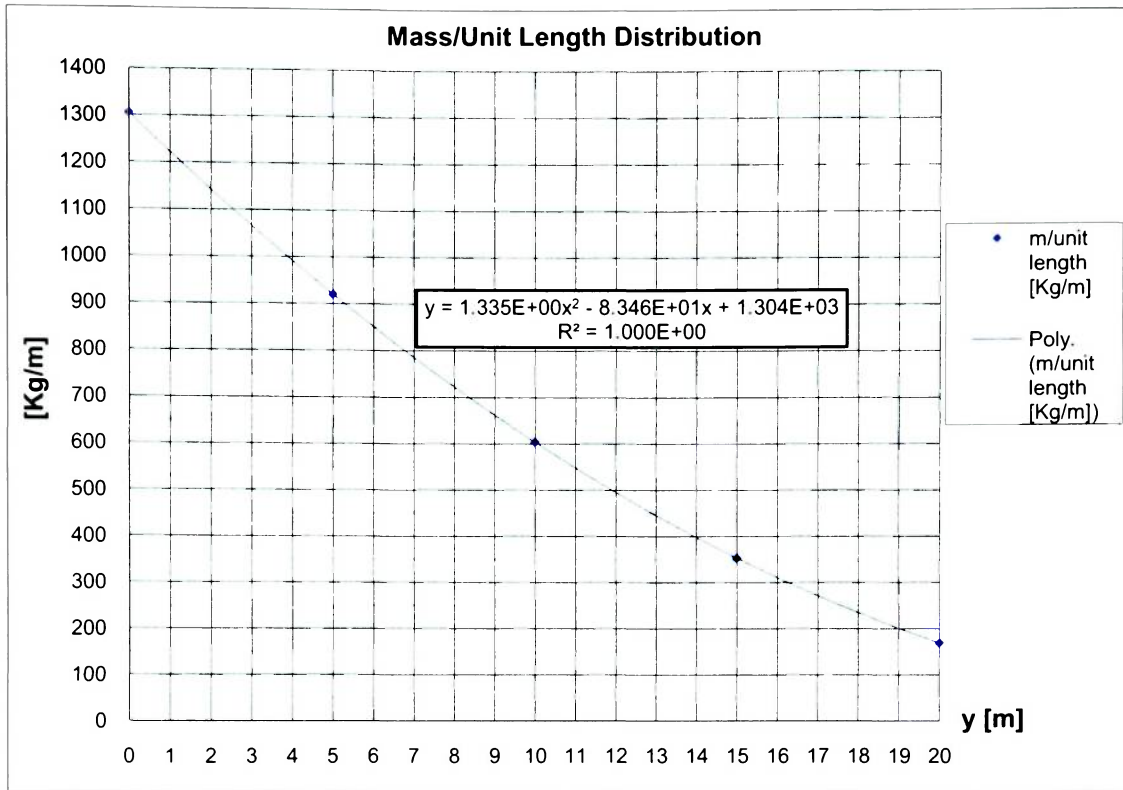


Figure 2.1g- Mass per unit length distribution.

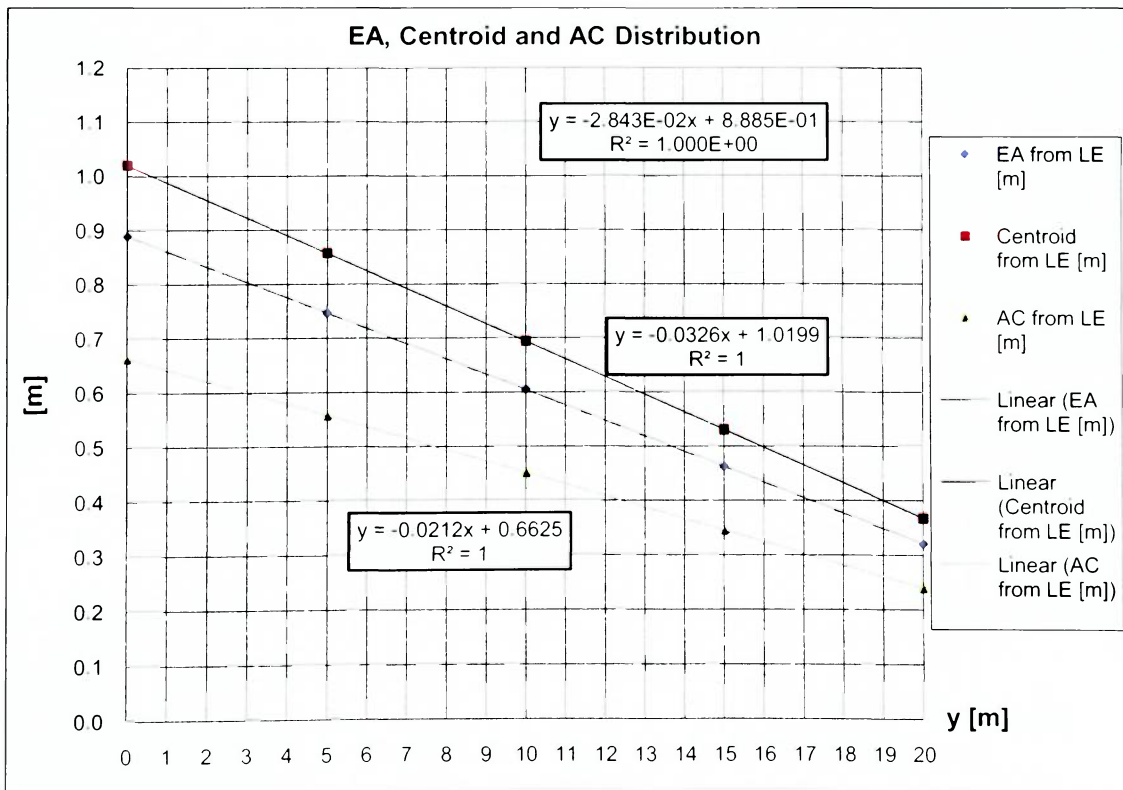


Figure 2.1h- Location of EA, CG and AC.

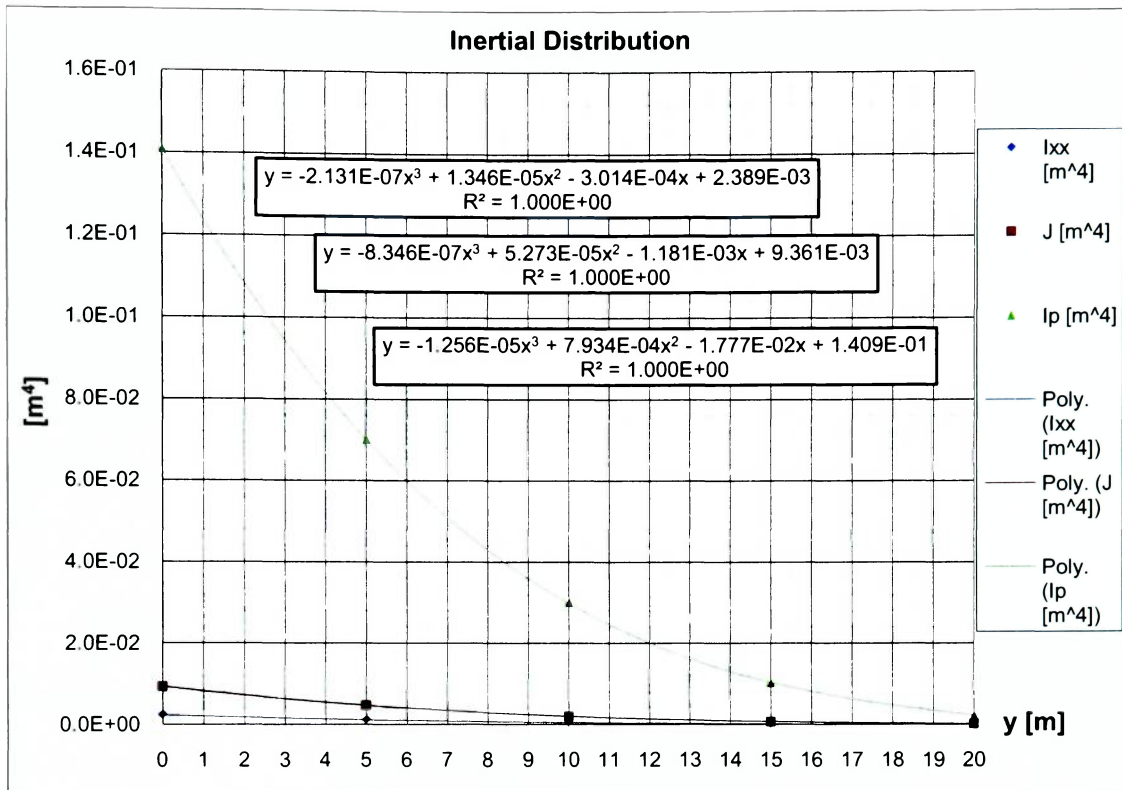


Figure 2.1i- Inertial and torsional constant distribution.

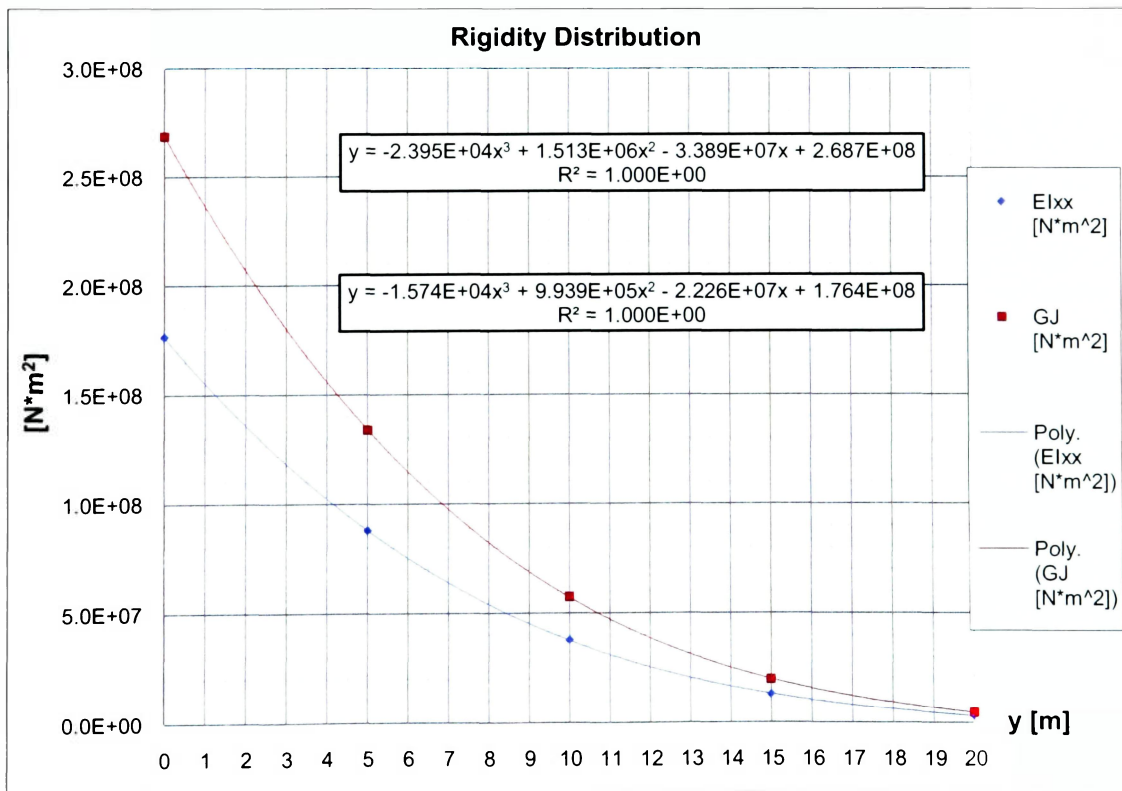


Figure 2.1j- Rigidity distribution.

From figure 2.1e, the distributions of chord (c), mass unbalance (b , distance from CG to EA) and aerodynamic unbalance (a , distance from AC to EA) are obtained (all values in $[m]$):

$$\begin{cases} c(y) = 2.5 - 0.08y \\ b(y) = 0.1314 - 4.203e^{-3}y \\ a(y) = 0.226 - 7.233e^{-3}y \end{cases} \quad (2.1-1)$$

From figure 2.1f, the distribution of cross-sectional area (A) is obtained (all values in $[m^2]$):

$$A(y) = 4.8290e^{-4}y^2 - 3.018e^{-2}y + 4.716e^{-1} \quad (2.1-2)$$

From figure 2.1g, the distribution of mass per unit length (\bar{m}) is given by (all values in $[Kg/m]$):

$$\bar{m}(y) = 1.335y^2 - 83.46y + 1304 \quad (2.1-3)$$

From figure 2.1h, the distributions of location from LE for EA , AC and CG are expressed as (all values in $[m]$):

$$\begin{cases} x_{EA}(y) = -2.843e^{-2}y + 8.885e^{-1} \\ x_{CG}(y) = -0.0326y + 1.0199 \\ x_{AC}(y) = -0.0212y + 0.6625 \end{cases} \quad (2.1-4)$$

From figure 2.1i, the distributions of moment of inertia (I_{xx}), torsional constant (J) and polar moment of inertia (I_p) are given as (all values in $[m^4]$):

$$\begin{cases} I_{xx}(y) = -2.131e^{-7}y^3 + 1.346e^{-5}y^2 - 3.014e^{-4}y + 2.389e^{-3} \\ J(y) = -8.346e^{-7}y^3 + 5.273e^{-5}y^2 - 1.181e^{-4}y + 9.361e^{-3} \\ I_p(y) = -1.256e^{-5}y^3 + 7.934e^{-4}y^2 - 1.777e^{-2}y + 1.409e^{-1} \end{cases} \quad (2.1-5)$$

Finally, from figure 2.1j, the distributions of bending rigidity (EI_{xx}) and torsional rigidity (GJ) are (all values in $[Nm^2]$):

$$\begin{cases} EI_{xx}(y) = -1.574e^4y^3 + 9.939e^5y^2 - 2.226e^7y + 1.7642e^8 \\ GJ(y) = -2.395e^4y^3 + 1.513e^6y^2 - 3.389e^7y + 2.6879e^8 \end{cases} \quad (2.1-6)$$

3. FORMULATION OF EQUATIONS OF MOTION

Consider current wing's planform is sketched in the following figure, where the coordinate system is aligned with the *EA* (similar approach used in [1] by the author and [2] by Dhainaut):

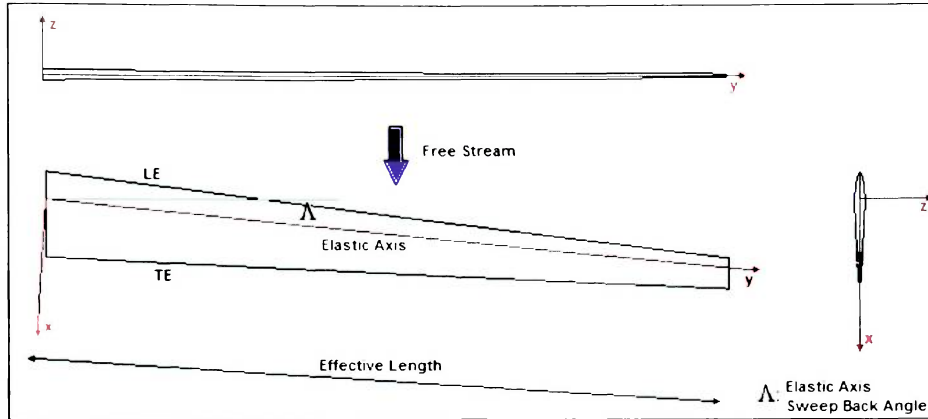


Figure 3a: Wing's planform and coordinate system.

Any deformation is then referenced to the elastic axis, and described by two quantities: bending and pitching about this axis. The sweep back angle of the elastic axis (*EA*) is referred as Δ . At any span-wise location, these quantities can be denoted by a set of generalized coordinates:

$$\begin{cases} h(y,t) = b_0 \phi_h(y) q_h(t) \\ \alpha(y,t) = \phi_\alpha(y) q_\alpha(t) \end{cases} \quad (3-1)$$

where:

- $q_h(t)$: generalized coordinate for bending as function of time.
- $q_\alpha(t)$: generalized coordinate for torsion as function of time.
- $\phi_h(y)$: shape function of deformation for bending [*m*].
- $\phi_\alpha(y)$: shape function of deformation for torsion [*rad*].
- b_0 : reference length [*m*].

3.1. Aerodynamic Forces

The aerodynamic loads will be treated by means of the *Strip-Theory* [7], which states that for any arbitrary span-wise station (Δy), the aerodynamic lift force (ΔL) can be expressed by

$$\Delta L = Q_\infty C_{l\alpha} \alpha_T c \Delta y \quad (3.1-1)$$

where

- Q_∞ free stream dynamic pressure [Pa]
- c local chord [m]
- $C_{l\alpha}$ local aerodynamic lift slope [1/rad]
- α_T streamwise angle of attack (AOA) [rad]

Assuming semi-rigid chord-wise segments, it is derived from figure 3b that the streamwise AOA resulting from elastic deformation is made out of a component due to pitch, and another one due to bending slope, as follows

$$\alpha_T = \alpha \cos \Lambda + \frac{\partial h}{\partial y} \sin \Lambda \quad (3.1-2)$$

Where Λ , is the wing's sweepback angle of the aerodynamic center line

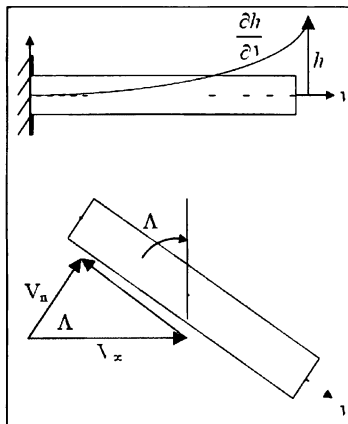


Figure 3.1a: Streamwise AOA [2]

Substituting expression 3.1-2 into expression 3.1-1, integrating across the semi-span's effective length (l_{eff}) and dividing by two, the aerodynamic lift force is obtained for half-wing:

$$L|_{\text{half-wing}} = \frac{Q_{\infty} C_{L\alpha}}{2} \int_0^{l_{eff}} c \left[\alpha \cos \Lambda + \frac{\partial h}{\partial y} \sin \Lambda \right] dy \quad (3.1-3)$$

In the previous expression, the effective semi-span length is:

$$l_{eff} = \frac{b_w / 2}{\cos \Lambda} \quad (3.1-4)$$

Now some empirical correction factor must be introduced in order to compute the wing's lift coefficient ($C_{L\alpha}$) as accurately as possible. For a subsonic wing ($M < 0.85$) a fairly enough approximation for a three-dimensional wing is given by [7] as follows:

$$C_{L\alpha} = \frac{\pi AR}{1 + \sqrt{1 + \left(\frac{\pi AR}{C_{l\alpha} \cos \Lambda_{AC}} \right)^2}} \quad (3.1-5)$$

Recalling the semi-rigid assumption for streamwise segments, the moment produced by the lift about the elastic axis, unaffected by wing deformations, is:

$$M_{EA} = La \quad (3.1-6)$$

Where a is the distance between the aerodynamic center (AC) and the elastic axis (EA) as shown in the following figure:

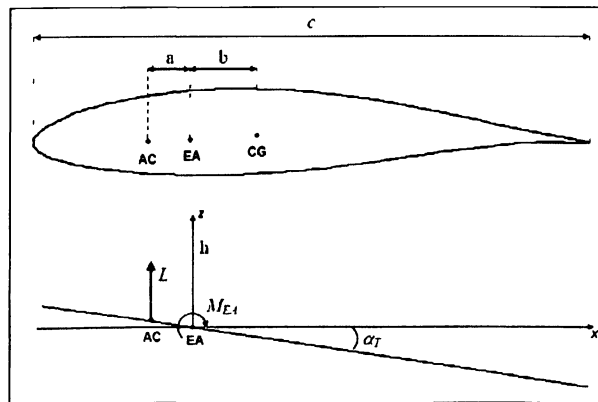


Figure 3.1b: Airfoil cross-section and aerodynamic forces diagram.

It is to be noted that only the influence of the aerodynamic lift force is considered for the analysis while the drag and moment are neglected.

The generalized non-conservative force term for Lagrange's equations of motion can be derived by applying the principle of virtual work. Thus the partial work done by the aerodynamic lift force is:

$$\delta W_{NC} = -\frac{L}{2}(\delta z_{AC}) = -\frac{L}{2}\delta(h - a\alpha_T) \quad (3.1-7)$$

Substituting expressions 3-1, 3.1-2 and 3.1-3 into 3.1-7, it yields:

$$\begin{aligned} \delta W_{NC} = & \frac{Q_\infty C_{L\alpha}|_{\text{semiwing}}}{2} \int_0^{l_{eff}} c \left\{ -\delta q_h q_h \left[\phi_h \frac{\partial \phi_h}{\partial y} \sin \Lambda - a \left(\frac{\partial \phi_h}{\partial y} \right)^2 \sin^2 \Lambda \right] + \right. \\ & \dots - \delta q_h q_\alpha \left[\phi_h \phi_\alpha \cos \Lambda - a \frac{\partial \phi_h}{\partial y} \phi_\alpha \sin \Lambda \cos \Lambda \right] + \\ & \dots + \delta q_\alpha q_h \left[a \frac{\partial \phi_h}{\partial y} \phi_\alpha \sin \Lambda \cos \Lambda \right] + \\ & \left. \dots + \delta q_\alpha q_\alpha \left[a \phi_\alpha^2 \cos^2 \Lambda \right] \right\} dy \end{aligned} \quad (3.1-8)$$

3.2. Kinetic Energy

While the wing is in motion the total kinetic energy ($[J/m]$) per unit span can be written as:

$$\overline{K_e} = \frac{1}{2} \overline{m} v^2 + \frac{1}{2} \overline{I} \omega^2 \quad (3.2-1)$$

Where the terms involved represent the kinetic energy due to bending and torsion respectively. Integrating the previous expression across the semi-span's effective length (l_{eff}), it yields:

$$\overline{K_e} = \frac{1}{2} \int_0^{l_{eff}} \overline{m} (\dot{h} + b\dot{\alpha})^2 dy + \frac{1}{2} \int_0^{l_{eff}} \overline{I}_{CG} \dot{\alpha}^2 dy \quad (3.2-2)$$

where:

- \bar{m} : wing's mass per unit length [Kg/m].
- \dot{h} : bending velocity [m/s].
- b : distance from center of mass (CG) to elastic axis (EA) [m].
- $\dot{\alpha}$: pitching velocity [rad/s].
- \bar{I}_{CG} : wing's mass moment of inertia per unit length [Kg*m].

Substituting expression 4-1 into 4.2-2, the total kinetic energy per unit span is: •

$$\bar{K}_e = \frac{1}{2} \int_0^{l_{eff}} \bar{m} \left[b_0^2 \dot{q}_h^2 \phi_h^2 + 2bb_0 \dot{q}_h \dot{q}_\alpha \phi_h \phi_\alpha + b^2 \dot{q}_\alpha^2 \phi_\alpha^2 \right] dy + \frac{1}{2} \int_0^{l_{eff}} \bar{I}_{CG} \dot{q}_\alpha^2 \phi_\alpha^2 dy \quad (3.2-3)$$

3.3. Potential Energy

The strain energy ([J/m]) per unit span can be written as the contribution from both the uncoupled modes for bending and torsion as follows:

$$\bar{V}_e = \frac{1}{2} K_{hh} q_h^2 + \frac{1}{2} K_{\alpha\alpha} q_\alpha^2 \quad (3.3-1)$$

where:

- $K_{hh} = \omega_h^2 M_{hh}$ and $K_{\alpha\alpha} = \omega_\alpha^2 M_{\alpha\alpha}$.
- ω_h : fundamental uncoupled bending frequency [rad/s].
- ω_α : fundamental uncoupled torsion frequency [rad/s].
- M_{hh} and $M_{\alpha\alpha}$: wing's mass terms (see following section).

Therefore, the total potential energy per unit span can be rewritten as:

$$\boxed{\bar{V}_e = \frac{1}{2} \omega_h^2 M_{hh} q_h^2 + \frac{1}{2} \omega_\alpha^2 M_{\alpha\alpha} q_\alpha^2} \quad (3.3-2)$$

3.4 Lagrange's Equation

The general expression for the Lagrange's equations of motion is:

$$\frac{\partial}{\partial t} \left(\frac{\partial \bar{L}}{\partial \dot{q}_i} \right) - \frac{\partial \bar{L}}{\partial q_i} = Q_{i-NC} = \delta W_{i-NC} \quad (3.4-1)$$

where:

- $\boxed{\bar{L} = \bar{K}_e - \bar{V}_e}$: is the Lagrangian.
- q_i : generalized coordinate.
- $Q_{i-NC} = \delta W_{i-NC}$: work done by non-conservative forces.

Combining expressions 3.2-3 and 3.3-2, the Lagrangian becomes:

$$\boxed{\bar{L} = \frac{1}{2} \left\{ \int_0^{l_{eff}} \bar{m} [b_0^2 \dot{q}_h^2 \phi_h^2 + 2bb_0 \dot{q}_h \dot{q}_\alpha \phi_h \phi_\alpha + b^2 \dot{q}_\alpha^2 \phi_\alpha^2] dy + \int_0^{l_{eff}} \bar{I}_{CG} \dot{q}_\alpha^2 \phi_\alpha^2 dy - [\omega_h^2 M_{hh} q_h^2 + \omega_\alpha^2 M_{\alpha\alpha} q_\alpha^2] \right\}} \quad (3.4-2)$$

Substituting expression 3.4-2 into the left hand side of expression 3.4-1:

$$\begin{aligned} \rightarrow \frac{\partial}{\partial t} \left(\frac{\partial \bar{L}}{\partial \dot{q}_h} \right) &= \ddot{q}_h \int_0^{l_{eff}} \bar{m} (b_0^2 \phi_h^2) dy + \dot{q}_\alpha \int_0^{l_{eff}} \bar{m} (b_0 b \phi_h \phi_\alpha) dy \\ \rightarrow \frac{\partial}{\partial t} \left(\frac{\partial \bar{L}}{\partial \dot{q}_\alpha} \right) &= \ddot{q}_\alpha \int_0^{l_{eff}} (\bar{m} b^2 + \bar{I}_{CG}) \phi_\alpha^2 dy + \dot{q}_h \int_0^{l_{eff}} \bar{m} (b_0 b \phi_h \phi_\alpha) dy \\ \rightarrow \frac{\partial \bar{L}}{\partial q_h} &= -q_h \omega_h^2 M_{hh} \\ \rightarrow \frac{\partial \bar{L}}{\partial q_\alpha} &= -q_\alpha \omega_\alpha^2 M_{\alpha\alpha} \end{aligned} \quad (3.4-3)$$

Identifying terms from the previous expression, the mass matrix for the system is:

$$\left. \begin{aligned}
 M_{hh} &= \int_0^{l_{eff}} \bar{m} \phi_h^2 dy \\
 M_{h\alpha} &= \int_0^{l_{eff}} \bar{m} b \phi_h \phi_\alpha dy = M_{\alpha h} \\
 M_{\alpha\alpha} &= \int_0^{l_{eff}} \underbrace{(\bar{m} b^2 + \bar{I}_{CG})}_{\bar{I}_{EA}} \phi_\alpha^2 dy
 \end{aligned} \right\} \rightarrow [M] = \begin{bmatrix} M_{hh} b_0^2 & M_{h\alpha} b_0 \\ M_{\alpha h} b_0 & M_{\alpha\alpha} \end{bmatrix} \quad (3.4-4)$$

And the stiffness matrix is:

$$\left. \begin{aligned}
 K_{hh} &= \omega_h^2 \int_0^{l_{eff}} \bar{m} \phi_h^2 dy \\
 K_{h\alpha} &= 0 = K_{\alpha h} \\
 K_{\alpha\alpha} &= \omega_\alpha^2 \int_0^{l_{eff}} \underbrace{(\bar{m} b^2 + \bar{I}_{CG})}_{\bar{I}_{EA}} \phi_\alpha^2 dy
 \end{aligned} \right\} \rightarrow [K] = \begin{bmatrix} K_{hh} b_0^2 & 0 \\ 0 & K_{\alpha\alpha} \end{bmatrix} \quad (3.4-5)$$

The right hand side of the Lagrange's equations of motion has been derived previously; therefore, from expression 3.1-8 the aerodynamic loads matrix is assembled by identifying the following terms:

$$\left. \begin{aligned}
 A_{hh} &= \frac{-C_{L\alpha}|_{semiring}}{2} \int_0^{l_{eff}} c \left[\phi_h \frac{\partial \phi_h}{\partial y} \sin \Lambda - a \left(\frac{\partial \phi_h}{\partial y} \right)^2 \sin^2 \Lambda \right] dy \\
 A_{h\alpha} &= \frac{-C_{L\alpha}|_{semiring}}{2} \int_0^{l_{eff}} c \left[\phi_h \phi_\alpha \cos \Lambda - a \frac{\partial \phi_h}{\partial y} \phi_\alpha \sin \Lambda \cos \Lambda \right] dy \\
 A_{\alpha h} &= \frac{C_{L\alpha}|_{semiring}}{2} \int_0^{l_{eff}} c \left[a \frac{\partial \phi_h}{\partial y} \phi_\alpha \sin \Lambda \cos \Lambda \right] dy \\
 A_{\alpha\alpha} &= \frac{C_{L\alpha}|_{semiring}}{2} \int_0^{l_{eff}} c \left[a \phi_\alpha^2 \cos^2 \Lambda \right] dy
 \end{aligned} \right\} \rightarrow [A] = \begin{bmatrix} A_{hh} b_0^2 & A_{h\alpha} b_0 \\ A_{\alpha h} b_0 & A_{\alpha\alpha} \end{bmatrix}$$

(3.4-6)

Combining the matrices from expressions 3.4-4, 3.4-5 and 3.4-6, and rearranging for the corresponding degrees of freedom, the equations of motion for the system are obtained:

$$\underbrace{\begin{bmatrix} M_{hh}b_0^2 & M_{h\alpha}b_0 \\ M_{\alpha h}b_0 & M_{\alpha\alpha} \end{bmatrix}}_{[M]} \underbrace{\begin{Bmatrix} \ddot{q}_h \\ \ddot{q}_\alpha \end{Bmatrix}}_{\{q\}} + \underbrace{\begin{bmatrix} K_{hh}b_0^2 & 0 \\ 0 & K_{\alpha\alpha} \end{bmatrix}}_{[K]} \underbrace{\begin{Bmatrix} q_h \\ q_\alpha \end{Bmatrix}}_{\{q\}} = Q_\infty \underbrace{\begin{bmatrix} A_{hh}b_0^2 & A_{h\alpha}b_0 \\ A_{\alpha h}b_0 & A_{\alpha\alpha} \end{bmatrix}}_{[A]} \underbrace{\begin{Bmatrix} q_h \\ q_\alpha \end{Bmatrix}}_{\{q\}} \quad (3.4-7)$$

3.5. The Flutter Problem

Assuming a harmonic solution, for the equation in expression 3.4-7, of the form:

$$\underbrace{\begin{Bmatrix} q_h \\ q_\alpha \end{Bmatrix}}_{\{q\}} = \underbrace{\begin{Bmatrix} q_{h0} \\ q_{\alpha 0} \end{Bmatrix}}_{\{q_0\}} e^{i\omega t} \quad (3.5-1)$$

After rearranging expression 3.4-7, the equations of motion for the problem are:

$$\Rightarrow \left[\begin{bmatrix} K_{hh}b_0^2 - Q_\infty A_{hh}b_0^2 & -Q_\infty A_{h\alpha}b_0 \\ -Q_\infty A_{\alpha h}b_0 & K_{\alpha\alpha} - Q_\infty A_{\alpha\alpha} \end{bmatrix} - \omega^2 \begin{bmatrix} M_{hh}b_0^2 & M_{h\alpha}b_0 \\ M_{\alpha h}b_0 & M_{\alpha\alpha} \end{bmatrix} \right] \{q_0\} e^{i\omega t} = \{0\}$$

$$\therefore \boxed{\left[\left[[K] - Q_\infty [A] \right] - \omega^2 [M] \right] \{q_0\} e^{i\omega t} = \{0\}} \quad (3.5-2)$$

The matrix $[[K]-Q_\infty[A]]$ is a function of the dynamic pressure (Q_∞). For a given value of this dynamic pressure, the stability behavior of the system can be studied by solving the eigenvalue problem. As the dynamic pressure increases, the eigenvalues (ω^2) for the different modes (in the case under study, the shape modes considered are the first uncoupled mode for bending and the first for torsion) merge to a complex conjugate pair that leads to an unstable system. The real part of the complex conjugate is the flutter uncoupled frequency, while the imaginary part represents the structural damping ratio. The transition from stable to unstable defines the flutter boundary, as seen on figure 3.5a:

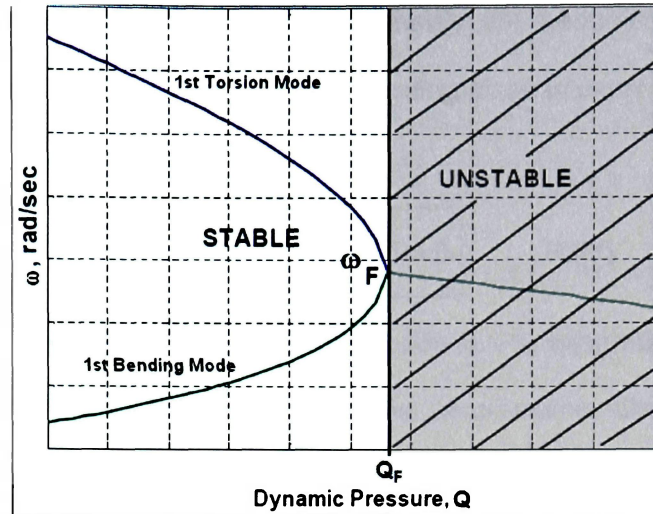


Figure 3.5a: Flutter boundary for a two-mode analysis [2].

From figure 3.5a, the flutter boundary is established and is represented by a particular value for the dynamic pressure (and therefore, flight speed for a given flight altitude). At this point, the structure is said to be at the flutter condition, and the motion is governed by a combination of bending and torsion modes acting at the same time and constant amplitude. Any increase in the dynamic pressure (or flight speed) will turn this phenomenon to the unstable region, where the amplitude of motion increases and could cause, if not take any corrective action, catastrophic damage to the structure.

3.6. The Divergence Problem

The wing divergence is a situation where, at very low angle of attack (AOA) and high speed, the pressure centers develop, pushing the front portion of the wing downward and the rear portion upward. This aerodynamic twisting effect on the wing structure while the rest of the aircraft is following the flight path decreases the AOA even more. The action finally exceeds the capability of the wing structure to resist the torsion stress, and causes the wing to separate from the airframe with no warning.

Once again, semi-rigid chord-wise segments are assumed, but this time the divergence state occurs when the term due to bending slope in expression 3.1-2 becomes negative:

$$\alpha_T = \alpha \cos \Lambda - \frac{\partial h}{\partial y} \sin \Lambda \quad (3.6-1)$$

Substituting expression 3.6-1 into expression 3.1-1, integrating across the semi-span's effective length and dividing by two, the aerodynamic divergence lift force is obtained for half-wing:

$$L|_{\text{semwing}} = \frac{Q_\infty C_{L\alpha}}{2} \int_0^{l_{\text{eff}}} c \left[\alpha \cos \Lambda - \frac{\partial h}{\partial y} \sin \Lambda \right] dy \quad (3.6-2)$$

Identically as for section 3.1, the same assumptions apply for the lift coefficient and for the moment produced by the lift about the elastic axis:

$$M_{EA} = La \quad (3.6-3)$$

As before, the influence of the aerodynamic drag force and aerodynamic moment are not taken into account here either, according to the theory developed by Dhainaut [2].

Substituting expressions 3.6-1, 3.6-2 and 3-1 into expression 3.1-7 results:

$$\begin{aligned} \delta W_{NC} = & \frac{Q_\infty C_{L\alpha}|_{\text{semwing}}}{2} \int_0^{l_{\text{eff}}} c \left\{ \delta q_h q_h \left[\phi_h \frac{\partial \phi_h}{\partial y} \sin \Lambda + a \left(\frac{\partial \phi_h}{\partial y} \right)^2 \sin^2 \Lambda \right] + \right. \\ & \dots - \delta q_h q_\alpha \left[\phi_h \phi_\alpha \cos \Lambda + a \frac{\partial \phi_h}{\partial y} \phi_\alpha \sin \Lambda \cos \Lambda \right] + \\ & \dots - \delta q_\alpha q_h \left[a \frac{\partial \phi_h}{\partial y} \phi_\alpha \sin \Lambda \cos \Lambda \right] + \\ & \left. \dots - \delta q_\alpha q_\alpha \left[a \phi_\alpha^2 \cos^2 \Lambda \right] \right\} dy \end{aligned} \quad (3.6-4)$$

Recalling the expressions developed in sections 3.2 and 3.3, the kinetic and potential energy per unit span are, respectively:

$$\overline{K}_e = \frac{1}{2} \int_0^{l_{eff}} \overline{m} \left[b_0^2 \dot{q}_h^2 \phi_h^2 + 2bb_0 \dot{q}_h \dot{q}_\alpha \phi_h \phi_\alpha + b^2 \dot{q}_\alpha^2 \phi_\alpha^2 \right] dy + \frac{1}{2} \int_0^{l_{eff}} \overline{I}_{CG} \dot{q}_\alpha^2 \phi_\alpha^2 dy \quad (3.6-5)$$

$$\overline{V}_e = \frac{1}{2} \omega_h^2 M_{hh} q_h^2 + \frac{1}{2} \omega_\alpha^2 M_{\alpha\alpha} q_\alpha^2 \quad (3.6-6)$$

In addition, the Lagrange's equation applies to obtain the equations of motion for this particular problem. Recalling the Lagrangian from expression 3.4-2, and carrying out a similar analysis as in section 4.4, the mass matrix, the stiffness matrix and the aerodynamic divergence loads matrix become, respectively:

$$\left. \begin{aligned} M_{hh} &= \int_0^{l_{eff}} \overline{m} \phi_h^2 dy \\ M_{h\alpha} &= \int_0^{l_{eff}} \overline{m} b \phi_h \phi_\alpha dy = M_{\alpha h} \\ M_{\alpha\alpha} &= \int_0^{l_{eff}} \underbrace{(\overline{m} b^2 + \overline{I}_{CG})}_{\overline{I}_{EA}} \phi_\alpha^2 dy \end{aligned} \right\} \rightarrow [M] = \begin{bmatrix} M_{hh} b_0^2 & M_{h\alpha} b_0 \\ M_{\alpha h} b_0 & M_{\alpha\alpha} \end{bmatrix} \quad (3.6-7)$$

$$\left. \begin{aligned} K_{hh} &= \omega_h^2 \int_0^{l_{eff}} \overline{m} \phi_h^2 dy \\ K_{h\alpha} &= 0 = K_{\alpha h} \\ K_{\alpha\alpha} &= \omega_\alpha^2 \int_0^{l_{eff}} \underbrace{(\overline{m} b^2 + \overline{I}_{CG})}_{\overline{I}_{EA}} \phi_\alpha^2 dy \end{aligned} \right\} \rightarrow [K] = \begin{bmatrix} K_{hh} b_0^2 & 0 \\ 0 & K_{\alpha\alpha} \end{bmatrix} \quad (3.6-8)$$

$$\left. \begin{aligned} A_{hh} &= \frac{C_{L\alpha}|_{semiwing}}{2} \int_0^{l_{eff}} c \left[\phi_h \frac{\partial \phi_h}{\partial y} \sin \Lambda + a \left(\frac{\partial \phi_h}{\partial y} \right)^2 \sin^2 \Lambda \right] dy \\ A_{h\alpha} &= \frac{-C_{L\alpha}|_{semiwing}}{2} \int_0^{l_{eff}} c \left[\phi_h \phi_\alpha \cos \Lambda + a \frac{\partial \phi_h}{\partial y} \phi_\alpha \sin \Lambda \cos \Lambda \right] dy \\ A_{\alpha h} &= \frac{-C_{L\alpha}|_{semiwing}}{2} \int_0^{l_{eff}} c \left[a \frac{\partial \phi_h}{\partial y} \phi_\alpha \sin \Lambda \cos \Lambda \right] dy \\ A_{\alpha\alpha} &= \frac{-C_{L\alpha}|_{semiwing}}{2} \int_0^{l_{eff}} c \left[a \phi_\alpha^2 \cos^2 \Lambda \right] dy \end{aligned} \right\} \rightarrow [A] = \begin{bmatrix} A_{hh} b_0^2 & A_{h\alpha} b_0 \\ A_{\alpha h} b_0 & A_{\alpha\alpha} \end{bmatrix} \quad (3.6-9)$$

Combining the previous matrices and rearranging for the corresponding degrees of freedom, the equations of motion for the divergence problem turn out to be:

$$\underbrace{\begin{bmatrix} K_{hh}b_0^2 & 0 \\ 0 & K_{\alpha\alpha} \end{bmatrix}}_{[K]} \underbrace{\begin{Bmatrix} q_h \\ q_\alpha \end{Bmatrix}}_{\{q\}} = Q_\infty \underbrace{\begin{bmatrix} A_{hh}b_0^2 & A_{h\alpha}b_0 \\ A_{\alpha h}b_0 & A_{\alpha\alpha} \end{bmatrix}}_{[A]} \underbrace{\begin{Bmatrix} q_h \\ q_\alpha \end{Bmatrix}}_{\{q\}} \quad (3.6-10)$$

Since the divergence phenomenon is a static problem, the solution of the system can be found by rearranging expression 3.6-10:

$$\Rightarrow \begin{bmatrix} K_{hh}b_0^2 - Q_\infty A_{hh}b_0^2 & -Q_\infty A_{h\alpha}b_0 \\ -Q_\infty A_{\alpha h}b_0 & K_{\alpha\alpha} - Q_\infty A_{\alpha\alpha} \end{bmatrix} \begin{Bmatrix} q_h \\ q_\alpha \end{Bmatrix} = \{0\}$$

$$\boxed{\therefore [K - Q_\infty A] \{q\} = \{0\}} \quad (3.6-11)$$

Again, the matrix $[[K]-Q_\infty[A]]$ is function of the dynamic pressure (Q_∞). Solving the problem, the lowest value gives the divergence dynamic pressure, and therefore the speed at this condition.

3.7. Correction for Compressibility Effects: Theodorsen's Curve

Due to the fact that the wing under study travels at speeds higher than $M=0.3$ (considered the limit where compressibility effect may be neglected) compressibility corrections must be taken into account. In order to do so, a curve provided from experimental analysis by the work done by Theodorsen (taken from [2]) is employed.

This experimental curve allows the correction by compressibility effects of a particular flutter speed. Inputting a dimensionless parameter (called here x_f) a factor is obtained that relates the new corrected speed to the original one.

Table 3.7-1 and figure 3.7a illustrate Theodorsen's experiment data and his correction factor curve, where k_f represents the ratio of corrected to uncorrected speeds, ($V_{corrected}/V$). In the abscise axis the dimensionless parameter x_f is defined as:

$$x_f = \frac{C_{75\%b/2} \omega_{flutter}}{KTAS_{flutter}} \quad (3.7-1)$$

where:

- $C_{75\%b/2}$: chord at 75% of semi-span [ff].
- $\omega_{flutter}$: flutter frequency [rad/s].
- $KTAS_{flutter}$: flutter air speed [kts].

Table 3.7-1: Theodorsen's experimental data.

x_f	k_f	x_f	k_f	x_f	k_f	x_f	k_f
0.00	1.000	0.60	1.260	1.20	1.340	1.70	1.370
0.20	1.100	0.80	1.300	1.30	1.350	1.80	1.375
0.30	1.175	0.90	1.310	1.40	1.355	1.90	1.380
0.40	1.210	1.00	1.320	1.50	1.360	2.00	1.385
0.50	1.240	1.10	1.330	1.60	1.365		

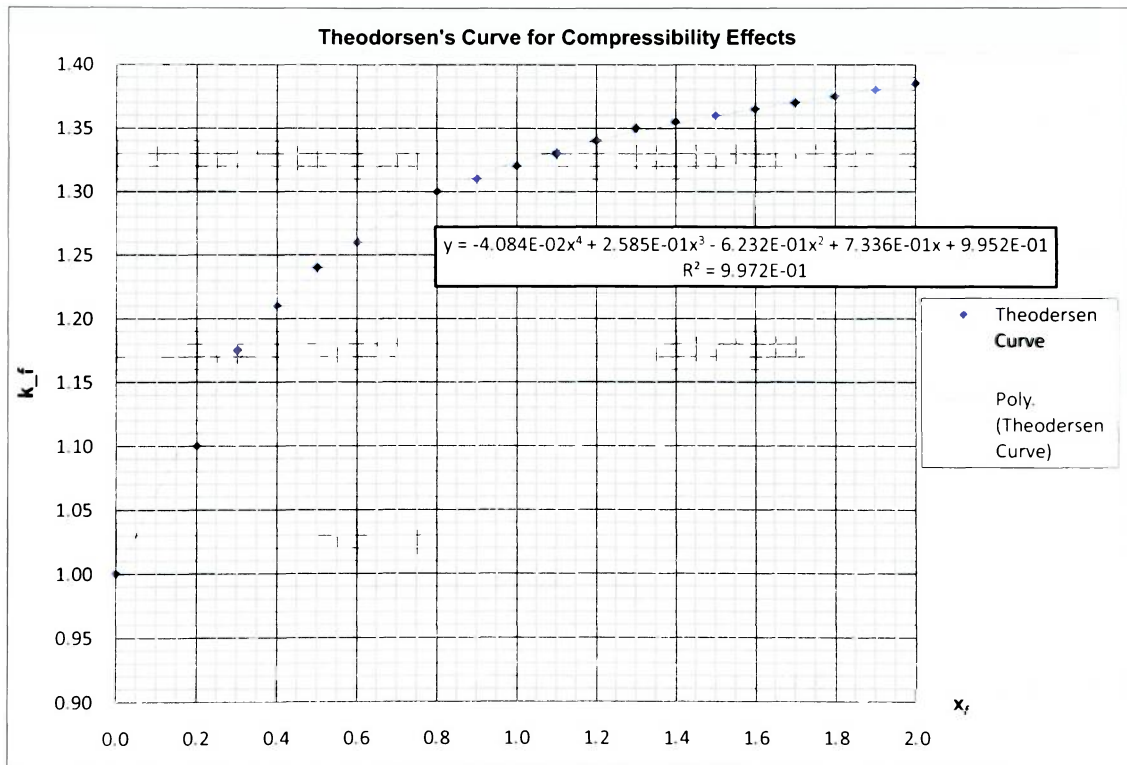


Figure 3.7a- Theodorsen's curve.

The Theodorsen's curve is represented by a trend line that best fits the experimental data; thus:

$$k_f = -4.084e^{-2}x_f^4 + 2.585e^{-1}x_f^3 - 6.232e^{-1}x_f^2 + 7.336e^{-1}x_f + 9.952e^{-1} \quad (3.7-2)$$

4. FREE VIBRATION ANALYSIS

The analysis of the system under free vibration provides the natural frequencies, which are associated with a particular vibration mode of the structures. Of all these vibration modes, and their corresponding natural frequencies, only two are of interest: the fundamental natural frequency for bending (this is the lowest natural frequency associated with the first bending mode), and the natural frequency for torsion (which is the lowest value for natural frequencies associated with the first torsion mode). The reason these two particular frequencies are so important is due to the facts that this particular flutter problem is studied assuming only two uncoupled vibration modes: first bending mode and first torsion mode. When these two modes start coupling, the structure exhibits flutter behavior, and at this point the harmonic oscillations the wing undergoes have no-damping; therefore, any increase in the airspeed will lead to higher-amplitude oscillations and, consequently, to catastrophic failure of the structure.

In order to compute the natural frequencies adequately, two different procedures (programmed in Matlab by the author) are employed: Rayleigh-Ritz method and Finite Element Method. Both of these techniques, are later validated by means of NASTRAN, and compared to each other.

4.1. Rayleigh-Ritz Method (RRM) [10]

This method is an extension of the Rayleigh's method (RM), and is based on the principle of conservation of energy. The Rayleigh-Ritz method assumes a deflection mode shape ($\phi(y)$), that's satisfies all boundary conditions, which is a combination of several functions multiplied by a constant ($a_i \phi_i(y)$):

$$\phi(y) = a_1 \phi_1(y) + a_2 \phi_2(y) + \dots + a_n \phi_n(y) \quad (4.1-1)$$

The number of frequencies that can be obtained with this technique depends on the number of independent functions combined for the deflection curve, and in general, the main advantage of RRM with respect to RM is that not only the first natural frequency can be obtained, but all the subsequent ones $\omega_1, \omega_2 \dots \omega_n$, with a better accuracy than its predecessor.

The frequencies are found, as a function of the constants $a_1, a_2 \dots a_n$, after the maximum kinetic energy (K_{e-max}) is equated with the maximum potential energy (V_{e-max}):

$$\boxed{K_{e-max} = V_{e-max}} \quad (4.1-2)$$

From this point, the condition that the frequency is a minimum results in:

$$\boxed{\frac{\partial R}{\partial a_i} = 0} \quad (4.1-3)$$

4.1.1. The Bending Problem (BF_RRM)

The functions that are selected must satisfy the boundary conditions of the problem, in the case of a cantilever wing, the coordinate system lays on the elastic axis (y -axis) and, since is a clamped beam, the boundary conditions are:

$$@ y = 0 \rightarrow \begin{cases} \phi = 0 \\ \frac{\partial \phi}{\partial y} = 0 \end{cases} \quad @ y = l_{eff} \rightarrow \begin{cases} \frac{\partial^2 \phi}{\partial y^2} = 0 \\ \frac{\partial^3 \phi}{\partial y^3} = 0 \end{cases} \quad (4.1.1-1)$$

This indicates that at the root, the beam has neither deflection nor slope, and at the free end, the beam is stress free and has no shear loading.

A deflection curve, based on two terms, that satisfies all boundary conditions is:

$$\phi(y) = a_1\phi_1(y) + a_2\phi_2(y) \rightarrow \begin{cases} \phi_1(y) = \left(\frac{y}{l_{eff}}\right)^2 \\ \phi_2(y) = 1 - \cos\left(\frac{\pi y}{2l_{eff}}\right) \end{cases} \quad (4.1.1-2)$$

The kinetic and potential energy for the beam under transverse motion is:

$$\begin{cases} K_e = \frac{1}{2} \int_0^{l_{eff}} \bar{m} \left(\frac{\partial \phi}{\partial t}\right)^2 dy \\ V_e = \frac{1}{2} \int_0^{l_{eff}} EI_{xx} \left(\frac{\partial^2 \phi}{\partial y^2}\right)^2 dy \end{cases} \quad (4.1.1-3)$$

If the beam is assumed to vibrate in harmonic motion, then the transverse displacement at EA ($w(y,t)$) can be expressed as:

$$w(y,t) = \phi(y) \sin \omega t \quad (4.1.1-4)$$

Plugging this expression into 4.1.1-3, the maximum kinetic energy (K_{e-max}) and the maximum potential energy (V_{e-max}) result:

$$\begin{cases} K_{e-max} = \frac{\omega^2}{2} \int_0^{l_{eff}} \bar{m} \phi^2 dy \\ V_{e-max} = \frac{1}{2} \int_0^{l_{eff}} EI_{xx} \left(\frac{d^2 \phi}{dy^2}\right)^2 dy \end{cases} \quad (4.1.1-5)$$

Equating the maximum kinetic energy to the maximum potential energy, the general expression for the natural frequencies is found to be:

$$\omega^2 = \frac{\int_0^{l_{eff}} EI_{xx} \left(\frac{d^2 \phi}{dy^2}\right)^2 dy}{\int_0^{l_{eff}} \bar{m} \phi^2 dy} \quad (4.1.1-6)$$

Rearranging the previous expression, a new function R is defined as:

$$R = \left[\int_0^{l_{eff}} EI_{xx} \left(\frac{d^2 \phi}{dy^2}\right)^2 dy - \omega^2 \int_0^{l_{eff}} \bar{m} \phi^2 dy \right] \quad (4.1.1-7)$$

Now, if the condition on expression 4.1-3 is applied to expression 4.1.1-7, the following system of equations results:

$$\begin{aligned} \frac{\partial}{\partial a_1} \left[\int_0^{l_{eff}} EI_{xx} \left(\frac{d^2 \phi}{dy^2} \right)^2 dy - \omega^2 \int_0^{l_{eff}} m \phi^2 dy \right] &= 0 \\ \frac{\partial}{\partial a_2} \left[\int_0^{l_{eff}} EI_{xx} \left(\frac{d^2 \phi}{dy^2} \right)^2 dy - \omega^2 \int_0^{l_{eff}} m \phi^2 dy \right] &= 0 \end{aligned} \quad (4.1.1-8)$$

Solution to this system of equations provides the first and second natural frequencies for bending (since only a two term deflection curve was assumed originally). From these two solutions, the minimum value represents the fundamental bending frequency.

In order to reduce the amount of calculations, this method is included in the Matlab code for this project under the name BF_RRM, and is used for the validation of the free vibration model along with FEM and NASTRAN.

4.1.2. The Torsion Problem (TF_RRM)

Similarly as stated in the preceding sub-section, the torsion problem is also approached with the Rayleigh-Ritz method; in this case, the boundary conditions are:

$$@ y = 0 \rightarrow \phi = 0 \quad @ y = l_{eff} \rightarrow \frac{\partial^2 \phi}{\partial y^2} = 0 \quad (4.1.2-1)$$

This indicates that at the root, the beam has no rotation about the elastic axis, and at the free end, the beam is stress free. Again, a two-term deflection curve that satisfies all boundary conditions is:

$$\phi(y) = a_1 \phi_1(y) + a_2 \phi_2(y) \rightarrow \begin{cases} \phi_1(y) = \frac{y}{l_{eff}} \\ \phi_2(y) = \sin\left(\frac{\pi y}{2l_{eff}}\right) \end{cases} \quad (4.1.2-2)$$

The kinetic and potential energy for the beam under transverse motion is:

$$\begin{cases} K_e = \frac{1}{2} \int_0^{l_{eff}} \bar{I}_{EA} \left(\frac{\partial \phi}{\partial t} \right)^2 dy \\ V_e = \frac{1}{2} \int_0^{l_{eff}} GJ \left(\frac{\partial \phi}{\partial y} \right)^2 dy \end{cases} \quad (4.1.2-3)$$

The beam is assumed to vibrate in harmonic motion, then the rotational displacement ($\theta(y,t)$) can be expressed as:

$$\theta(y,t) = \phi(y) \sin \omega t \quad (4.1.2-4)$$

Plugging this expression into 4.1.2-3, the maximum kinetic energy (K_{e-max}) and the maximum potential energy (V_{e-max}) result:

$$\begin{cases} K_{e-max} = \frac{\omega^2}{2} \int_0^{l_{eff}} \bar{I}_{EA} \phi^2 dy \\ V_{e-max} = \frac{1}{2} \int_0^{l_{eff}} GJ \left(\frac{d\phi}{dy} \right)^2 dy \end{cases} \quad (4.1.2-5)$$

Equating the maximum kinetic energy to the maximum potential energy, the general expression for the natural frequencies is found to be:

$$\omega^2 = \frac{\int_0^{l_{eff}} GJ \left(\frac{d\phi}{dy} \right)^2 dy}{\int_0^{l_{eff}} \bar{I}_{EA} \phi^2 dy} \quad (4.1.2-6)$$

Rearranging the previous expression, a new function R is defined as:

$$R = \left[\int_0^{l_{eff}} GJ \left(\frac{d\phi}{dy} \right)^2 dy - \omega^2 \int_0^{l_{eff}} \bar{I}_{EA} \phi^2 dy \right] \quad (4.1.2-7)$$

Once again the condition on expression 4.1-3 is applied to expression 4.1.2-7, resulting:

$$\frac{\partial}{\partial a_1} \left[\int_0^{l_{eff}} GJ \left(\frac{d\phi}{dy} \right)^2 dy - \omega^2 \int_0^{l_{eff}} \bar{I}_{EA} \phi^2 dy \right] = 0$$

$$\frac{\partial}{\partial a_2} \left[\int_0^{l_{eff}} GJ \left(\frac{d\phi}{dy} \right)^2 dy - \omega^2 \int_0^{l_{eff}} \bar{I}_{EA} \phi^2 dy \right] = 0$$

(4.1.2-8)

Solution to this system of equations provides the first and second natural frequencies for torsion (only a two term deflection curve was assumed). From these two solutions, the minimum value represents the fundamental torsion frequency.

Also in this case the method is included in the Matlab code under the name TF_RRM, and is used for the validation of the free vibration model along with FEM and NASTRAN.

4.2. Finite Element Method (FEM) [13]

The Finite Element Method (FEM) is a numerical technique to find approximate solutions of partial differential equations (PDE) as well as of integral equations. For this particular problem, the wing is modeled as a beam in which all the mechanical properties are known and expressed as function of the semi-span coordinate y along the elastic axis.

The previous section treated the beam as a continuous function; in the FEM approach the beam will be divided into several elements (each of them defined with two nodes, one located at the beginning of the element and another one at the end) that, combined with each other, will provide a matrix system of equations.

In order to find the solution for the system, the eigenvalue problem is solved, from which the natural frequencies are obtained (there are as many solutions as degrees of freedom has the system).

In general, the FEM solution gives very good accuracy when compared to RRM, and it can be increased by adjusting the number of elements chosen. The main purpose

to have a FEM model is that it gives the capability to modify the mechanical properties in each element, providing the means that will allow the simulation of elastic foundations.

4.2.1. The Bending Problem (BF_FEM)

In FEM, the free vibration analysis of a beam undergoing transverse motion can be represented with the following equation:

$$\boxed{[M]\{\ddot{q}\} + [K]\{q\} = \{0\}} \quad (4.2.1-1)$$

Where $[M]$ is the mass matrix, $[K]$ is the stiffness matrix, and $\{q\}$ is the vector of generalized coordinates.

In order to gain accuracy, the entire beam will be divided into many small elements; their mechanical, geometrical and mass properties are known since all these parameters have already been defined for the entire wing in section 2. These properties are then evaluated at each node, and their average values represent the properties in the corresponding element.

Since the beam is divided into several elements, each of these elements will have a total of four degrees of freedom (DOF), two at each node: a transverse displacement (w , along z-axis) and a rotation (θ , around x-axis):

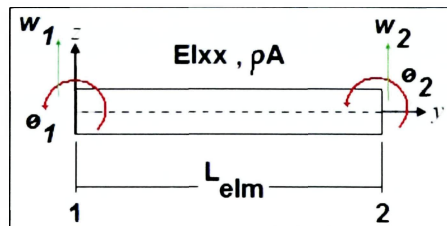


Figure 4.2.1a: Beam element for bending analysis with FEM.

The mass matrix of the beam element for bending analysis (from Galerkin's method) is:

$$[M]_{elm} = \frac{\rho_{elm} A_{elm} L_{elm}}{420} \begin{bmatrix} 156 & 22L_{elm} & 54 & -13L_{elm} \\ 22L_{elm} & 4L_{elm}^2 & 13L_{elm} & -3L_{elm}^2 \\ 54 & 13L_{elm} & 156 & -22L_{elm} \\ -13L_{elm} & -3L_{elm}^2 & -22L_{elm} & 4L_{elm}^2 \end{bmatrix} \quad (4.2.1-2)$$

And the stiffness matrix for the element is:

$$[K]_{elm} = \frac{E_{elm} I_{xx-elm}}{L_{elm}^3} \begin{bmatrix} 12 & 6L_{elm} & -12 & 6L_{elm} \\ 6L_{elm} & 4L_{elm}^2 & -6L_{elm} & 2L_{elm}^2 \\ -12 & -6L_{elm} & 12 & -6L_{elm} \\ 6L_{elm} & 2L_{elm}^2 & -6L_{elm} & 4L_{elm}^2 \end{bmatrix} \quad (4.2.1-3)$$

Assuming a harmonic solution for the equation of motion of the system (expression 4.2.1-1) of the form:

$$\{q\} = \{C\} e^{i\omega t} \quad (4.2.1-4)$$

In the previous expression C is a vector containing constants for the corresponding DOF's. Plugging this expression into 4.2.1-1, the system reduces to:

$$\boxed{[[K] - \omega^2 [M]] = 0} \quad (4.2.1-5)$$

Expression 4.2.1-5 represents the eigenvalue problem for the system; its solution gives the natural frequencies for the beam undergoing transverse vibration. The minimum value of these frequencies corresponds to the fundamental bending natural frequency.

In order to make a program accurate enough and reducing the amount of calculations, this method is included in the Matlab code under the name BF_FEM, and is used for the validation of the free vibration model along with RRM and NASTRAN.

4.2.2. The Torsion Problem (TF_FEM)

In this case the equation of motion for the rod undergoing rotational vibration is:

$$\boxed{[I]\{\ddot{\theta}\} + [K]\{\theta\} = \{0\}} \quad (4.2.2-1)$$

Where $[I]$ is the mass moment of inertia matrix, $[K]$ is the stiffness matrix, and $\{\theta\}$ is the vector of generalized coordinates.

Once again, the rod is divided into several elements; each of these elements has a total of two DOF, one per node: a rotation (θ , around y-axis):

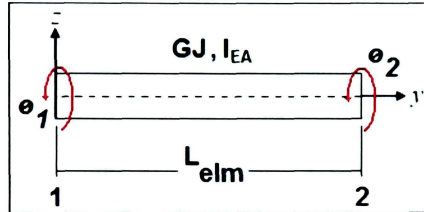


Figure 4.2.2a: Rod element for torsion analysis with FEM

The mass moment of inertia about EA matrix of the rod element for torsion analysis (lumped method) is:

$$[I]_{elm} = \frac{\bar{I}_{EA-elm} L_{elm}}{2} \begin{bmatrix} 1 & 0 \\ 0 & 1 \end{bmatrix} \quad (4.2.2-2)$$

And the stiffness matrix for the element is:

$$[K]_{elm} = \frac{G_{elm} J_{elm}}{L_{elm}} \begin{bmatrix} 1 & -1 \\ -1 & 1 \end{bmatrix} \quad (4.2.2-3)$$

Similarly as before, a harmonic solution is assumed:

$$\{\theta\} = \{C\} e^{i\omega t} \quad (4.2.2-4)$$

C is a vector containing constants for the corresponding DOF's. Plugging this expression into 4.2.2-1, the system reduces to:

$$\boxed{[K] - \omega^2 [I] = 0} \quad (4.2.2-5)$$

The solution of expression 4.2.2-5 gives the natural frequencies for the rod undergoing rotational vibration. The minimum value of these frequencies corresponds to the fundamental torsion natural frequency.

This method is included in the Matlab code under the name TF_FEM, and is used for the validation of the free vibration model along with RRM and NASTRAN.

4.3. Validation of Free Vibration Model (RRM-FEM-NASTRAN)

The validation consists in the comparison of the two analytical methods described before (RRM and FEM), with the addition of NASTRAN.

The result from RRM and FEM are obtained simultaneously in Matlab when the program runs. In the case of the results shown below, the FEM model has been run with 100 elements.

The NASTRAN analysis is taken as the reference parameter, and is based on the model created in CATIA; its geometry is then imported with NASTRAN and a normal modes/eigenvalues analysis is run using the Aluminum 20204 T351 material properties from NASTRAN's library.

All figures and direct program output from the Matlab code are shown in the Appendix A, section A3.

The following table presents the values of this comparison, along with the percentage of error in each case:

Table 4.3-1: Free vibration model validation

Fundamental Frequencies [Hz]					
Method	RRM		FEM		NASTRAN
Case		% error		% error	
Bending	0.76230	1.79284	0.75734	1.13011	0.74887
Torsion	19.26600	-0.17120	19.04410	-1.32100	19.29904(*)
Ratio	25.27		25.15		25.77

From this table, it can be seen that both methods, RRM and FEM, are very accurate with overall error lower than 2%. Although the RRM results are more accurate than the ones obtained from FEM, it cannot simulate the elastic foundation, and will not be employed in the further analysis.

Note (*): although NASTRAN does not provide the natural frequency of torsion when it performs the free vibration analysis, this value has been found to be the closest to the theoretical calculations by RRM and FEM, and therefore is taken just as a reference (see Appendix A3).

5. METHOD OF RESOLUTION

The flutter analysis is carried out completely in Matlab thanks to a code specially designed for this purpose. The Matlab code has a main program which uses a series of subroutines through the different stages of calculation. These details are given in the following subsection.

5.1. Program Flow and Subroutines

As mentioned before, the code uses a main program that calls different subroutines to analyze the problem. These different subroutines are listed below:

Flutter Analysis FEM EF: this is the main program, contains the principal loops, and calls the other subroutines, plots and displays all the results in the Matlab Command Window. For a given problem, this is the only program that has to be run.

Data Input: this is the first subroutine called by the main program; it contains the information of the wing (mechanical, geometrical and mass properties) and converts the atmospheric parameters used later by the other subroutines.

BF FEM EF: this program computes the fundamental natural frequency of vibration in bending with the elastic effects taken into account.

TF FEM EF: this program computes the fundamental natural frequency of vibration in torsion with the elastic effects taken into account.

Flutter Subroutine: this subroutine computes the vibration frequencies of the structures and the corresponding air speed of the excitation, that are used later to calculate the flutter speed and frequency.

Divergence Subroutine: this subroutine computes the divergence speed of the wing that is employed later to calculate the limit speed of flight.

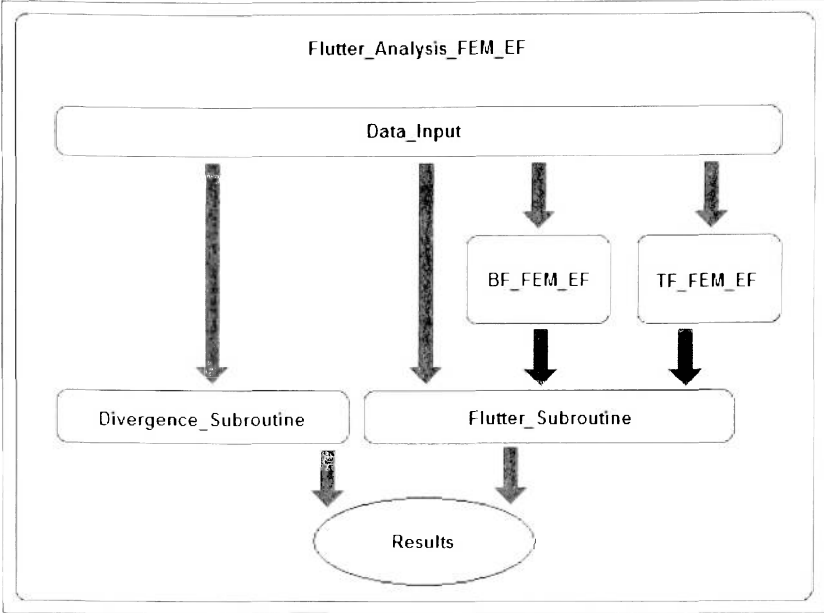


Figure 5.1a: Information flow within the Matlab code.

6. PROGRAM VALIDATION: THE GOLAND'S WING

The Goland's wing [3] is a very widely used case of study, because it provides an excellent tool to validate results. It consists of a rectangular-straight-cantilever wing, perfectly clamped at one end, and free in the opposite. The aerodynamic shape of this particular wing is considered to be an ideal thin airfoil. The flight speed is *400mph* ($\sim 178m/s$) and flight altitude is sea level (*SL*) under ISA (International Standard Atmosphere) conditions.

The Goland's wing is used to show that the results obtained from the Matlab code are consistent with the ones coming from another different theory, which proves right the use of this simplified approach.

6.1. Data Input File

In Appendix A1 there is an example of the Data Input file from the Matlab code (the units of the parameters used originally by Goland have been converted into SI system, for more details refer to [3]).

6.2. Validation

Running the program for the previous data input file, the results are the following:

```
-----Program Output-----
Uncoupled Bending Frequency: Omega_h = 8.05324 Hz
Uncoupled Torsion Frequency: Omega_a = 13.8465 Hz
Current Flight Altitude:      H = 0 m
-----Flutter Output-----
Flutter @ Q = 17590.1 Pa
Flutter @ V = 169.465 m/s
Flutter @ Mach = 0.498046
Flutter Frequency:           Omega_fl = 11.2442 Hz
```

From this data the plots have been omitted since all the important information is already provided above. When compared to the values from [3] the result is the following:

Table 6.2-1: Code validation with the Goland's wing

Method	Code	Goland	% error
Parameter			
V-flutter [m/s]	169.5	174.7	-2.96
Omega-flutter [Hz]	11.24	10.53	6.74

From table 6.2-1, it can be seen that the accuracy of the method used in the code gives a reasonable approximation to the data obtained by Goland (his results are not corrected by compressibility effects).

7. ELASTIC FOUNDATION MODEL

The following sub-sections deal with the contribution of the set of torsion springs at the root location of the wing's elastic axis and their effects on the FEM model.

7.1. Contribution Using FEM (FEM_EF)

As mentioned in the introduction, the elastic foundation will be simulated by adding a combination of torsion springs to some particular DOF's in the FEM model. These particular DOF's are: rotation or slope for bending at root (at the first node of the first beam element), and rotation for torsion at root (at the first node of the first rod element).

The contribution of these two torsion springs allows to simulate the elasticity that a real wing would have when mounted to the aircraft fuselage. Their stiffness values are variable, and are expressed as a percentage of the critical stiffness that simulates a perfect clamping condition (when these values are set to be 100%, they represent the perfect clamping condition).

7.1.1. The Bending Problem (BF_FEM_EF)

As stated on section 4.2.1, the free vibration analysis with FEM of a beam undergoing transverse motion can be represented with the following equation:

$$\boxed{[M]\{\ddot{q}\} + [K]\{q\} = \{0\}} \quad (7.1.1-1)$$

Where $[M]$ is the mass matrix, $[K]$ is the stiffness matrix, and $\{q\}$ is the vector of generalized coordinates.

The beam is divided into several elements; each of these elements has a total of four DOF's as detailed in section 4.2.1.

The contribution of the torsion spring is added to the boundary conditions of first element, which now has a rotation (θ , around x-axis), controlled by the torsion spring (K_B [N^*m]) at the first node:

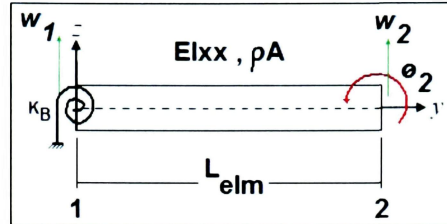


Figure 7.1.1a: First beam element and its elastic contribution.

The mass matrix of all the beam elements is exactly the same as the one shown in expression 4.2.1-2.

The stiffness matrix, however, is different for the first element since it has the contribution of the spring in the rotation of the first node (the second DOF out of four in the element), thus:

$$[K]_1 = \frac{E_1 I_{xx-1}}{L_1^3} \begin{bmatrix} 12 & 6L_1 & -12 & 6L_1 \\ 6L_1 & 4L_1^2 + \bar{K}_B & -6L_1 & 2L_1^2 \\ -12 & -6L_1 & 12 & -6L_1 \\ 6L_1 & 2L_1^2 & -6L_1 & 4L_1^2 \end{bmatrix} \quad (7.1.1-2)$$

In the previous expression the suffix indicates that this is only for the first element, and the term \bar{K}_B represents:

$$\bar{K}_B = \frac{K_B L_1^3}{E_1 I_{xx-1}} \quad (7.1.1-3)$$

The stiffness matrix for the rest of the beam elements remains exactly the same as in expression 4.2.1-3.

Once again, the harmonic solution is assumed; therefore, the system reduces to:

$$[[K] - \omega^2 [M]] = 0 \quad (7.1.1-4)$$

Solving the eigenvalue problem the natural frequencies of bending vibration are obtained. The minimum value of these frequencies corresponds to the fundamental natural bending frequency.

As before, this method is included in the Matlab code under the name BF_FEM_EF, and is used for the validation of the free vibration model along with TF_FEM_EF and NASTRAN.

7.1.2. The Torsion Problem (TF_FEM_EF)

From section 4.2.2, the free vibration analysis with FEM of a rod undergoing torsion motion can be represented with the following equation:

$$\boxed{[I]\{\ddot{\theta}\} + [K]\{\theta\} = \{0\}} \quad (7.1.2-1)$$

Where $[I]$ is the mass moment of inertia matrix, $[K]$ is the stiffness matrix, and $\{\theta\}$ is the vector of generalized coordinates.

The beam is once again divided into several elements; each of these elements has a total of two DOF's as detailed in section 5.2.2.

The contribution of the torsion spring is added to the boundary conditions of first element, which now has a rotation (θ , around y-axis), controlled by the torsion spring (K_T [N^*m]) at the first node:

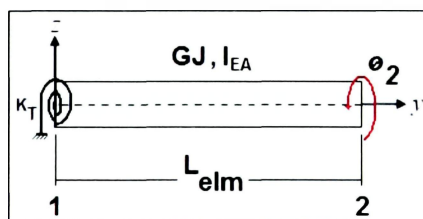


Figure 7.1.2a: First rod element and its elastic contribution.

The mass moment of inertia about EA matrix of all the beam elements is exactly the same as the one shown in expression 4.2.2-2.

The stiffness matrix, however, is different for the first element since it has the contribution of the spring in the rotation of the first node (the first DOF out of two in the element), thus:

$$[K]_1 = \frac{G_1 J_1}{L_1} \begin{bmatrix} 1 + \bar{K}_r & -1 \\ -1 & 1 \end{bmatrix} \quad (7.1.2-2)$$

In the previous expression the suffix indicates that this is only for the first element, and the term \bar{K}_r represents:

$$\bar{K}_r = \frac{K_r L_1}{G_1 J_1} \quad (7.1.2-3)$$

The stiffness matrix for the rest of the beam elements remains exactly the same as in expression 4.2.2-3.

Once again, the harmonic solution is assumed; therefore, the system reduces to:

$$[[K] - \omega^2 [I]] = 0 \quad (7.1.2-4)$$

Solving the eigenvalue problem the natural frequencies of torsion vibration are obtained. The minimum value of these frequencies corresponds to the fundamental natural torsion frequency.

As before, this method is included in the Matlab code under the name TF_FEM_EF, and is used for the validation of the free vibration model along with BF_FEM_EF and NASTRAN.

7.2. Validation of the Model (FEM_EF & FEM)

The validation consists in the comparison of the two FEM models with elastic foundation using spring values that simulate a perfect clamp, and the FEM model perfectly clamped. The preset values simulating the ideal clamp condition at the root are:

$$\begin{cases} K_B = 2.926e^{50} [Nm / rad] \\ K_T = 3.485e^{18} [Nm / rad] \end{cases} \quad (7.2-1)$$

The following table presents the values of this comparison; along with the percentage of error in each case (FEM model with 100 elements):

Table 7.2-1: Elastic foundation validation

Fundamental Frequencies [Hz]			
Method	FEM_EF	% error	FEM
Case			
Bending	0.75734	0.00000	0.75734
Torsion	18.97570	0.00000	18.97570
Ratio	25.06		25.06

From table 7.2-1 it can be seen that the values for the spring constants are large since they have been applied to a single point along the root (elastic axis), idealizing the flexibility of the complete structure that would support the wing in a real aircraft.

A slight modification in the expression 7.2-1 gives:

$$\begin{cases} K_B = 1.812e^{23} [Nm / rad] \\ K_T = 1.700e^{18} [Nm / rad] \end{cases} \quad (7.2-2)$$

This change on the springs produces a small error on the simulation of the clamp:

Table 7.2-2: Modified elastic foundation validation

Fundamental Frequencies [Hz]			
Method	FEM_EF	% error	FEM
Case			
Bending	0.75444	-0.38292	0.75734
Torsion	18.97230	-0.37702	19.04410
Ratio	25.15		25.15

These new values are smaller than the ones in expression 7.2-1, but their contribution to the fundamental frequencies is almost negligible; therefore, they will be used from now on in the simulation of the ideal clamp.

8. RESULTS

Different cases were analyzed in order to compute the effects of the main parameters involved: the torsion spring constants and the flight altitude. These cases are detailed as follows:

- Case I: the effects of the elasticity in torsion are studied.
- Case II: the effects of the elasticity in bending are studied.
- Case III: the effects of the flight altitude are studied.

8.1. Case I: Effects of Elastic Foundation in Torsion

In this case the bending mode is analyzed as clamped, whereas the torsion mode has the possibility to change its spring elastic constant at root, for cruise flight altitude. The variation of the elasticity depends on an input vector that changes the ratio of the preset torsion spring of the ideal clamp condition:

$$K_T = R_{K_T} 1.700e^{18} [Nm / rad] \quad (8.1-1)$$

The vector or elastic ratio is:

$$R_{K_T} = \left[2e^{-4} \quad 3e^{-4} \quad 4e^{-4} \quad 5e^{-4} \quad 6e^{-4} \right] \quad (8.1-2)$$

The results are shown in Appendix A2 in order of appearance according to the elastic ratio vector.

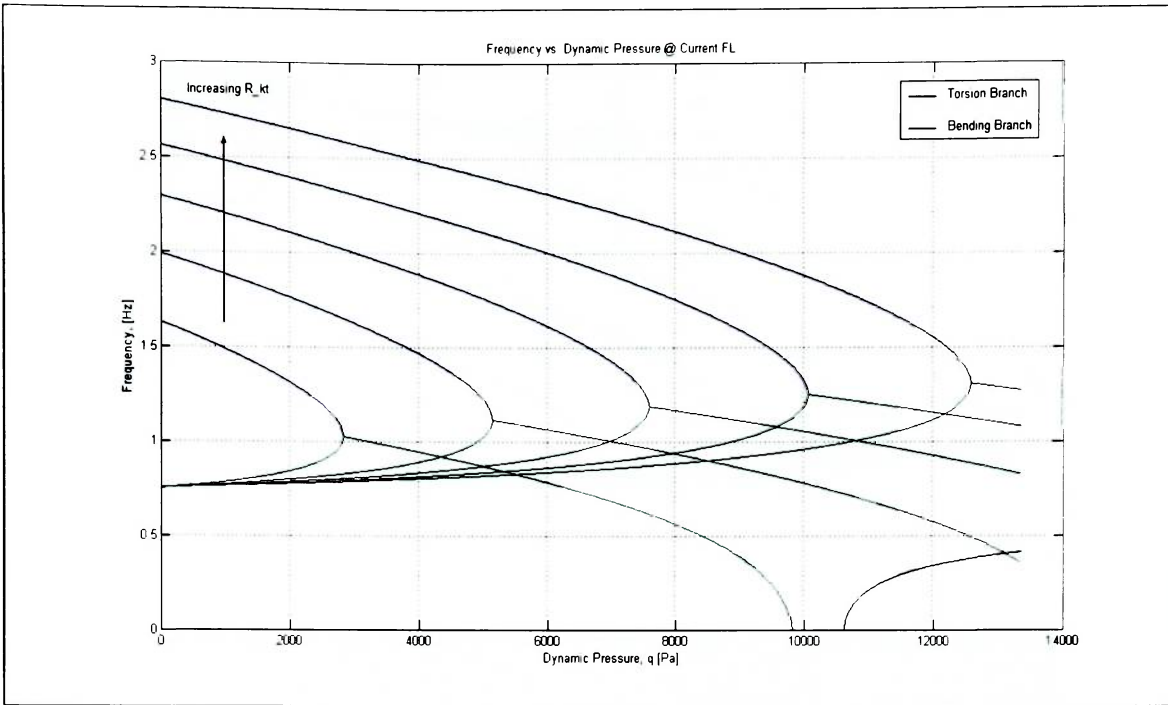


Figure 8.1a: Frequency vs. dynamic pressure.

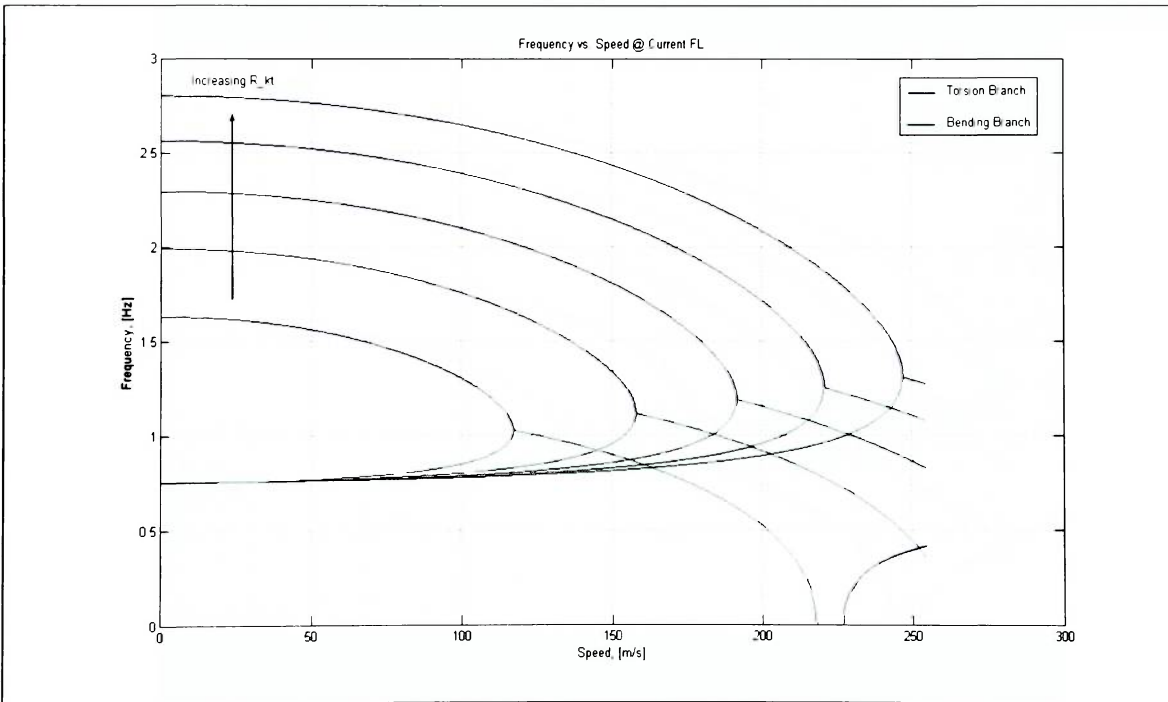


Figure 8.1b: Frequency vs. speed.

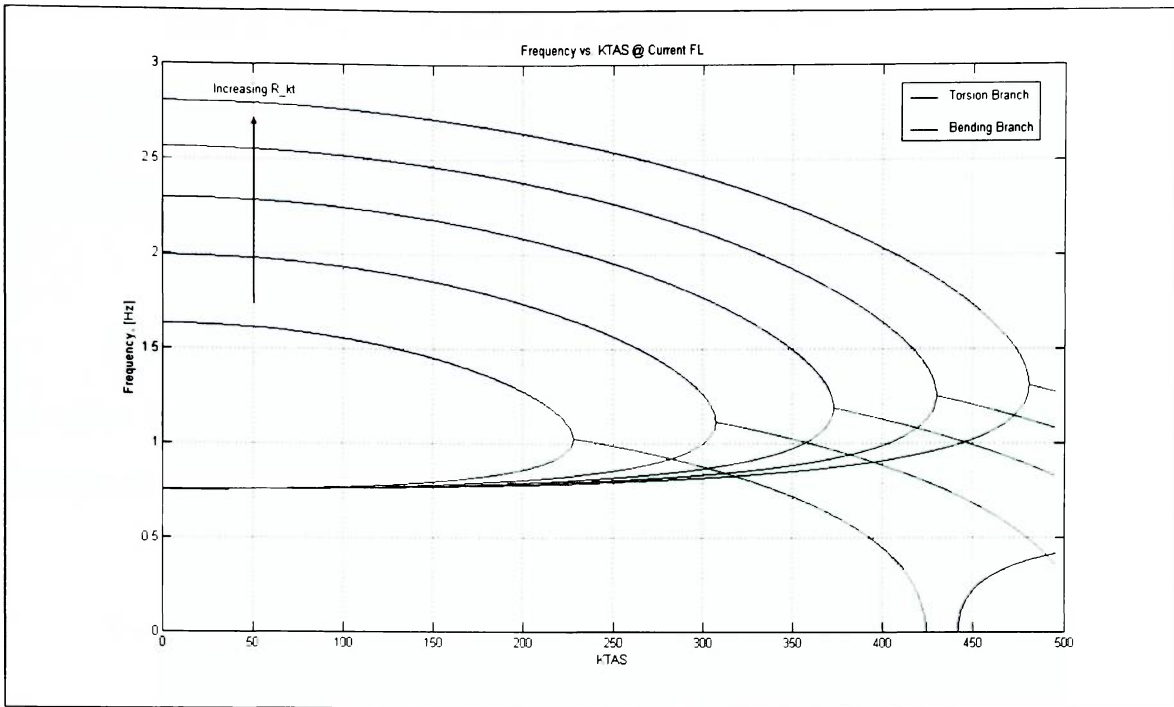


Figure 8.1c: Frequency vs. KTAS.

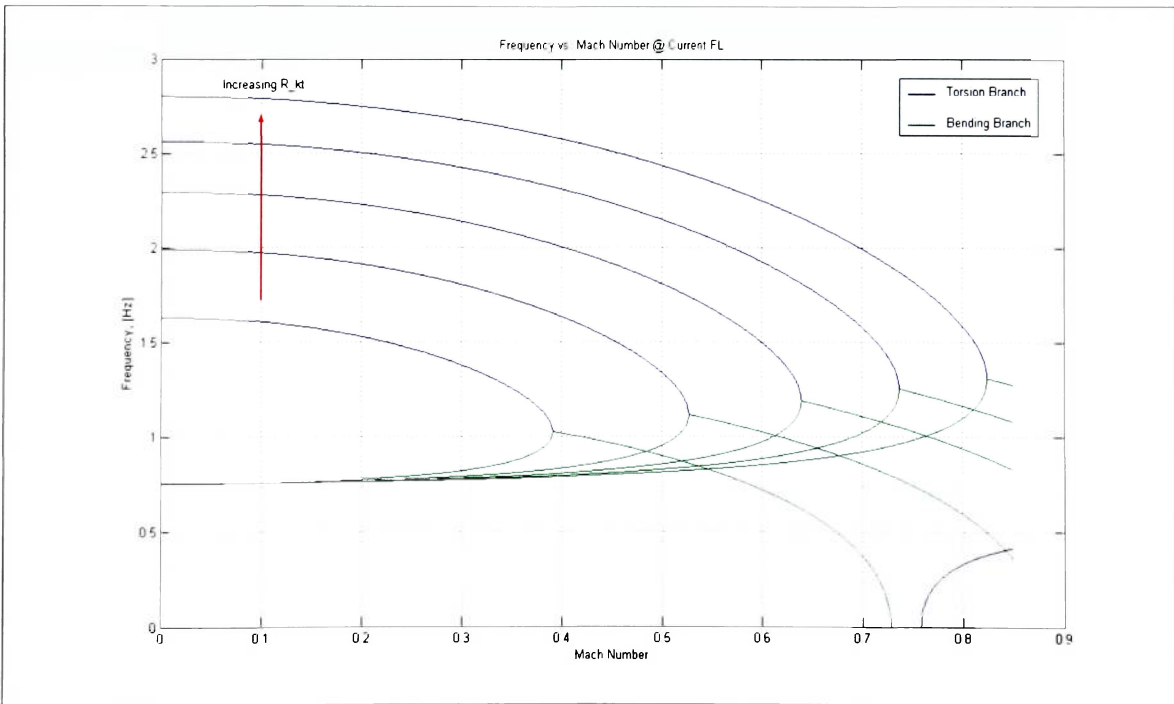


Figure 8.1d: Frequency vs. Mach number.

8.2. Case II: Effects of Elastic Foundation in Bending

In this case the torsion mode is analyzed with the highest elasticity ratio that produced flutter in Case I:

$$\boxed{R_{K_B} = 6e^{-4}} \quad (8.2-1)$$

The bending mode has the possibility to change its spring elastic constant at root, for cruise flight altitude. The variation of the elasticity depends on an input vector that changes the ratio of the preset bending spring of the ideal clamp condition:

$$K_B = R_{K_B} 1.812e^{23} [Nm / rad] \quad (8.2-2)$$

The vector or elastic ratio is:

$$\boxed{R_{K_B} = [1e^{-9} \quad 1e^{-7} \quad 1e^{-5} \quad 1e^{-3} \quad 1e^0]} \quad (8.2-3)$$

The results are shown in Appendix A2 in order of appearance according to the elastic ratio vector.

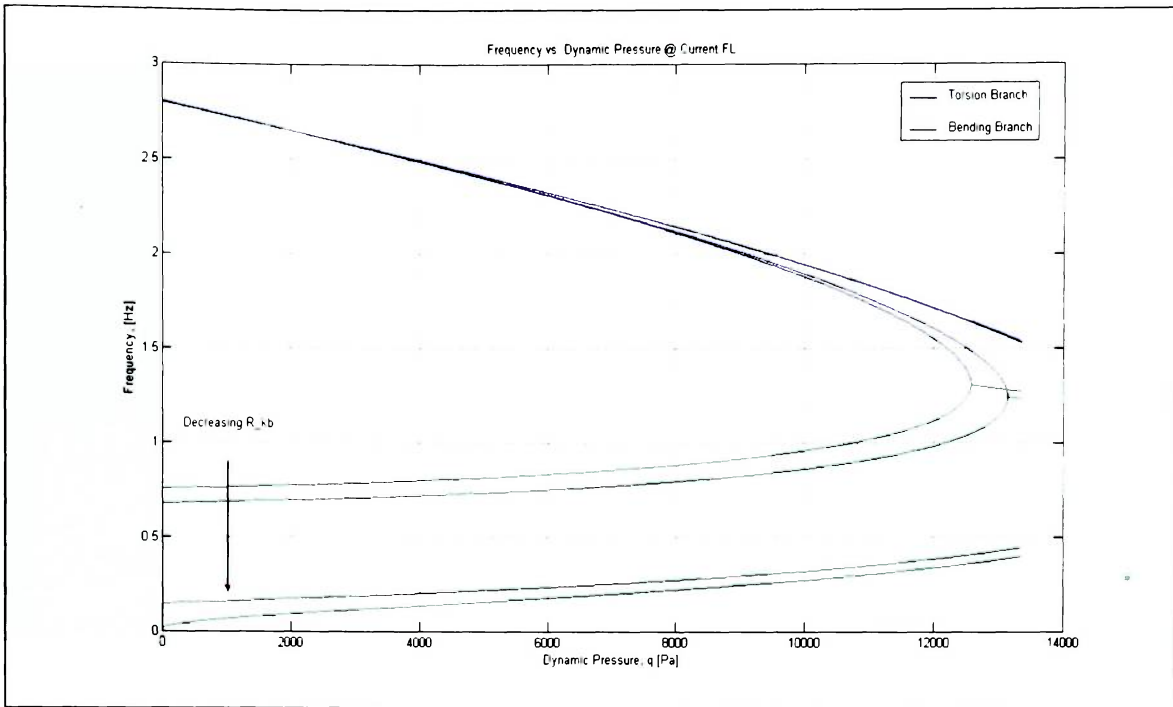


Figure 8.2a: Frequency vs. dynamic pressure.

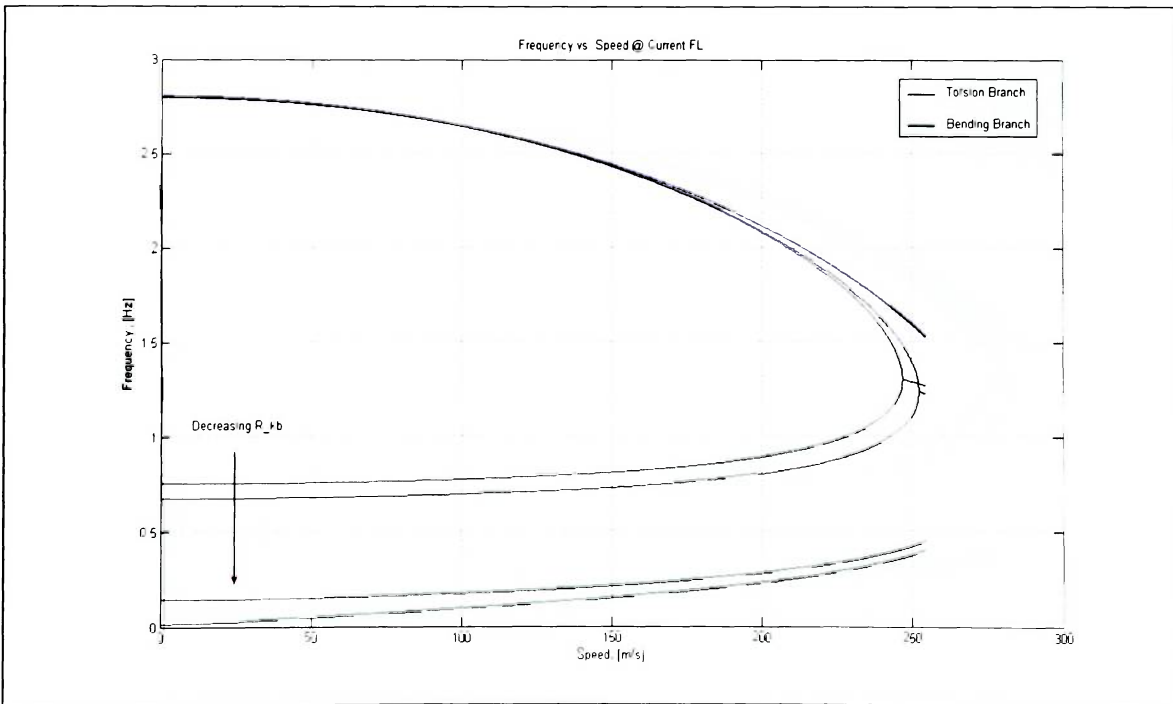


Figure 8.2b: Frequency vs. speed.

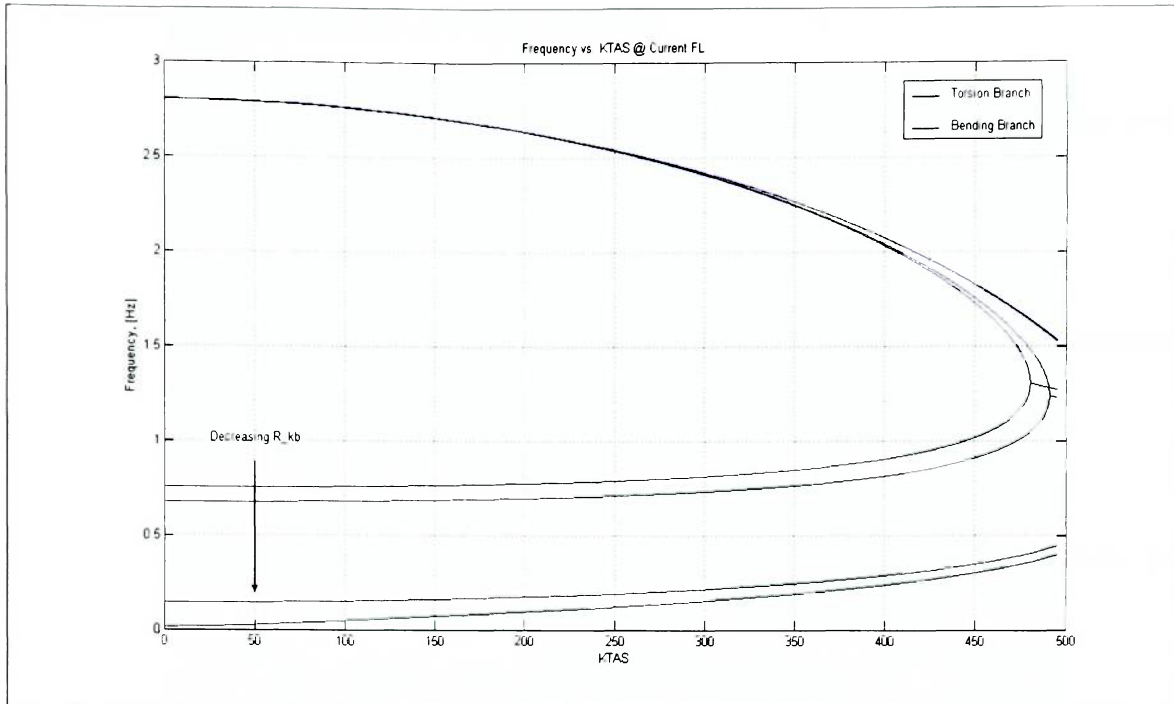


Figure 8.2c: Frequency vs. KTAS.

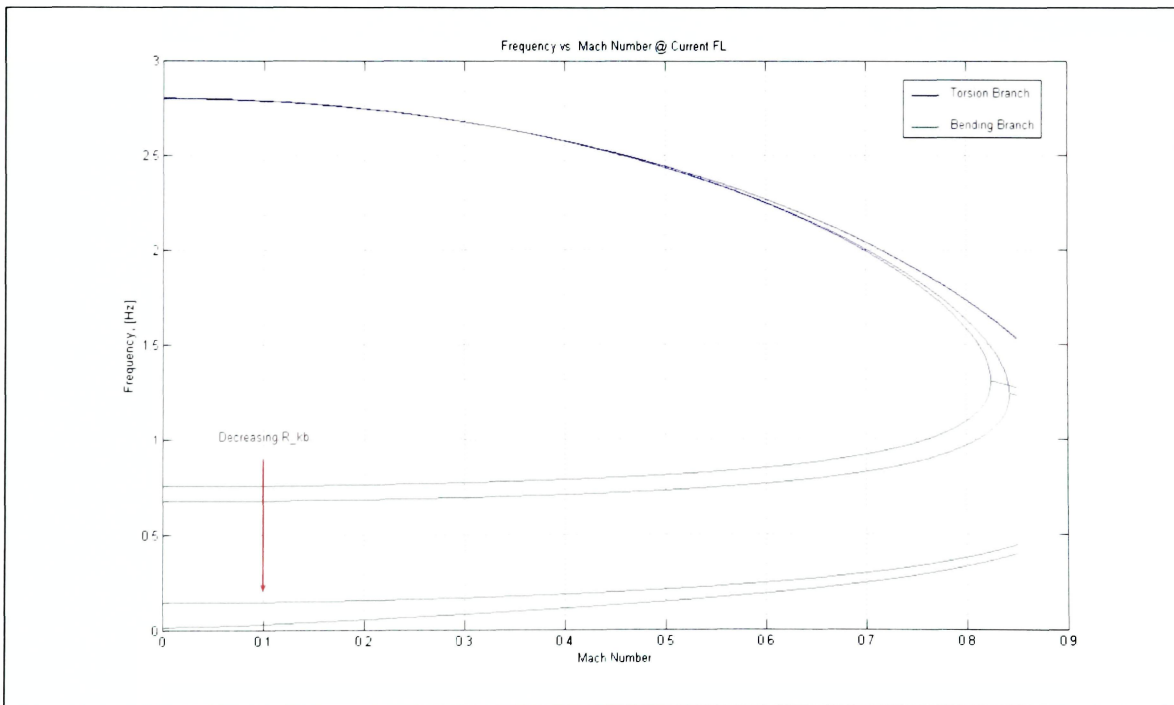


Figure 8.2d: Frequency vs. Mach number.

8.3. Case III: Effects of Flight Altitude

In this case the torsion mode is analyzed with the highest elasticity ratio that produced flutter in Case I:

$$R_{K_r} = 6e^{-4} \quad (8.3-1)$$

The bending mode is considered to have an elasticity ratio to clamp condition equal to one (highest value from Case II):

$$R_{K_B} = 1 \quad (8.3-2)$$

Since the effects of flight altitude want to be studied, the input this time will be an altitude vector, expressed as:

$$H_{fl} = [0 \quad 2500 \quad 5000 \quad 7500 \quad 10000][m] \quad (8.3-3)$$

The results are shown in Appendix A2 in order of appearance according to the altitude vector.

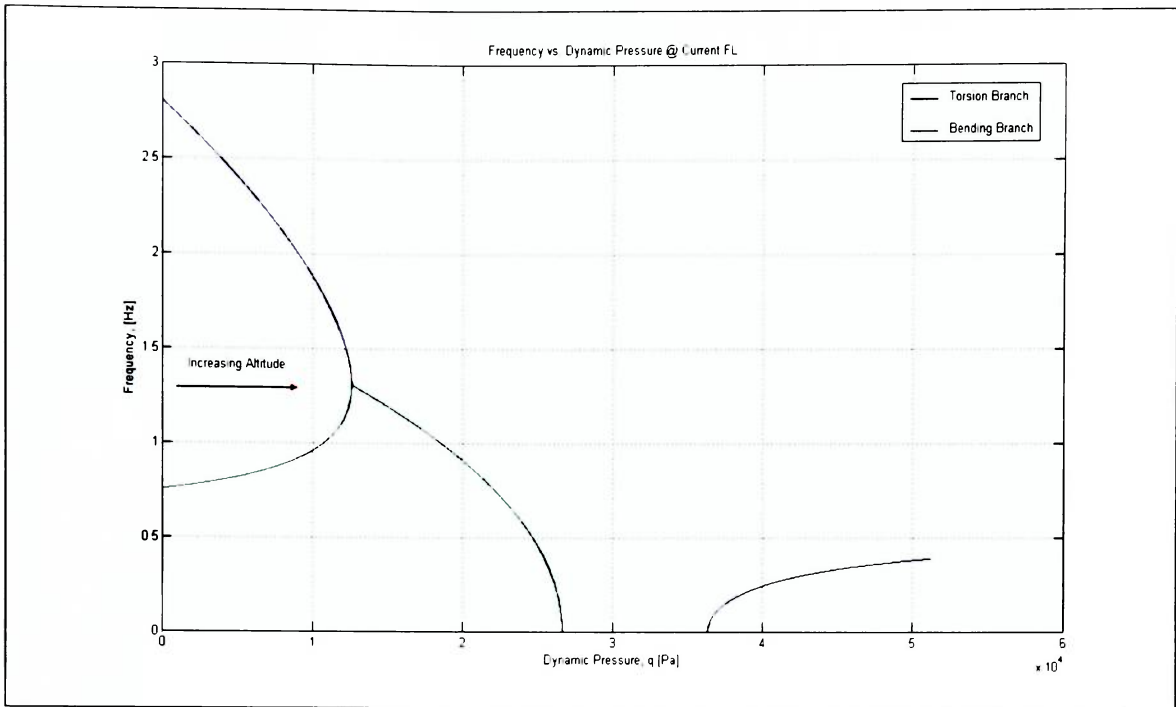


Figure 8.3a: Frequency vs. dynamic pressure.

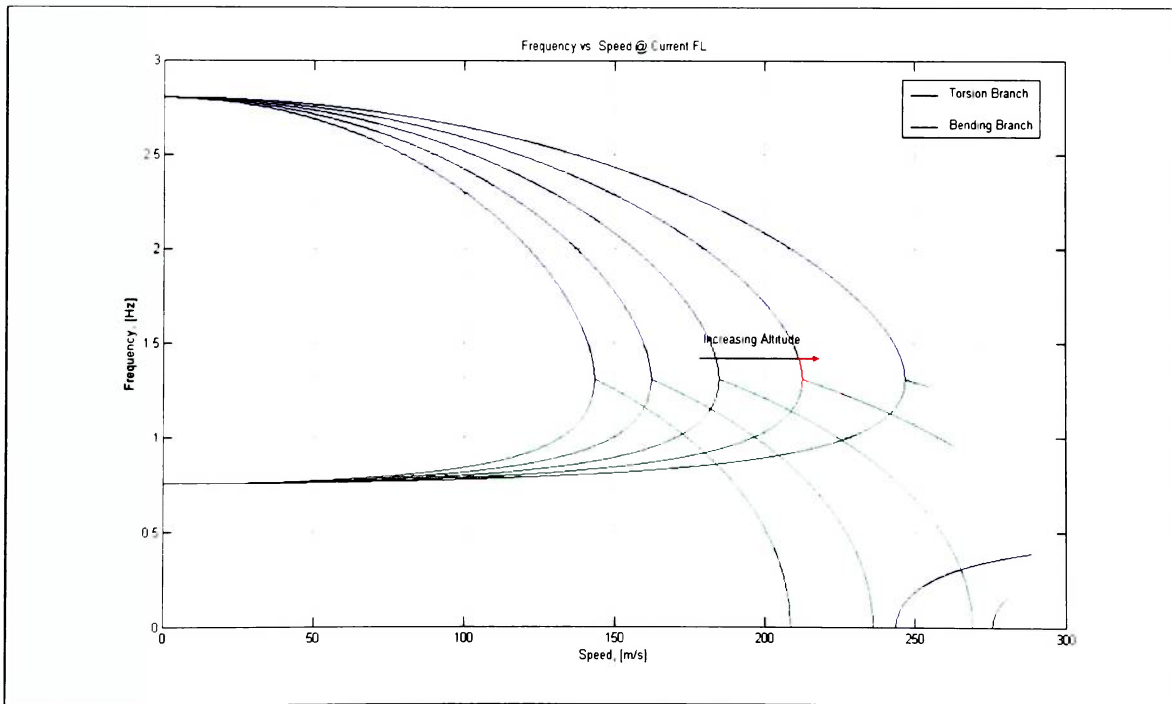


Figure 8.3b: Frequency vs. speed.

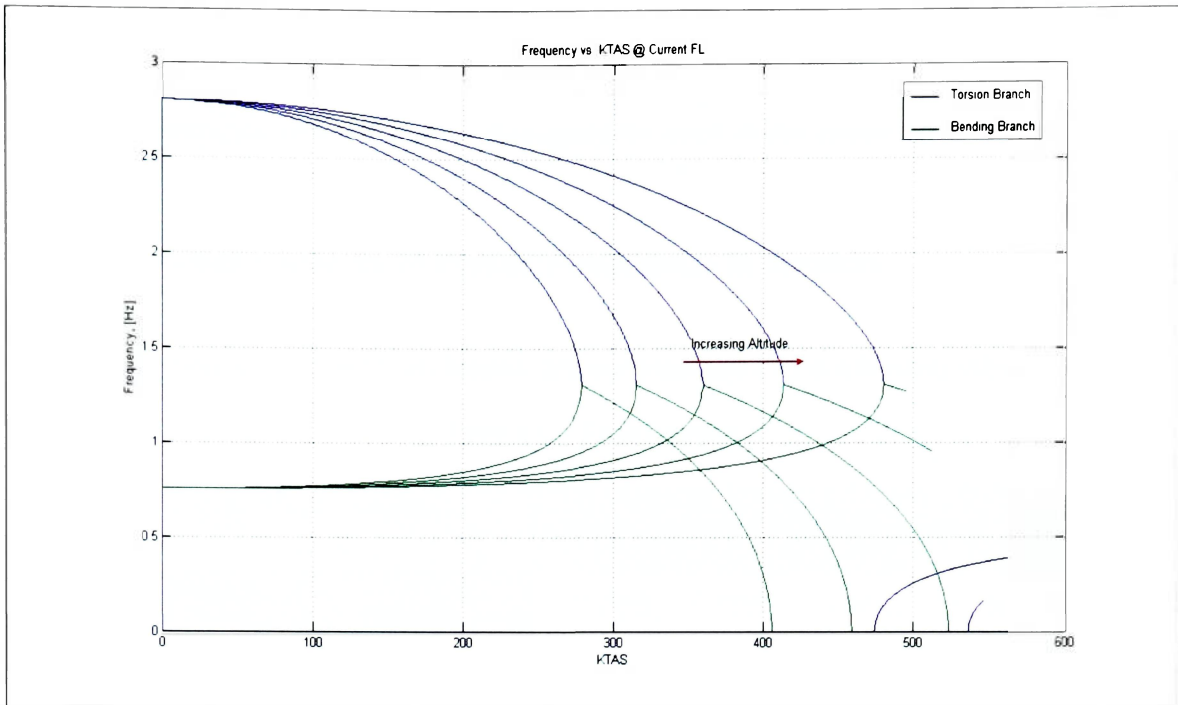


Figure 8.3c: Frequency vs. KTAS.

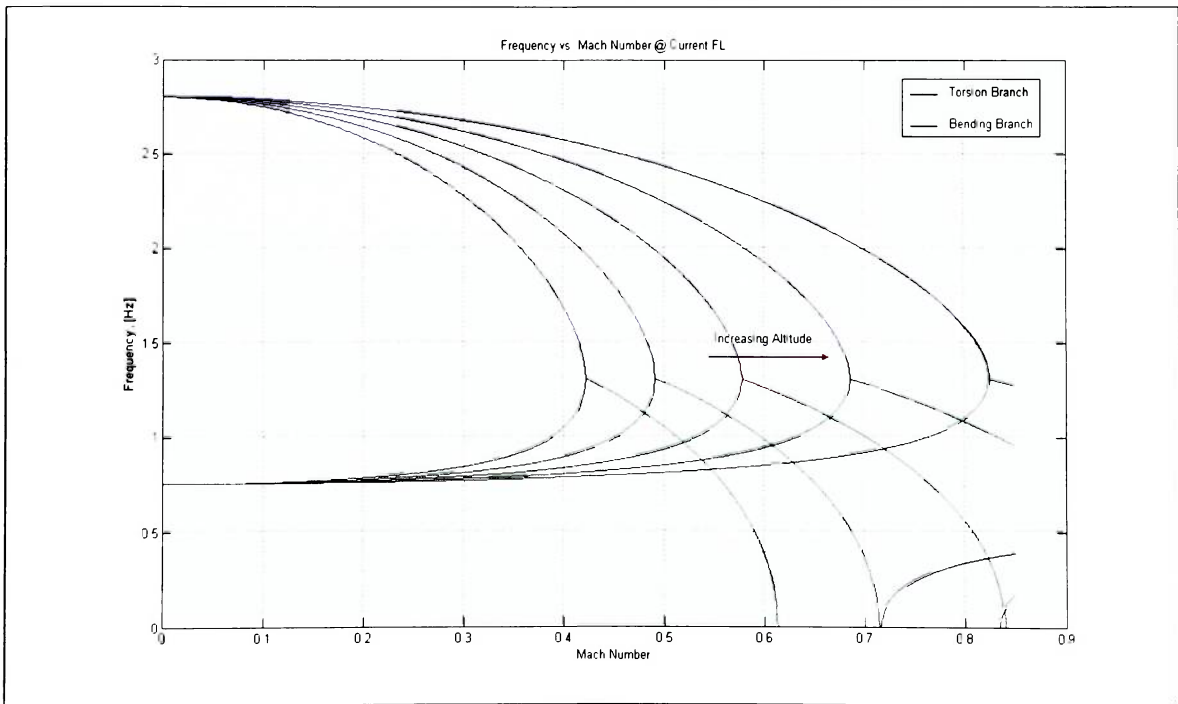


Figure 8.3d: Frequency vs. Mach number.

9. ANALYSIS

The analysis of the results is discussed for each of the cases described previously.

9.1. Case I: Effects of Elastic Foundation in Torsion

The results obtained from Matlab are summarized in the following table:

Table 9.1-1: Case I results

CASE I					
Torsion Elasticity Ratio	2.00E-04	3.00E-04	4.00E-04	5.00E-04	6.00E-04
Parameter					
Bending Frequency [Hz]	0.7544	0.7544	0.7544	0.7544	0.7544
Torsion Frequency [Hz]	1.5917	1.9475	2.2465	2.5092	2.7459
Frequency Ratio (Torsion/Bending)	2.11	2.58	2.98	3.33	3.64
Flutter Frequency [Hz]	1.0231	1.1135	1.1863	1.2494	1.3062
Flutter Dynamic Pressure-Corr [Pa]	3273.7	5790.7	8409.0	11068.6	13746.5
Flutter Speed-Corr [m/s]	126.0	167.5	201.9	231.6	258.1
Flutter Mach-Corr	0.4207	0.5595	0.6742	0.7735	0.8620
Reduced Flutter Frequency-Corr	0.0434	0.0355	0.0314	0.0288	0.0270
Divergence Dynamic Pressure [Pa]	9440.9	13821.7	18029.0	22089.5	26023.4
Divergence Speed [m/s]	213.9	258.8	295.6	327.2	355.1
Divergence Mach	0.7144	0.8643	0.9872	1.0927	1.1860

From table 9.1-1, the suffix “*corr*” means that the current value has been already corrected for compressibility effects by Theodorsen's curve.

In order to interpret these results properly, plots of the most important parameters (such as: torsion frequency and flutter frequency, flutter dynamic pressure, flutter Mach, etc.) are provided to observe their variation with the elastic foundation:

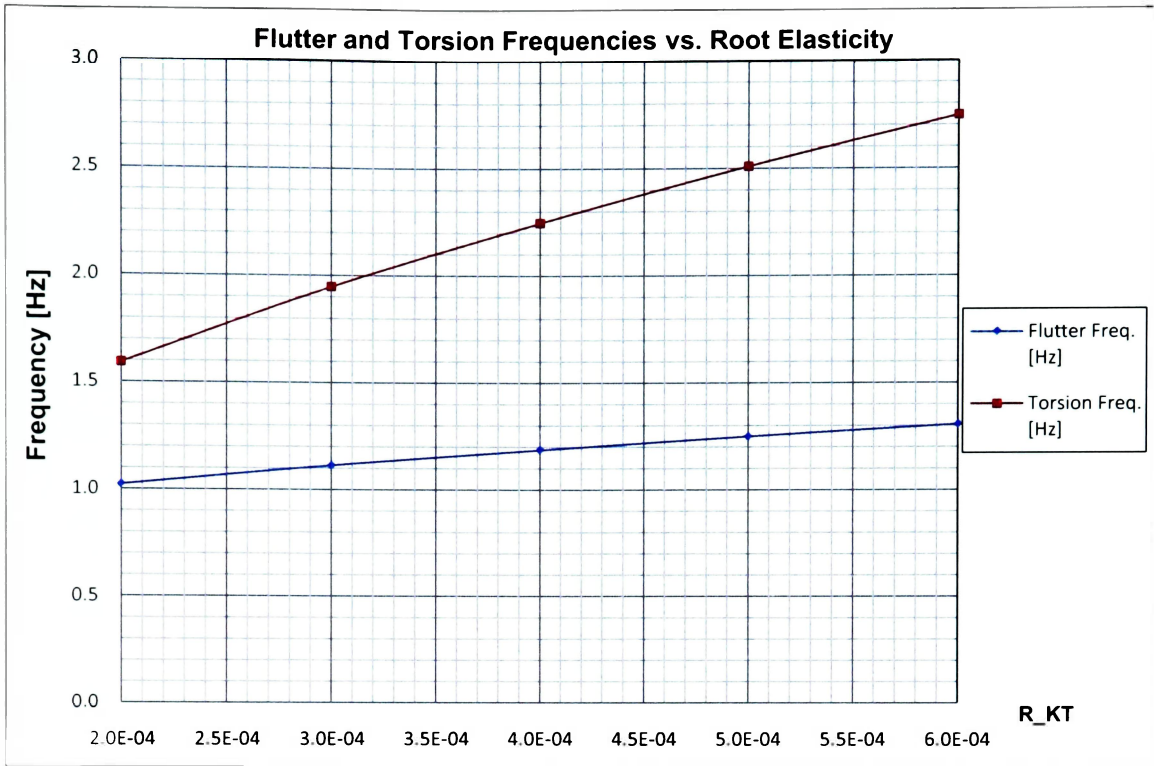


Figure 9.1a: Effect on flutter and torsion frequencies.

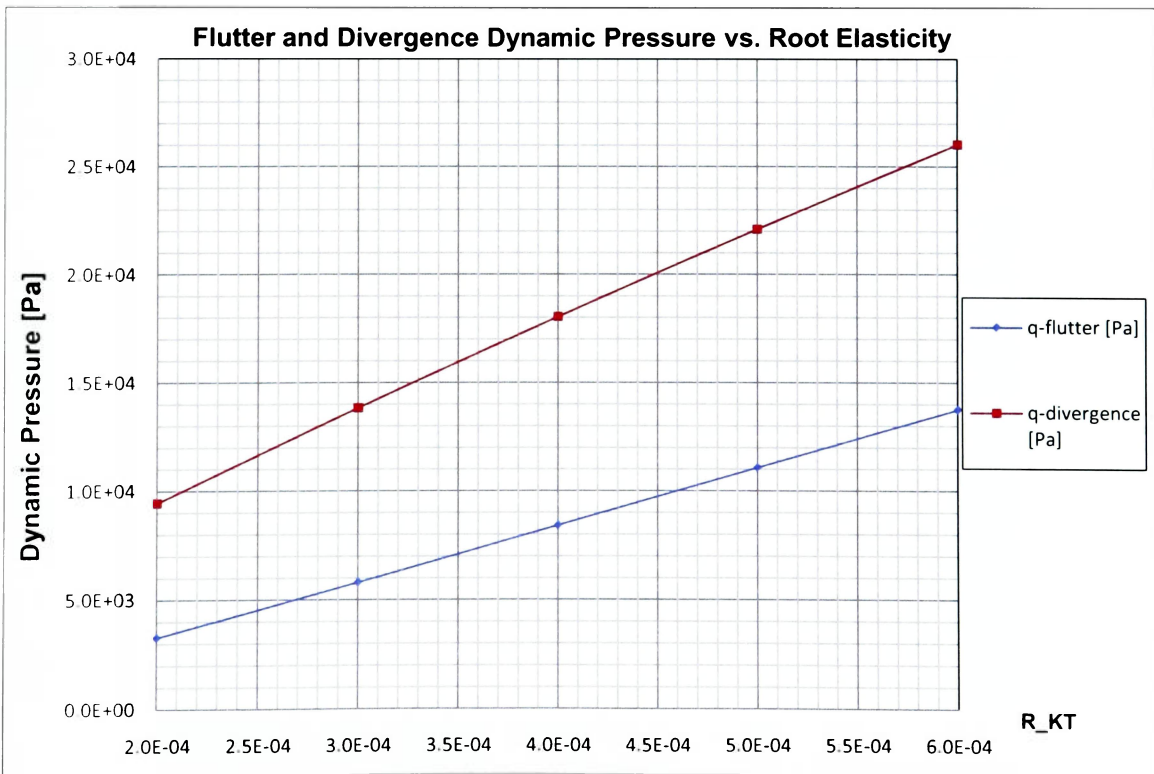


Figure 9.1b: Effect on flutter and divergence dynamic pressure.

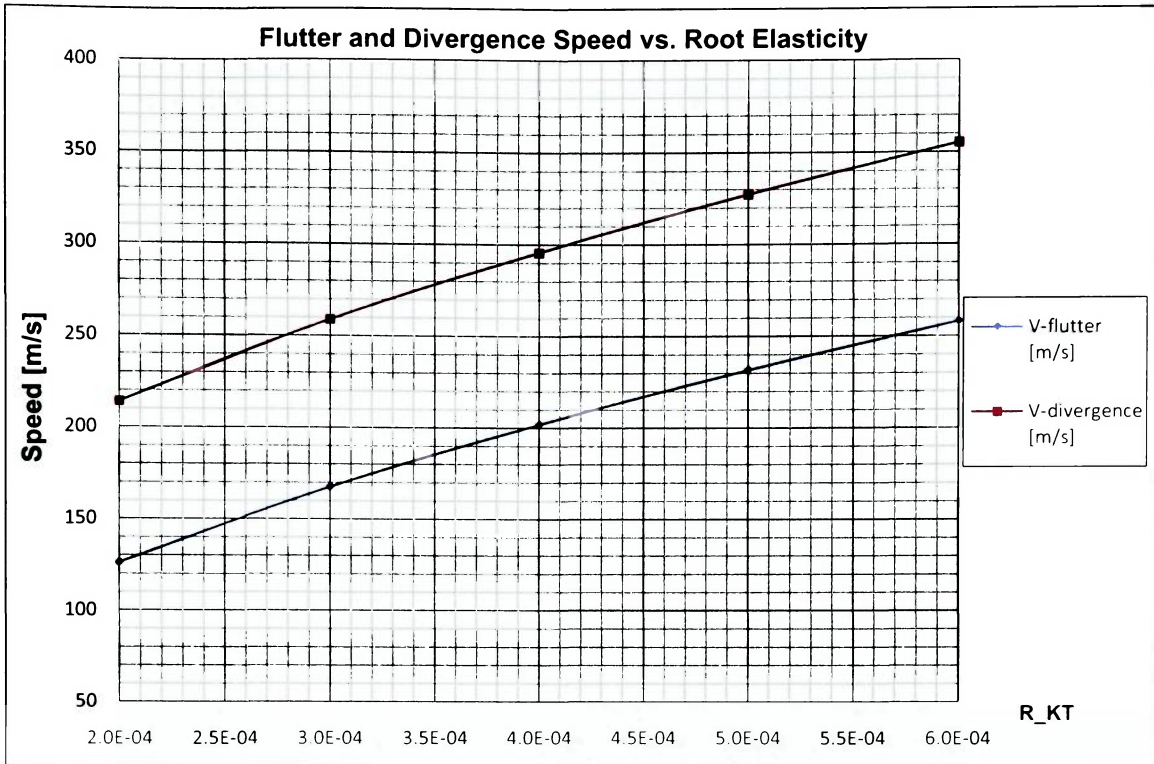


Figure 9.1c: Effect on flutter and divergence speed.

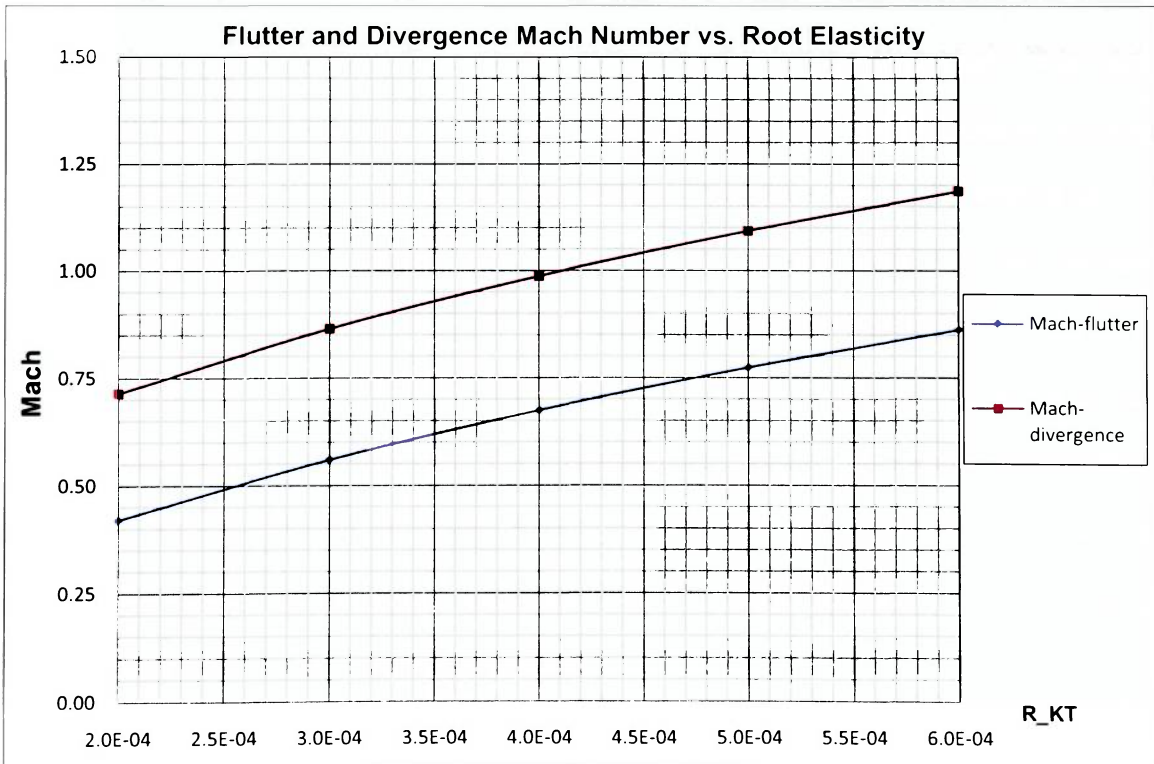


Figure 9.1d: Effect on flutter and divergence Mach number.

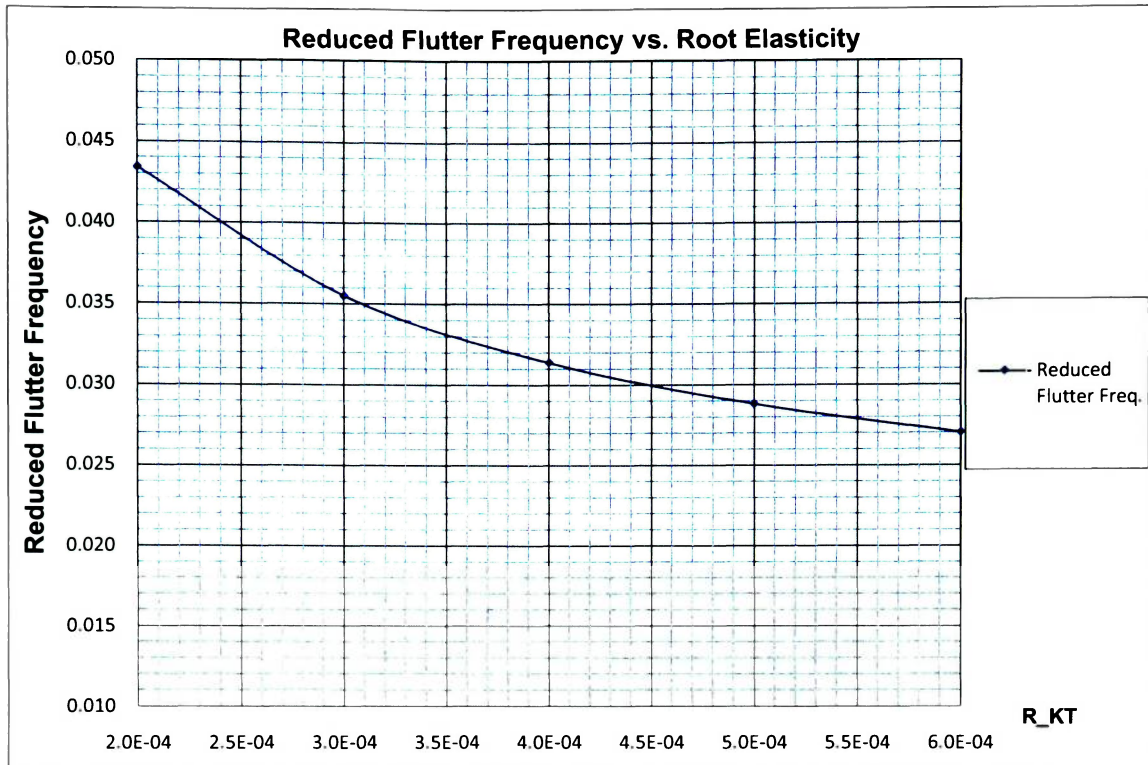


Figure 9.1e: Effect on flutter reduced frequency.

It can be seen from figure 9.1a, that both the flutter frequency and the natural torsion frequency increase when the elasticity ratio for torsion increases. This makes sense, provided that a high enough value for the elasticity ratio would produce a perfect clamp condition, in which case this wing in particular does not experience flutter at all.

The following three figures, 9.1b, c and d, are related since they all represent either speed (true air speed, TAS) or functions depending on this parameter (such as dynamic pressure or Mach number). From there the curves for divergence and flutter are given, both varying increasingly with the elasticity ratio. Again, the same reason applies here since any increase in the elasticity ratio will carry an increase in the root flexibility, and therefore the flutter envelopes displace to higher levels of speed. This fact is clearly seen on figures 8.1a to d, in the results section.

Figure 9.1e shows the reduced flutter frequency (also referred to as Strouhal number in [9]), a dimensionless parameter that relates the flutter frequency, the *MGC* and the flutter

speed. The benefit of this parameter is that flutter speed and frequency can be analyzed at the same time. The reason it decays in that fashion is due to the fact that although the flutter frequency increases, the flutter speed also does it, but faster.

It can be concluded that the contribution of the elasticity in the foundation for torsion vibration is extremely important; when flutter occurs, any change in this value will automatically change drastically the flutter envelope, as seen on figures 8.1a to d, and this means that a wing could be flutter free if the elasticity in the torsion at the root is strong enough.

9.2. Case II: Effects of Elastic Foundation in Bending

The results obtained from Matlab are summarized in the following table:

Table 9.2-1: Case II results

CASE II					
Bending Elasticity Ratio	1.00E-09	1.00E-07	1.00E-05	1.00E-03	1.00E+00
Parameter					
Bending Frequency [Hz]	0.0147	0.1443	0.6771	0.7544	0.7544
Torsion Frequency [Hz] (R_KT=6e-4)	2.7459	2.7459	2.7459	2.7459	2.7459
Frequency Ratio (Torsion/Bending)	187.17	19.03	4.06	3.64	3.64
Flutter Frequency [Hz]	-	-	1.2390	1.3062	1.3062
Flutter Dynamic Pressure-Corr [Pa]	-	-	14280.5	13746.6	13746.5
Flutter Speed-Corr [m/s]	-	-	263.1	258.1	258.1
Flutter Mach-Corr	-	-	0.8786	0.8620	0.8620
Reduced Flutter Frequency-Corr	-	-	0.0252	0.0270	0.0270
Divergence Dynamic Pressure [Pa]	14860.3	17009.2	25463.0	26023.4	26023.4
Divergence Speed [m/s]	268.4	287.1	351.3	355.1	355.1
Divergence Mach	0.8962	0.9588	1.1732	1.1860	1.1860

Notice that for the first two values of bending elasticity ratio, the wing does not experience flutter at all.

In order to better interpret these results, plots of the most important parameters (such as: bending frequency, flutter frequency, flutter dynamic pressure, flutter Mach, etc.) are provided to observe their variation with the elastic foundation:

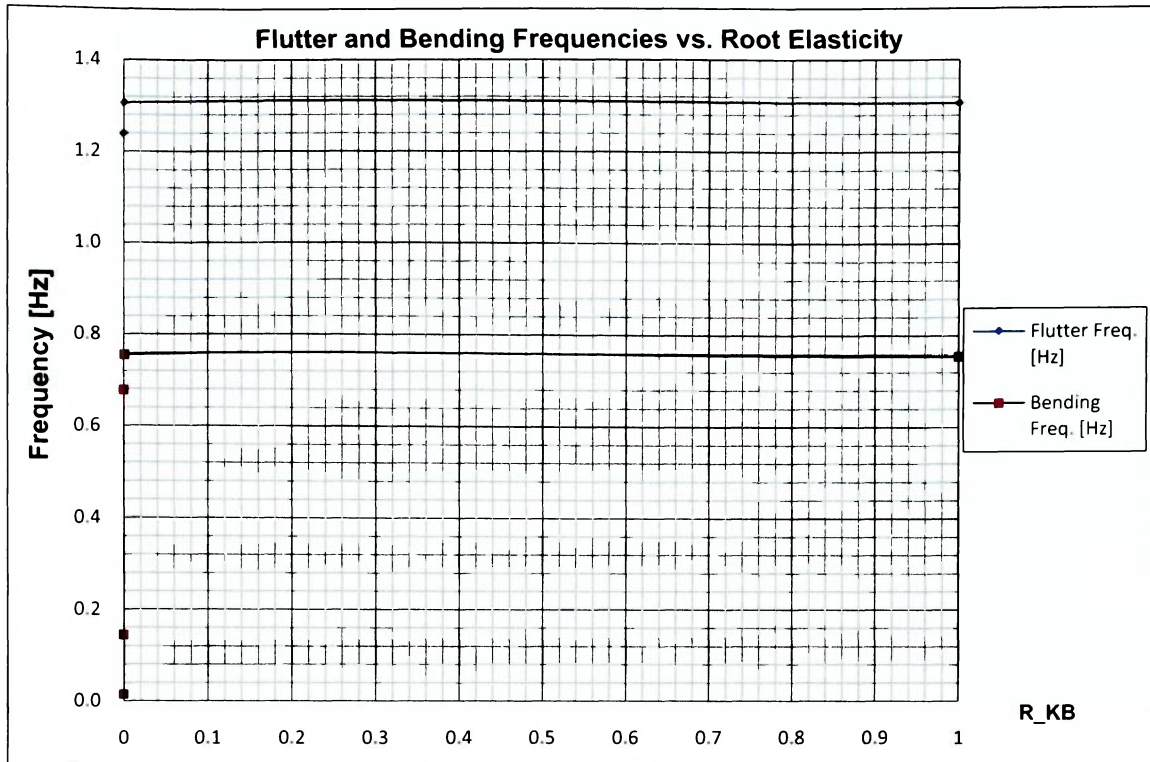


Figure 9.2a: Effect on flutter and torsion frequencies.

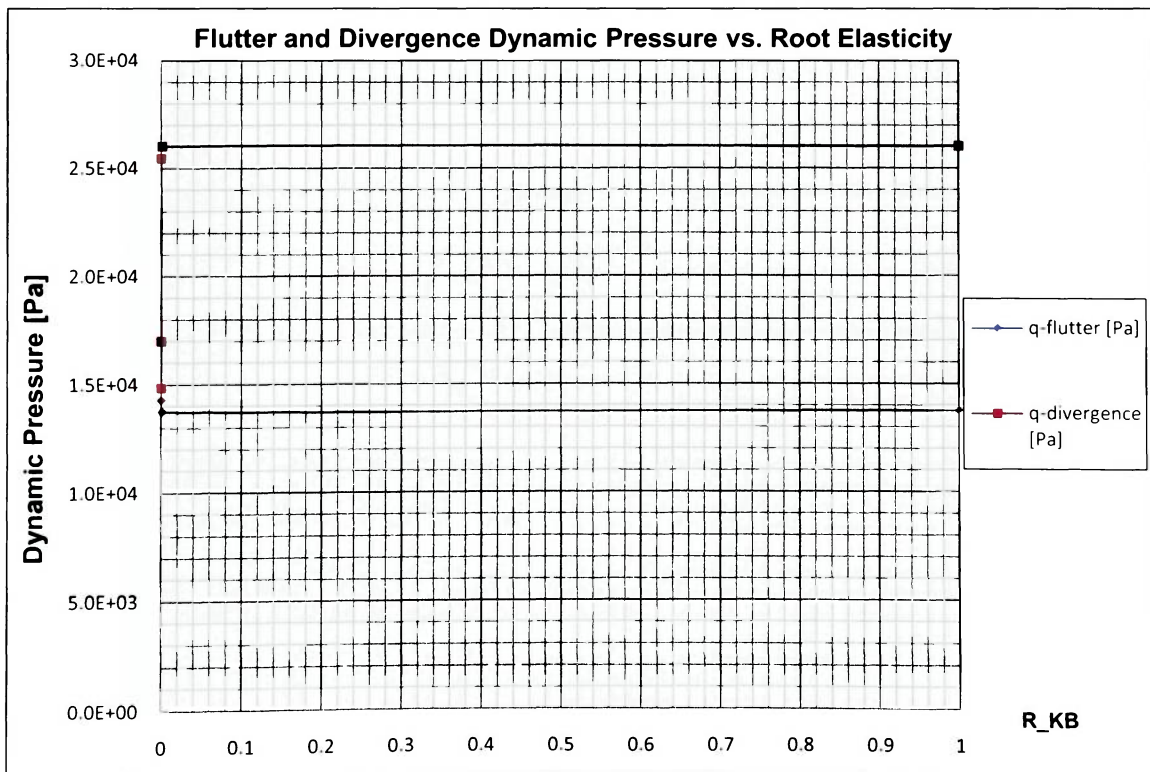


Figure 9.2b: Effect on flutter and divergence dynamic pressure.

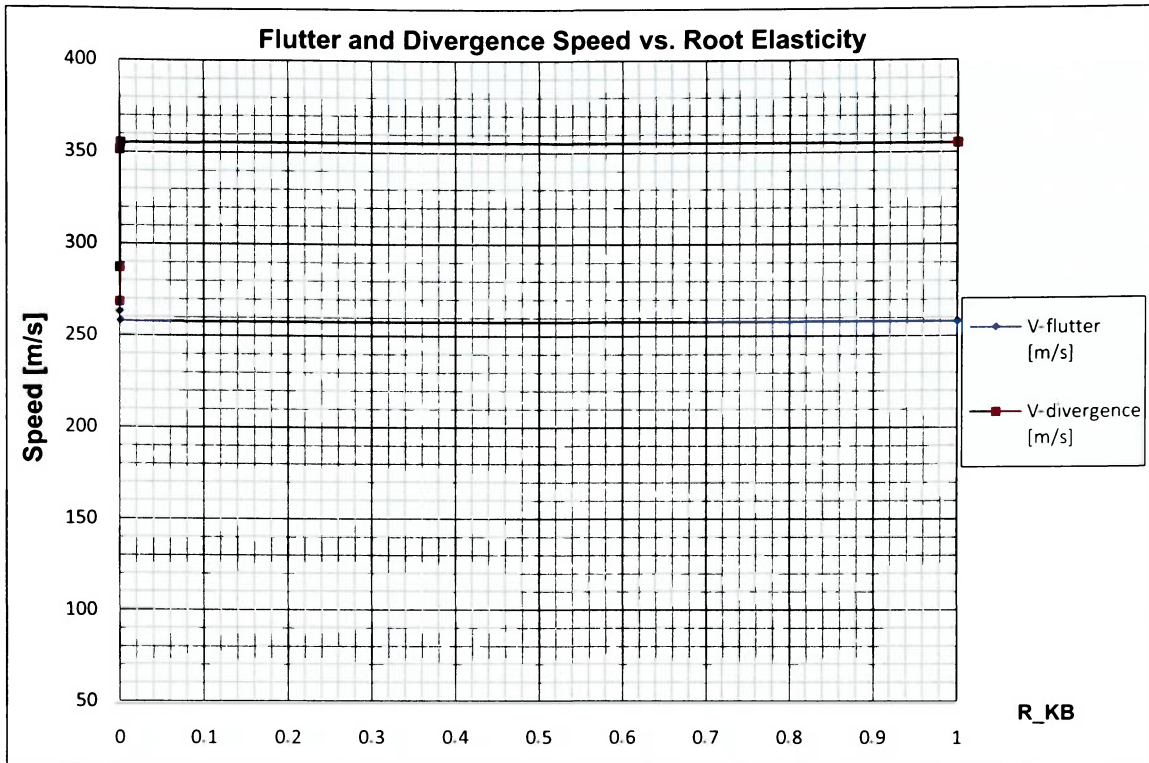


Figure 9.2c: Effect on flutter and divergence speed.

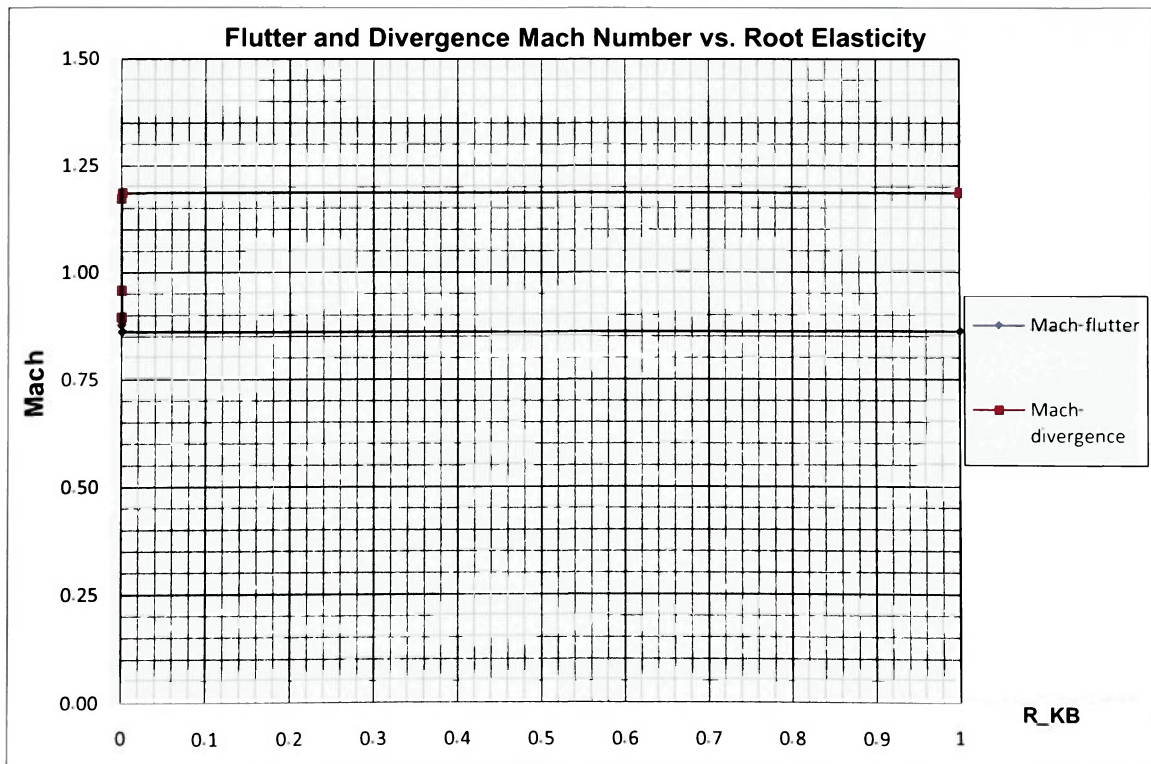


Figure 9.2d: Effect on flutter and divergence Mach number.

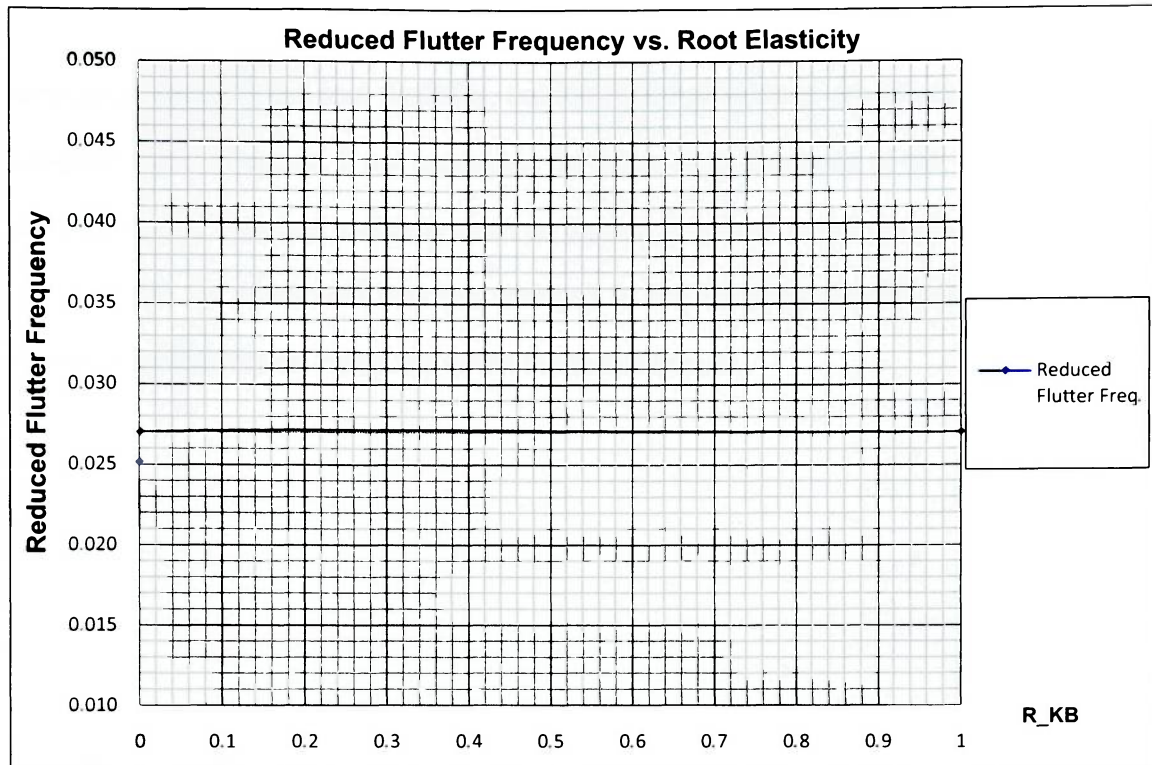


Figure 9.2e: Effect on flutter reduced frequency.

It can be seen from figure 9.2a, that both the flutter frequency and the natural torsion frequency have the same tendency: first they increase when the elasticity ratio for torsion increases at very low ranges, and then remain steady from that point until reaching the unity. This behavior is due to the fact that in order to make significant changes in the fundamental bending frequency, the values of elasticity ratios have to be important, and this means reducing the spring constant almost to a point where the wing changes the root's boundary condition from a clamp to a hinged support. In a case like this, the wing is flutter free, since the very low frequencies of vibration in bending are not important enough to couple the torsion mode to produce the flutter critical point.

The three following three figures, 9.2b, c and d, are related too (they represent true air speed, dynamic pressure and Mach number); there the curves for divergence and flutter are shown, both presenting the same phenomenon explained above when the elastic ratios change. The same happens to the reduced flutter frequency.

Overall, any increase in the elasticity ratio (this is making the connection stiffer) will carry an increase in the root flexibility, but the flutter envelopes are displaced only slightly to higher levels of speed, if not producing no flutter at all (because of the weakness of the bending mode). This fact is clearly seen on figures 8.1a to d, in the results section.

It can be concluded that the changes in the bending elasticity ratios are not as important as the torsion ratios are when the flutter occurs.

9.3. Case III: The Effects of Flight Altitude

The results obtained from Matlab are summarized in the following table:

Table 9.3-1: Case III results

CASE III					
Flight Altitude [m]	0	2500	5000	7500	10000
Parameter					
Bending Frequency [Hz] (R_KB=1)	0.7544	0.7544	0.7544	0.7544	0.7544
Torsion Frequency [Hz] (R_KT=6e-4)	2.7459	2.7459	2.7459	2.7459	2.7459
Frequency Ratio (Torsion/Bending)	3.64	3.64	3.64	3.64	3.64
Flutter Frequency [Hz]	1.3050	1.3063	1.3056	1.3056	1.3062
Flutter Dynamic Pressure-Corr [Pa]	14641.9	14377.3	14170.6	13958.1	13746.5
Flutter Speed-Corr [m/s]	154.6	173.4	196.2	224.0	258.1
Flutter Mach-Corr	0.4544	0.5245	0.6122	0.7221	0.8620
Reduced Flutter Frequency-Corr	0.0451	0.0402	0.0355	0.0311	0.0270
Divergence Dynamic Pressure [Pa]	26023.4	26023.4	26023.4	26023.4	26023.4
Divergence Speed [m/s]	206.1	233.2	265.9	305.8	355.1
Divergence Mach	0.6058	0.7056	0.8297	0.9860	1.1860

In order to better interpret these results, plots of the most important parameters (such as: flutter frequency, flutter dynamic pressure, flutter Mach, etc.) are provided to observe their variation with the flight altitude:

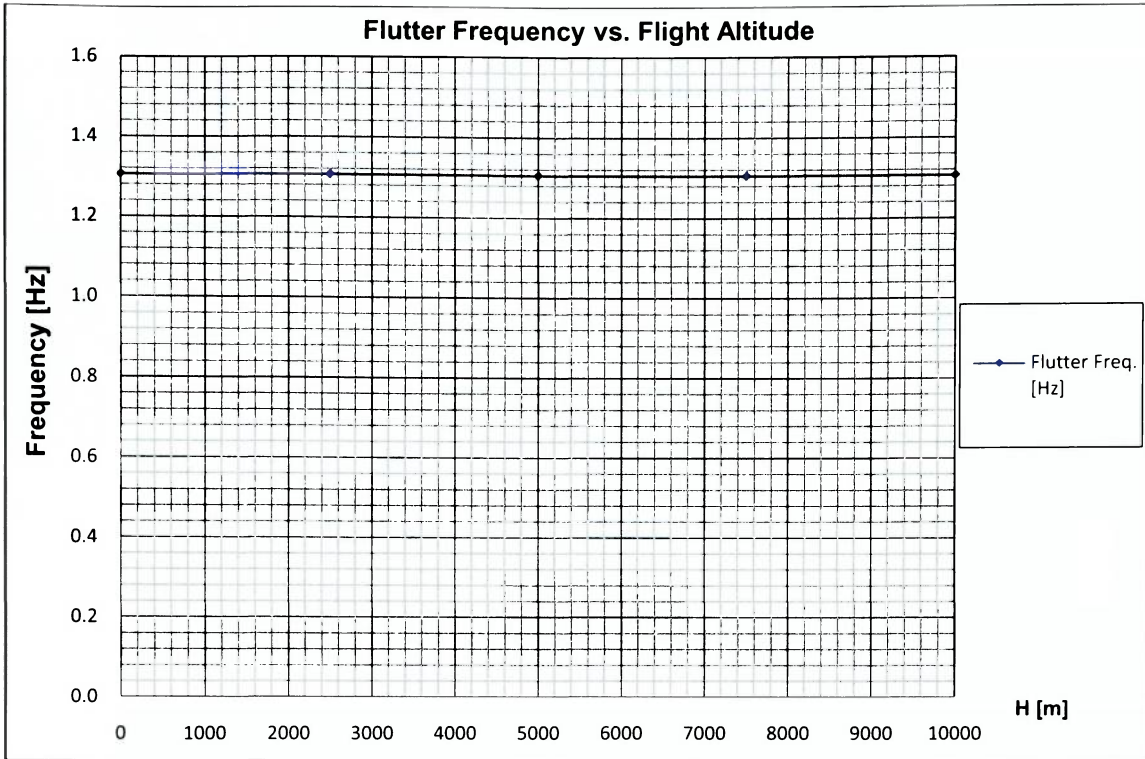


Figure 9.3a: Effect on flutter frequency.

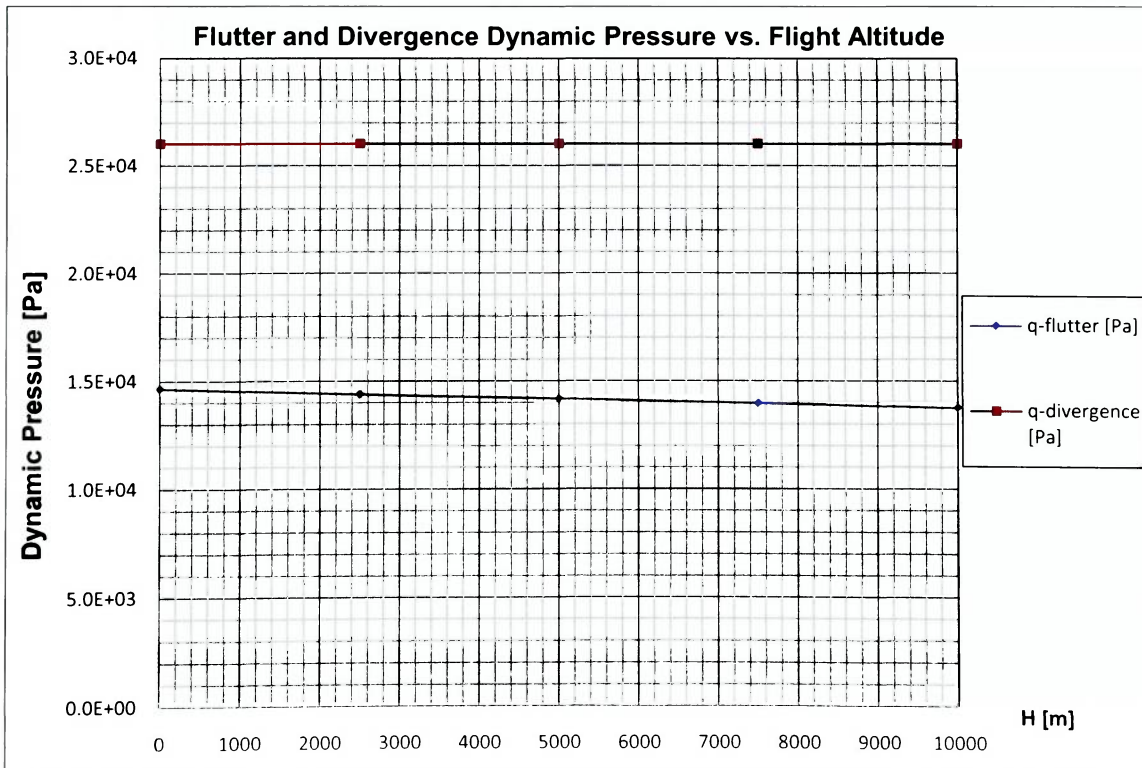


Figure 9.3b: Effect on flutter and divergence dynamic pressure.

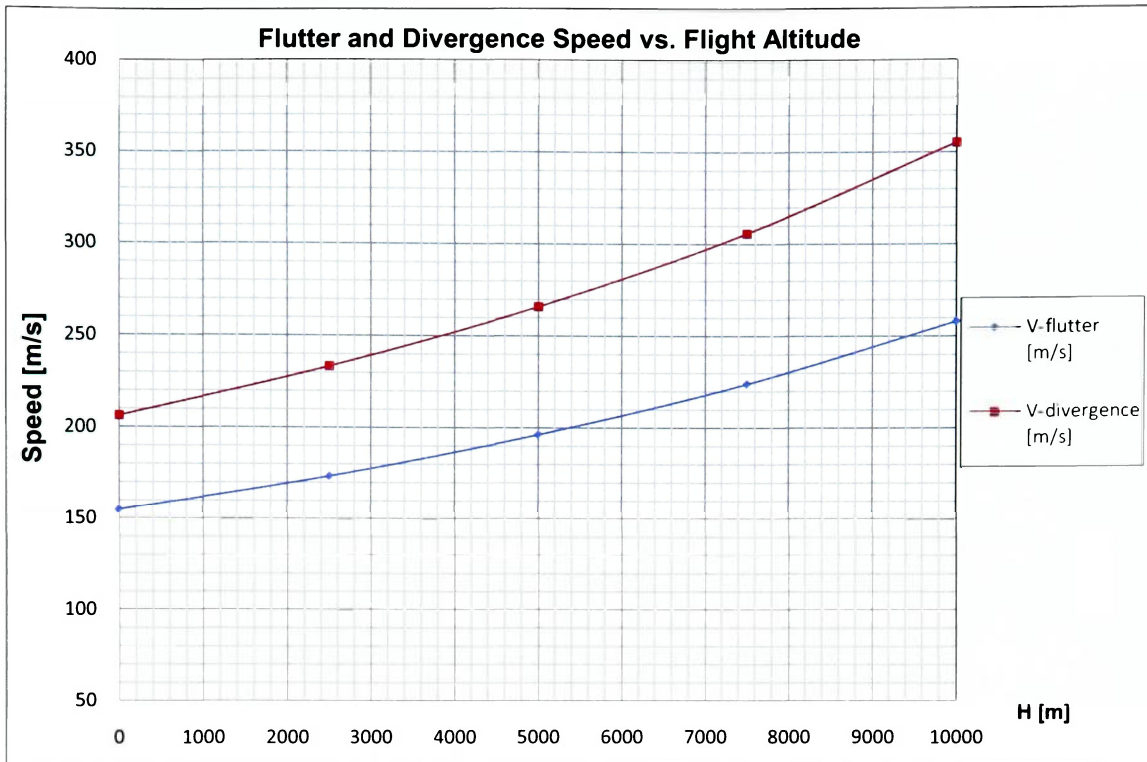


Figure 9.3c: Effect on flutter and divergence speed.

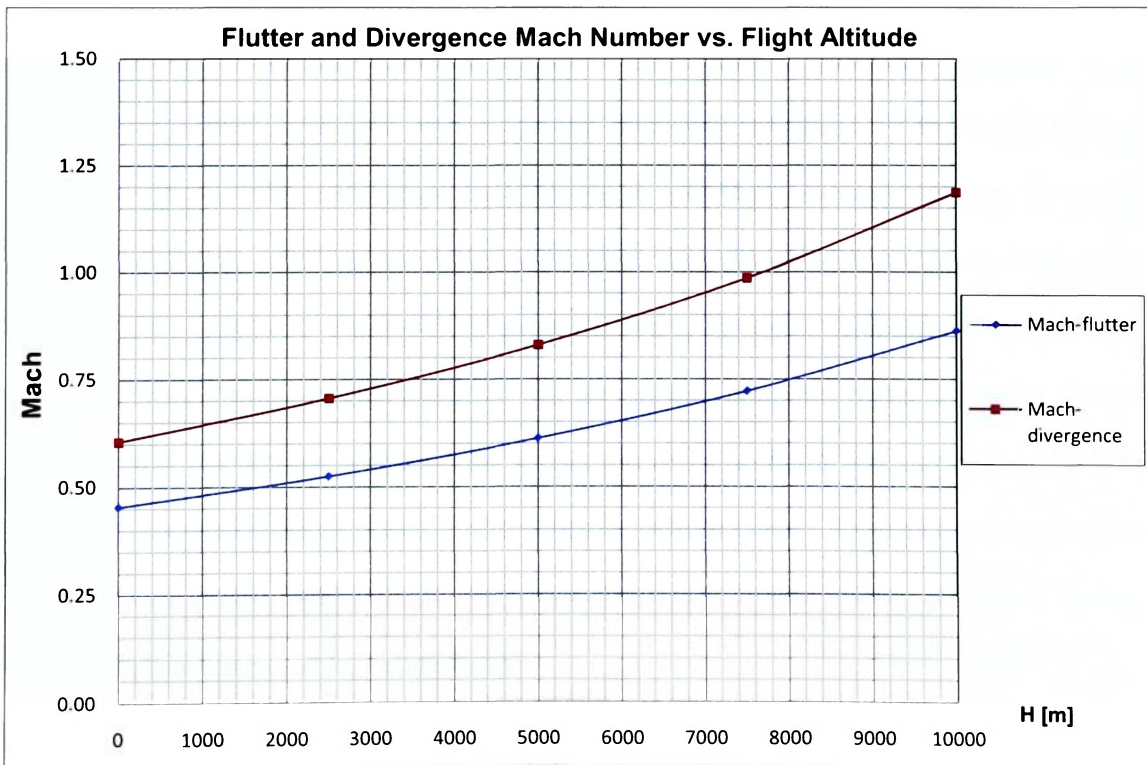


Figure 9.3d: Effect on flutter and divergence Mach number.

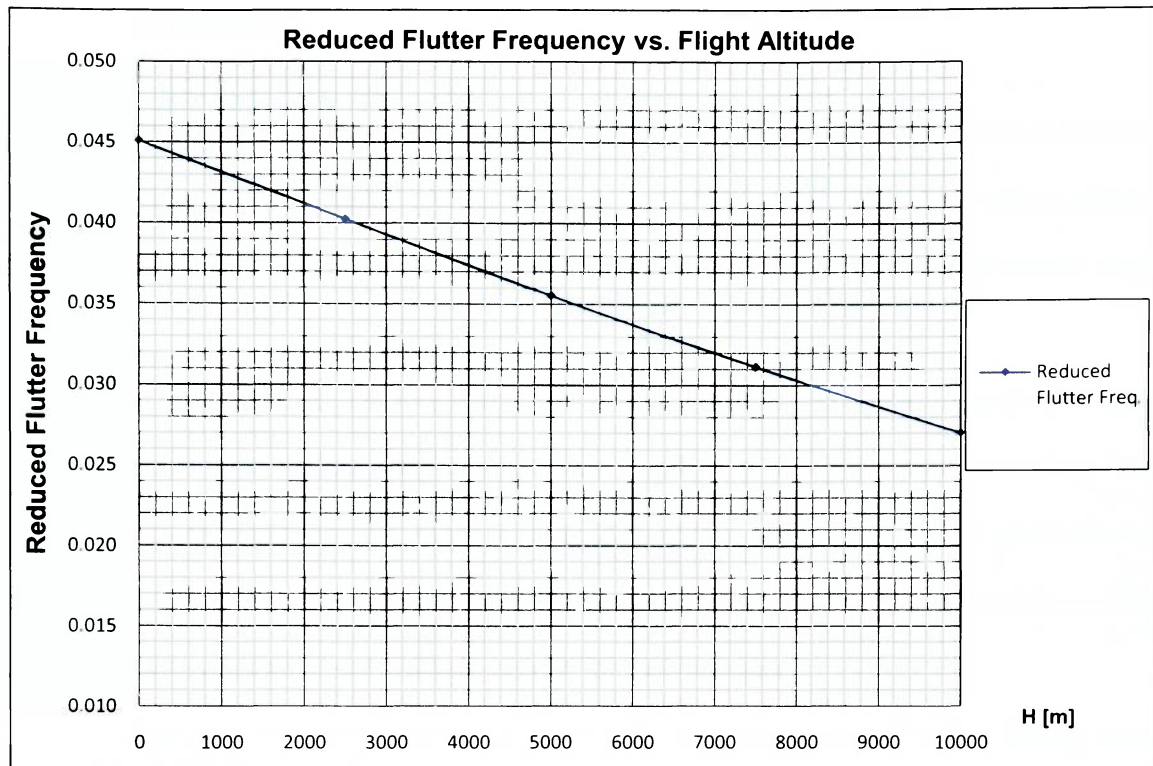


Figure 9.3e: Effect on flutter reduced frequency.

From figure 9.3a it can be seen that the flutter frequency has a linear tendency, at a constant value around 1.305Hz . Figure 9.3b shows a constant behavior of the divergence dynamic pressure, and a linearly decaying tendency for the flutter dynamic pressure. Figures 9.3c and d show that the speed and Mach number increase when flight altitude increases, which is consistent with what was observed from figure 9.3b, for an almost linear variation of the flutter dynamic pressure, the rise in altitude will carry a rise in the associated flutter speeds because the air density changes faster than the dynamic pressure with the altitude. Figure 9.3e shows the reduced flutter frequency, and its linear decay can be explained as it was in the figure 9.1e from Case I. Overall it is observed that the increment in the flight altitude increases the flutter critical speed, therefore, giving a larger flutter free zone at higher altitudes.

10. CONCLUSIONS

Throughout this work there are many details observed and many lessons learned. It is clear now that the flutter phenomenon is not trivial at all, and even when using a simplified approach, the complexity in the procedure and the processing of results might be tedious.

The very first obstacle found was the lack of examples to solve completely a flutter problem, even for a typical wing configuration such as a straight rectangular wing. This was a complete disadvantage, since almost 90% of the papers and books deal with this problem and less than 5% percent have the procedures complete. The other drawback is that many references did not validate results for their models.

Either way, the formulation of such a difficult problem started with a theory using Lagrangian formulations ([1] and [2]) and an old paper (Goland's wing [3]).

It was clear since the very beginning that the results obtained from this problem would be difficult to validate, and the idea of a wind tunnel model came to picture. However, as it was found out later, the wind tunnel model construction proved to be really difficult, and its completion to validate this model was out of the reach of this work. Without this, the theoretical approach employed to study the effects of elastic foundations in the flutter behavior a high-aspect ratio wing with varying properties along the semi-span will remain unconcluded until a wind tunnel model can be properly designed and tested.

The selection of the type of wing to be studied came with the idea to contribute with new data to what has been done so far in the subject, as mentioned previously, most of the examples deal with rectangular straight wings; therefore the choose of a very high-aspect ratio wing with non-constant properties along the semi-span, made out of metal with a particular set of torsion springs at the root would give a valuable piece of information to be considered in future studies.

The use of CATIA, NASTRAN, and Matlab helped to accomplish the goals of this thesis. The wing was first designed in CATIA based on the wing of the Northrop-Grumman RQ-4 Block 20 “*Global Hawk*”; this geometric model was imported from NASTRAN and the cross-section properties were obtained for a determined number of span-wise stations. This information was later introduced in Excel tables where all the cross-section properties (mass and mechanical) were plotted and obtained them as functions of the span-wise coordinate (y-axis), as shown in section 3.

Later the free vibration analysis was carried out in NASTRAN to compute natural frequencies and validate the theoretical models: Rayleigh-Ritz Method (RRM) and Finite Element Method (FEM). As it was proven in section 4.3, where the overall errors were less than 2%, validating the theoretical methods.

At this point, a Matlab code able to calculate the flutter envelope of a clamped wing was ready to be used, therefore validation was necessary. To do so, the Goland's wing [3] was employed by simply changing some data input parameters in the Matlab code; after validation (section 7.2) the error for flutter frequency was less than 7% and less than 3% in the case of flutter speed, demonstrating the accuracy of the code.

Further modifications were made to the code in order to simulate the elasticity in the foundation. The contribution of a pair of torsion springs was added to the FEM models (section 7.1), and their results were once again validated using values to replicate those from an ideal clamp condition (section 7.2), resulting in errors less than 0.4%.

With the Matlab code ready, the analysis was conducted in different steps, to properly account the effects of each of the main parameters to be studied (characterized as cases in section 8). Particularly in Case I the values of the elasticity ratio had to be manipulated in such a way that, for a perfect clamp in the bending mode, would produce flutter (the wing analyzed as perfectly clamped is flutter free). In each case, the elapsed time was about 300 seconds.

After analyzing all the cases, it was observed that the contribution of the torsion mode elasticity is extremely remarkable on the flutter behavior, and even of greater importance than the bending mode elasticity, as it was pointed out in sections 9.1 and 2. Also, the effect of the flight altitude on the flutter limit speed has been proven to be beneficiary, since the increase in the altitude enlarges the flutter free zone (section 9.3).

The work done so far with this project allows the study of basic structural parameters such as the elastic foundation in the dynamic behavior of a wing, but is not limited to it. Besides the elastic foundation or flight altitude, the effect of aspect ratio can also be studied, or the sweep back angle, etc.

The author of this work has some recommendations for future research project: the improvement of the post-processing tools or development of new ones to be coupled to the Matlab code; the improvement of the aerodynamic loading by using in a first stage Lifting Line Method, and later Vortex Lattice Method; improvement of the FEM model; development of a non-stationary model, etc.

Also, it is highly recommended that future students or researchers continue with this line of work and validate the theoretical model with experimental data obtained from wind tunnel testing. That contribution would add the project a very respectable basis to be taken into account as a proper tool to study the elasticity effects on the flutter behavior.

11. REFERENCES

- [1] Sepic Kriskovich H., *"Preliminary Flutter Analysis of Wings Using a Simplified Lagrangian Formulation"*, AE-699, Embry-Riddle Aeronautical University, 2009.
- [2] Dhainaut J., *"Preliminary Conceptual Aeroelastic Design"*, Master's Thesis, Embry-Riddle Aeronautical University, 2000.
- [3] Goland M., *"The Flutter of a Uniform Cantilever Wing"*, Journal of Applied Mechanics, December 1945.
- [4] De Baets P., Battoo R., and Mavris D., *"Aeroelastic Analysis of a Composite Wingbox with Varying Root Flexibility"*, AIAA 2000-1623.
- [5] Dhainaut J., Desmond M., Gangadharan S, and Subramanian C., *"Measuring Aeroelastic Wing Characteristics Using Microsensor Systems (MEMS)"*, AIAA 2007-1266.
- [6] De Marqui Junior C., Rebolho D., Belo E., Marques F., *"Identification of Flutter Parameters for a Wing Model"*, Journal of the Brazilian Society of Mechanical Science and Engineering, July 2006.
- [7] Kuethe A., and Chow C., *"Foundations of Aerodynamics: Bases of Aerodynamic Design"*, 4th Edition, Wiley, 1996.
- [8] Bisplinghoff R., Ashley H., and Halfman R., *"Aeroelasticity"*, 2nd Edition, Addison-Wesley Publishing Company, Inc., November 1957.
- [9] Fung Y., *"An Introduction to the Theory of Aeroelasticity"*, 2nd Edition, Dover Publications, Inc., 1993.
- [10] Scanlan R., and Rosenbaum R., *"Aircraft Vibration and Flutter"*, 2nd Edition, Dover Publications, Inc., 1968.
- [11] Fox R., and McDonald A., *"Introduction to Fluid Mechanics"*, 2nd Edition, John Wiley & Sons, 1978.

[12] Abbot I., and Von Doenhoff A., *"Theory of Wing Sections: Including a Summary of Airfoil Data"*, Dover Publications, Inc., 1959.

[13] Eslami H., *"Finite Element Fundamentals"*, AE-514 Class Notes, Embry-Riddle Aeronautical University, 2007.

[14] www.defense-update.com

[15] www.flighglobal.com

[16] www.northropgrumman.com

[17] www.desktopaero.com/appliaero/appendices/stdatm.html

APPENDIX A

A1. DATA INPUT FILE SAMPLE

```

%*****
%-----DATA INPUT-----
%*****
%=====
%.....MATERIAL.....
%=====
E =7.385e10; % Al 2024 T-351 Young's Modulus [Pa].
G =2.870e10; % Al 2024 T-351 Shear Modulus [Pa].
Rho=2.765e3; % Al 2024 T-351 Material's density [Kg/m^3].
%=====
%.....GEOMETRY.....
%=====
L =6.296; % Semi-span, cantilever wing's length [m].
cr=1.829; % Root's cord [m].
ct=1.829; % Root's cord [m].
%-----
Sweep_ac=0.00; % AC Sweep back angle [degrees].
%-----
c= 1.829; % Chord distribution, [m].
b= 3.109e-1; % Distance from CG to EA, b=(Xcg-Xea) [m].
a= 1.463e-1; % Distance from EA to AC, a=(Xea-Xac) [m].

%=====
%.....CROS SECTIONAL PROPERTIES.....
%=====
EIxx= 1.132e9; % Flexural rigidity about x-axis, EIxx(y) [Pa].
GJ= 1.144e8; % Torsional rigidity, GJ(y) [Pa].
m= 35.7169; % Mass/unit length, m(y) [kg/m].
s= 6.525; % Unbalance mass/unit length, s(y) [Kg].
Iea= 8.643; % Mass moment of inertia about EA/unit length, Iea [Kg*m].
%=====
%.....AERODYNAMICS.....
%=====
CL_airfoil=2*pi; % Airfoil lift coefficient slope
% [1/rad].
CL_a=pi*(AR/(1+sqrt(1+(pi*AR/(CL_airfoil*cos(Delta_ac)))^2))); % Wing's
% lift coefficient.

```

A2. STUDY CASES PROGRAM OUTPUT

Case I: Effects of Elastic Foundation in Torsion

-----Program Output-----

Uncoupled Bending Frequency: $\Omega_h = 0.754437$ Hz

Uncoupled Torsion Frequency: $\Omega_a = 1.59171$ Hz

Fundamental Frequencies Ratio: Ratio = 0.473979

Current Flight Altitude: $H = 10000$ m

-----Divergence Output-----

Divergence @ $Q = 9440.86$ Pa

Divergence @ $V = 213.901$ m/s

Divergence @ $V = 770.043$ Km/h

Divergence @ KTAS = 416.24

Divergence @ Mach = 0.714353

-----Flutter Output-----

Flutter @ $Q = 2833.74$ Pa

Flutter @ $V = 117.189$ m/s

Flutter @ $V = 421.88$ Km/h

Flutter @ KTAS = 228.043

Flutter @ Mach = 0.391369

Flutter Frequency: $\Omega_{fl} = 1.02306$ Hz

Reduced Flutter Frequency (Strouhal): Str = 0.0466245

-----Data Corrected for Compressibility Effects by Theodorsen-----

Theodorsen X-factor (Equivalent Strouhal): $X_f = 0.119613$

Theodorsen Compressibility Correction Factor: $K_f = 1.07482$

Corrected Flutter Speed is: $V_{fl_corr} = 125.958$ m/s

Corrected Flutter Speed is: $V_{fl_corr} = 453.448$ Km/h

Corrected Flutter Speed is: KTAS_{corr} = 245.107

Corrected Flutter Speed is: $M_{corr} = 0.420653$

Corrected Flutter Dynamic Pressure is: $Q_{corr} = 3273.67$ Pa

Corrected Reduced Flutter Frequency (Strouhal): Str_{corr} = 0.0433787

-----Program Output-----

Uncoupled Bending Frequency: $\Omega_h = 0.754437$ Hz

Uncoupled Torsion Frequency: $\Omega_a = 1.94748$ Hz

Fundamental Frequencies Ratio: Ratio = 0.38739

Current Flight Altitude: $H = 10000$ m

-----Divergence Output-----

Divergence @ $Q = 13821.7$ Pa

Divergence @ $V = 258.814$ m/s

Divergence @ $V = 931.729$ Km/h

Divergence @ KTAS = 503.637

Divergence @ Mach = 0.864345

-----Flutter Output-----

Flutter @ $Q = 5146.18$ Pa

Flutter @ $V = 157.924$ m/s

Flutter @ $V = 568.528$ Km/h

Flutter @ KTAS = 307.312

Flutter @ Mach = 0.527411

Flutter Frequency: $\Omega_{fl} = 1.11351$ Hz

Reduced Flutter Frequency (Strouhal): $Str = 0.0376567$

-----Data Corrected for Compressibility Effects by Theodorsen-----

Theodorsen X-factor (Equivalent Strouhal): $X_f = 0.0966068$

Theodorsen Compressibility Correction Factor: $K_f = 1.06077$

Corrected Flutter Speed is: $V_{fl_corr} = 167.522$ m/s

Corrected Flutter Speed is: $V_{fl_corr} = 603.08$ Km/h

Corrected Flutter Speed is: $KTAS_{corr} = 325.989$

Corrected Flutter Speed is: $M_{corr} = 0.559464$

Corrected Flutter Dynamic Pressure is: $Q_{corr} = 5790.7$ Pa

Corrected Reduced Flutter Frequency (Strouhal): $Str_{corr} = 0.0354993$

-----Program Output-----

Uncoupled Bending Frequency: $\Omega_h = 0.754437$ Hz

Uncoupled Torsion Frequency: $\Omega_a = 2.24651$ Hz

Fundamental Frequencies Ratio: Ratio = 0.335826

Current Flight Altitude: $H = 10000$ m

-----Divergence Output-----

Divergence @ $Q = 18029$ Pa

Divergence @ $V = 295.592$ m/s

Divergence @ $V = 1064.13$ Km/h

Divergence @ KTAS = 575.207

Divergence @ Mach = 0.987172

-----Flutter Output-----

Flutter @ $Q = 7578.92$ Pa

Flutter @ $V = 191.651$ m/s

Flutter @ $V = 689.943$ Km/h

Flutter @ KTAS = 372.942

Flutter @ Mach = 0.640045

Flutter Frequency: $\Omega_{fl} = 1.18625$ Hz

Reduced Flutter Frequency (Strouhal): $Str = 0.0330571$

-----Data Corrected for Compressibility Effects by Theodorsen-----

Theodorsen X-factor (Equivalent Strouhal): $X_f = 0.0848066$

Theodorsen Compressibility Correction Factor: $K_f = 1.05334$

Corrected Flutter Speed is: $V_{fl_corr} = 201.874$ m/s

Corrected Flutter Speed is: $V_{fl_corr} = 726.746$ Km/h

Corrected Flutter Speed is: $KTAS_{corr} = 392.835$

Corrected Flutter Speed is: $M_{corr} = 0.674186$

Corrected Flutter Dynamic Pressure is: $Q_{corr} = 8409.04$ Pa

Corrected Reduced Flutter Frequency (Strouhal): $Str_{corr} = 0.0313831$

-----Program Output-----

Uncoupled Bending Frequency: $\Omega_h = 0.754437$ Hz

Uncoupled Torsion Frequency: $\Omega_a = 2.50916$ Hz

Fundamental Frequencies Ratio: Ratio = 0.300673

Current Flight Altitude: H = 10000 m

-----Divergence Output-----

Divergence @ Q = 22089.5 Pa

Divergence @ V = 327.19 m/s

Divergence @ V = 1177.88 Km/h

Divergence @ KTAS = 636.694

Divergence @ Mach = 1.0927

-----Flutter Output-----

Flutter @ Q = 10065.1 Pa

Flutter @ V = 220.86 m/s

Flutter @ V = 795.095 Km/h

Flutter @ KTAS = 429.781

Flutter @ Mach = 0.737592

Flutter Frequency: $\Omega_{fl} = 1.24935$ Hz

Reduced Flutter Frequency (Strouhal): Str = 0.0302112

-----Data Corrected for Compressibility Effects by Theodorsen-----

Theodorsen X-factor (Equivalent Strouhal): $X_f = 0.0775055$

Theodorsen Compressibility Correction Factor: $K_f = 1.04867$

Corrected Flutter Speed is: $V_{fl_corr} = 231.608$ m/s

Corrected Flutter Speed is: $V_{fl_corr} = 833.789$ Km/h

Corrected Flutter Speed is: $KTAS_{corr} = 450.697$

Corrected Flutter Speed is: $M_{corr} = 0.773488$

Corrected Flutter Dynamic Pressure is: $Q_{corr} = 11068.6$ Pa

Corrected Reduced Flutter Frequency (Strouhal): $Str_{corr} = 0.0288091$

-----Program Output-----

Uncoupled Bending Frequency: $\Omega_h = 0.754437$ Hz

Uncoupled Torsion Frequency: $\Omega_a = 2.74589$ Hz

Fundamental Frequencies Ratio: Ratio = 0.274751

Current Flight Altitude: $H = 10000$ m

-----Divergence Output-----

Divergence @ $Q = 26023.4$ Pa

Divergence @ $V = 355.131$ m/s

Divergence @ $V = 1278.47$ Km/h

Divergence @ KTAS = 691.066

Divergence @ Mach = 1.18601

-----Flutter Output-----

Flutter @ $Q = 12578.1$ Pa

Flutter @ $V = 246.896$ m/s

Flutter @ $V = 888.825$ Km/h

Flutter @ KTAS = 480.446

Flutter @ Mach = 0.824544

Flutter Frequency: $\Omega_{fl} = 1.30618$ Hz

Reduced Flutter Frequency (Strouhal): $Str = 0.0282544$

-----Data Corrected for Compressibility Effects by Theodorsen-----

Theodorsen X-factor (Equivalent Strouhal): $X_f = 0.0724856$

Theodorsen Compressibility Correction Factor: $K_f = 1.04542$

Corrected Flutter Speed is: $V_{fl_corr} = 258.109$ m/s

Corrected Flutter Speed is: $V_{fl_corr} = 929.192$ Km/h

Corrected Flutter Speed is: $KTAS_{corr} = 502.266$

Corrected Flutter Speed is: $M_{corr} = 0.861991$

Corrected Flutter Dynamic Pressure is: $Q_{corr} = 13746.5$ Pa

Corrected Reduced Flutter Frequency (Strouhal): $Str_{corr} = 0.027027$

Elapsed time is 308.616063 seconds.

Case II: Effects of Elastic Foundation in Bending

-----Program Output-----

Uncoupled Bending Frequency: $\Omega_h = 0.0146704$ Hz
Uncoupled Torsion Frequency: $\Omega_a = 2.74589$ Hz
Fundamental Frequencies Ratio: Ratio = 0.00534269
Current Flight Altitude: $H = 10000$ m

-----Divergence Output-----

Divergence @ $Q = 14860.3$ Pa
Divergence @ $V = 268.361$ m/s
Divergence @ $V = 966.101$ Km/h
Divergence @ KTAS = 522.217
Divergence @ Mach = 0.896231

-----Program Output-----

Uncoupled Bending Frequency: $\Omega_h = 0.144289$ Hz
Uncoupled Torsion Frequency: $\Omega_a = 2.74589$ Hz
Fundamental Frequencies Ratio: Ratio = 0.0525472
Current Flight Altitude: $H = 10000$ m

-----Divergence Output-----

Divergence @ $Q = 17009.2$ Pa
Divergence @ $V = 287.11$ m/s
Divergence @ $V = 1033.6$ Km/h
Divergence @ KTAS = 558.7
Divergence @ Mach = 0.958844

Note: the previous two sub-cases did not experience flutter.

```

*****
-----Program Output-----
Uncoupled Bending Frequency: Omega_h = 0.677056 Hz
Uncoupled Torsion Frequency: Omega_a = 2.74589 Hz
Fundamental Frequencies Ratio: Ratio = 0.246571
Current Flight Altitude:      H = 10000 m
-----Divergence Output-----
Divergence @   Q = 25463 Pa
Divergence @   V = 351.287 m/s
Divergence @   V = 1264.63 Km/h
Divergence @ KTAS = 683.585
Divergence @ Mach = 1.17317
-----Flutter Output-----
Flutter @   Q = 13152.8 Pa
Flutter @   V = 252.474 m/s
Flutter @   V = 908.906 Km/h
Flutter @ KTAS = 491.301
Flutter @ Mach = 0.843173
Flutter Frequency:      Omega_fl = 1.23897 Hz
Reduced Flutter Frequency (Strouhal): Str = 0.0262086
-----Data Corrected for Compressibility Effects by Theodorsen-----
Theodorsen X-factor (Equivalent Strouhal): X_f = 0.0672369
Theodorsen Compressibility Correction Factor: K_f = 1.04199
Corrected Flutter Speed is: V_fl_corr = 263.075 m/s
Corrected Flutter Speed is: V_fl_corr = 947.068 Km/h
Corrected Flutter Speed is: KTAS_corr = 511.929
Corrected Flutter Speed is: M_corr = 0.878575
Corrected Flutter Dynamic Pressure is:      Q_corr = 14280.5 Pa
Corrected Reduced Flutter Frequency (Strouhal): Str_corr = 0.0251525
*****

```

-----Program Output-----

Uncoupled Bending Frequency: $\Omega_h = 0.754438$ Hz

Uncoupled Torsion Frequency: $\Omega_a = 2.74589$ Hz

Fundamental Frequencies Ratio: Ratio = 0.274752

Current Flight Altitude: $H = 10000$ m

-----Divergence Output-----

Divergence @ $Q = 26023.4$ Pa

Divergence @ $V = 355.131$ m/s

Divergence @ $V = 1278.47$ Km/h

Divergence @ KTAS = 691.066

Divergence @ Mach = 1.18601

-----Flutter Output-----

Flutter @ $Q = 12578.1$ Pa

Flutter @ $V = 246.896$ m/s

Flutter @ $V = 888.825$ Km/h

Flutter @ KTAS = 480.446

Flutter @ Mach = 0.824544

Flutter Frequency: $\Omega_{fl} = 1.30618$ Hz

Reduced Flutter Frequency (Strouhal): $Str = 0.0282545$

-----Data Corrected for Compressibility Effects by Theodorsen-----

Theodorsen X-factor (Equivalent Strouhal): $X_f = 0.0724856$

Theodorsen Compressibility Correction Factor: $K_f = 1.04542$

Corrected Flutter Speed is: $V_{fl_corr} = 258.109$ m/s

Corrected Flutter Speed is: $V_{fl_corr} = 929.192$ Km/h

Corrected Flutter Speed is: $KTAS_{corr} = 502.266$

Corrected Flutter Speed is: $M_{corr} = 0.861991$

Corrected Flutter Dynamic Pressure is: $Q_{corr} = 13746.5$ Pa

Corrected Reduced Flutter Frequency (Strouhal): $Str_{corr} = 0.027027$

-----Program Output-----

Uncoupled Bending Frequency: $\Omega_h = 0.754437$ Hz

Uncoupled Torsion Frequency: $\Omega_a = 2.74589$ Hz

Fundamental Frequencies Ratio: Ratio = 0.274751

Current Flight Altitude: $H = 10000$ m

-----Divergence Output-----

Divergence @ $Q = 26023.4$ Pa

Divergence @ $V = 355.131$ m/s

Divergence @ $V = 1278.47$ Km/h

Divergence @ KTAS = 691.066

Divergence @ Mach = 1.18601

-----Flutter Output-----

Flutter @ $Q = 12578.1$ Pa

Flutter @ $V = 246.896$ m/s

Flutter @ $V = 888.825$ Km/h

Flutter @ KTAS = 480.446

Flutter @ Mach = 0.824544

Flutter Frequency: $\Omega_{fl} = 1.30618$ Hz

Reduced Flutter Frequency (Strouhal): $Str = 0.0282544$

-----Data Corrected for Compressibility Effects by Theodorsen-----

Theodorsen X-factor (Equivalent Strouhal): $X_f = 0.0724856$

Theodorsen Compressibility Correction Factor: $K_f = 1.04542$

Corrected Flutter Speed is: $V_{fl_corr} = 258.109$ m/s

Corrected Flutter Speed is: $V_{fl_corr} = 929.192$ Km/h

Corrected Flutter Speed is: $KTAS_{corr} = 502.266$

Corrected Flutter Speed is: $M_{corr} = 0.861991$

Corrected Flutter Dynamic Pressure is: $Q_{corr} = 13746.5$ Pa

Corrected Reduced Flutter Frequency (Strouhal): $Str_{corr} = 0.027027$

Elapsed time is 315.404327 seconds.

Case III: Effects of Flight Altitude

-----Program Output-----

Uncoupled Bending Frequency: $\Omega_h = 0.754437$ Hz

Uncoupled Torsion Frequency: $\Omega_a = 2.74589$ Hz

Fundamental Frequencies Ratio: Ratio = 0.274751

Current Flight Altitude: $H = 0$ m

-----Divergence Output-----

Divergence @ $Q = 26023.4$ Pa

Divergence @ $V = 206.124$ m/s

Divergence @ $V = 742.047$ Km/h

Divergence @ KTAS = 401.107

Divergence @ Mach = 0.605785

-----Flutter Output-----

Flutter @ $Q = 12603.8$ Pa

Flutter @ $V = 143.449$ m/s

Flutter @ $V = 516.416$ Km/h

Flutter @ KTAS = 279.144

Flutter @ Mach = 0.421586

Flutter Frequency: $\Omega_{fl} = 1.30502$ Hz

Reduced Flutter Frequency (Strouhal): $Str = 0.0485869$

-----Data Corrected for Compressibility Effects by Theodorsen-----

Theodorsen X-factor (Equivalent Strouhal): $X_f = 0.124648$

Theodorsen Compressibility Correction Factor: $K_f = 1.07782$

Corrected Flutter Speed is: $V_{fl_corr} = 154.613$ m/s

Corrected Flutter Speed is: $V_{fl_corr} = 556.606$ Km/h

Corrected Flutter Speed is: $KTAS_{corr} = 300.868$

Corrected Flutter Speed is: $M_{corr} = 0.454396$

Corrected Flutter Dynamic Pressure is: $Q_{corr} = 14641.9$ Pa

Corrected Reduced Flutter Frequency (Strouhal): $Str_{corr} = 0.0450787$

-----Program Output-----

Uncoupled Bending Frequency: $\Omega_h = 0.754437$ Hz

Uncoupled Torsion Frequency: $\Omega_a = 2.74589$ Hz

Fundamental Frequencies Ratio: Ratio = 0.274751

Current Flight Altitude: H = 2500 m

-----Divergence Output-----

Divergence @ Q = 26023.4 Pa

Divergence @ V = 233.225 m/s

Divergence @ V = 839.612 Km/h

Divergence @ KTAS = 453.844

Divergence @ Mach = 0.705618

-----Flutter Output-----

Flutter @ Q = 12575 Pa

Flutter @ V = 162.124 m/s

Flutter @ V = 583.646 Km/h

Flutter @ KTAS = 315.484

Flutter @ Mach = 0.490502

Flutter Frequency: $\Omega_{fl} = 1.30632$ Hz

Reduced Flutter Frequency (Strouhal): Str = 0.0430328

-----Data Corrected for Compressibility Effects by Theodorsen-----

Theodorsen X-factor (Equivalent Strouhal): $X_f = 0.110399$

Theodorsen Compressibility Correction Factor: $K_f = 1.06927$

Corrected Flutter Speed is: $V_{fl_corr} = 173.354$ m/s

Corrected Flutter Speed is: $V_{fl_corr} = 624.073$ Km/h

Corrected Flutter Speed is: $KTAS_{corr} = 337.337$

Corrected Flutter Speed is: $M_{corr} = 0.524477$

Corrected Flutter Dynamic Pressure is: $Q_{corr} = 14377.3$ Pa

Corrected Reduced Flutter Frequency (Strouhal): $Str_{corr} = 0.0402452$

```

*****
-----Program Output-----
Uncoupled Bending Frequency: Omega_h = 0.754437 Hz
Uncoupled Torsion Frequency: Omega_a = 2.74589 Hz
Fundamental Frequencies Ratio: Ratio = 0.274751
Current Flight Altitude:      H = 5000 m
-----Divergence Output-----
Divergence @   Q = 26023.4 Pa
Divergence @   V = 265.907 m/s
Divergence @   V = 957.265 Km/h
Divergence @ KTAS = 517.441
Divergence @ Mach = 0.82967
-----Flutter Output-----
Flutter @   Q = 12591.9 Pa
Flutter @   V = 184.967 m/s
Flutter @   V = 665.881 Km/h
Flutter @ KTAS = 359.935
Flutter @ Mach = 0.577124
Flutter Frequency:      Omega_fl = 1.30555 Hz
Reduced Flutter Frequency (Strouhal): Str = 0.0376964
-----Data Corrected for Compressibility Effects by Theodorsen-----
Theodorsen X-factor (Equivalent Strouhal): X_f = 0.0967084
Theodorsen Compressibility Correction Factor: K_f = 1.06084
Corrected Flutter Speed is: V_fl_corr = 196.22 m/s
Corrected Flutter Speed is: V_fl_corr = 706.391 Km/h
Corrected Flutter Speed is: KTAS_corr = 381.833
Corrected Flutter Speed is:  M_corr = 0.612235
Corrected Flutter Dynamic Pressure is:      Q_corr = 14170.6 Pa
Corrected Reduced Flutter Frequency (Strouhal): Str_corr = 0.0355345
*****

```

-----Program Output-----

Uncoupled Bending Frequency: $\Omega_h = 0.754437$ Hz

Uncoupled Torsion Frequency: $\Omega_a = 2.74589$ Hz

Fundamental Frequencies Ratio: Ratio = 0.274751

Current Flight Altitude: $H = 7500$ m

-----Divergence Output-----

Divergence @ $Q = 26023.4$ Pa

Divergence @ $V = 305.791$ m/s

Divergence @ $V = 1100.85$ Km/h

Divergence @ KTAS = 595.054

Divergence @ Mach = 0.985965

-----Flutter Output-----

Flutter @ $Q = 12591$ Pa

Flutter @ $V = 212.703$ m/s

Flutter @ $V = 765.73$ Km/h

Flutter @ KTAS = 413.908

Flutter @ Mach = 0.685819

Flutter Frequency: $\Omega_{fl} = 1.3056$ Hz

Reduced Flutter Frequency (Strouhal): $Str = 0.0327819$

-----Data Corrected for Compressibility Effects by Theodorsen-----

Theodorsen X-factor (Equivalent Strouhal): $X_f = 0.0841006$

Theodorsen Compressibility Correction Factor: $K_f = 1.05289$

Corrected Flutter Speed is: $V_{fl_corr} = 223.953$ m/s

Corrected Flutter Speed is: $V_{fl_corr} = 806.231$ Km/h

Corrected Flutter Speed is: $KTAS_{corr} = 435.801$

Corrected Flutter Speed is: $M_{corr} = 0.722093$

Corrected Flutter Dynamic Pressure is: $Q_{corr} = 13958.1$ Pa

Corrected Reduced Flutter Frequency (Strouhal): $Str_{corr} = 0.0311351$

-----Program Output-----

Uncoupled Bending Frequency: $\Omega_h = 0.754437$ Hz

Uncoupled Torsion Frequency: $\Omega_a = 2.74589$ Hz

Fundamental Frequencies Ratio: Ratio = 0.274751

Current Flight Altitude: $H = 10000$ m

-----Divergence Output-----

Divergence @ $Q = 26023.4$ Pa

Divergence @ $V = 355.131$ m/s

Divergence @ $V = 1278.47$ Km/h

Divergence @ KTAS = 691.066

Divergence @ Mach = 1.18601

-----Flutter Output-----

Flutter @ $Q = 12578.1$ Pa

Flutter @ $V = 246.896$ m/s

Flutter @ $V = 888.825$ Km/h

Flutter @ KTAS = 480.446

Flutter @ Mach = 0.824544

Flutter Frequency: $\Omega_{fl} = 1.30618$ Hz

Reduced Flutter Frequency (Strouhal): $Str = 0.0282544$

-----Data Corrected for Compressibility Effects by Theodorsen-----

Theodorsen X-factor (Equivalent Strouhal): $X_f = 0.0724856$

Theodorsen Compressibility Correction Factor: $K_f = 1.04542$

Corrected Flutter Speed is: $V_{fl_corr} = 258.109$ m/s

Corrected Flutter Speed is: $V_{fl_corr} = 929.192$ Km/h

Corrected Flutter Speed is: $KTAS_{corr} = 502.266$

Corrected Flutter Speed is: $M_{corr} = 0.861991$

Corrected Flutter Dynamic Pressure is: $Q_{corr} = 13746.5$ Pa

Corrected Reduced Flutter Frequency (Strouhal): $Str_{corr} = 0.027027$

Elapsed time is 315.055754 seconds.

A3. VALIDATION OF FREE VIBRATION MODEL OUTPUT

The fundamental natural frequency output from the program subroutines RRM_BF and RRM_TF is presented below (b1 denotes bending; t1 denotes torsion, all values in Hz):

Omega_b1 =

0.7623

ans =

0.7623

Omega_t1 =

19.2660

ans =

19.2660

The fundamental natural frequency output from the program subroutines FEM_BF and FEM_TF is shown below (all values in Hz):

Uncoupled Bending Frequency: Omega_h = 0.757337 Hz

ans =

0.7573

Uncoupled Torsion Frequency: Omega_a = 18.9757 Hz

ans =

18.9757

The fundamental natural frequency output from NASTRAN is detailed below (the torsion frequency represents an approximation given by NASTRAN):

Bending: *Omega_b = 0.7488739 Hz*

Torsion: *Omega_t = 19.29904 Hz*

The following figures have been taken from NASTRAN windows:

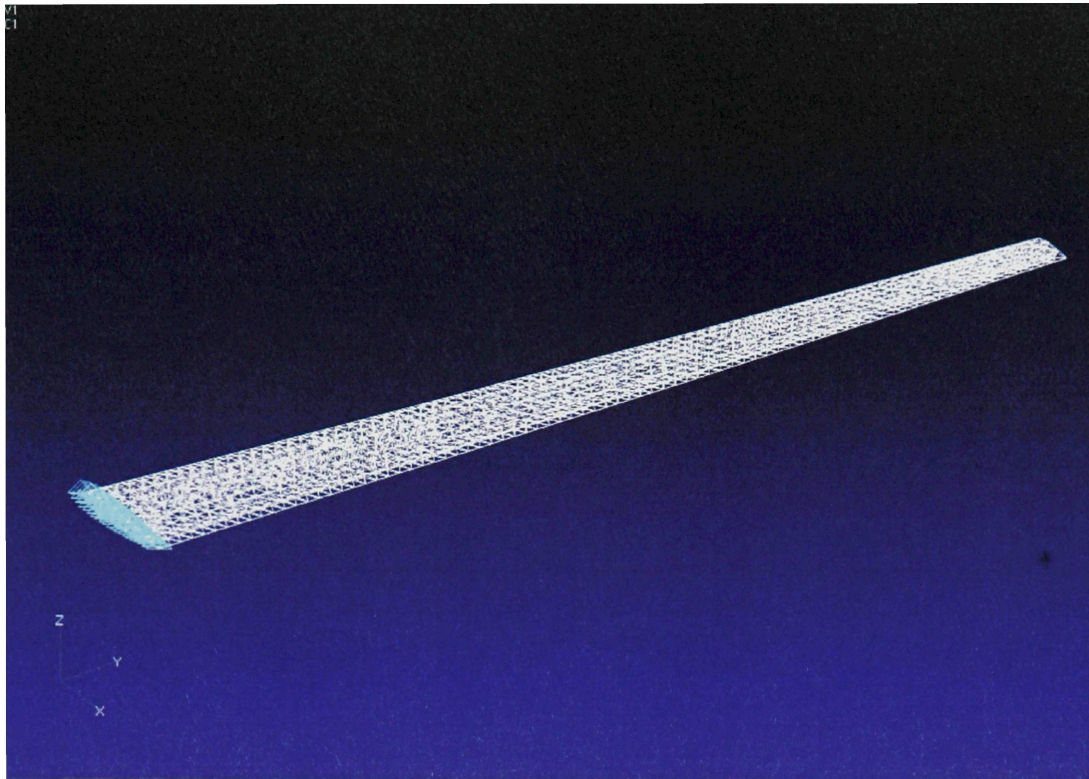


Figure A.3a: NASTRAN model already meshed and constrained.

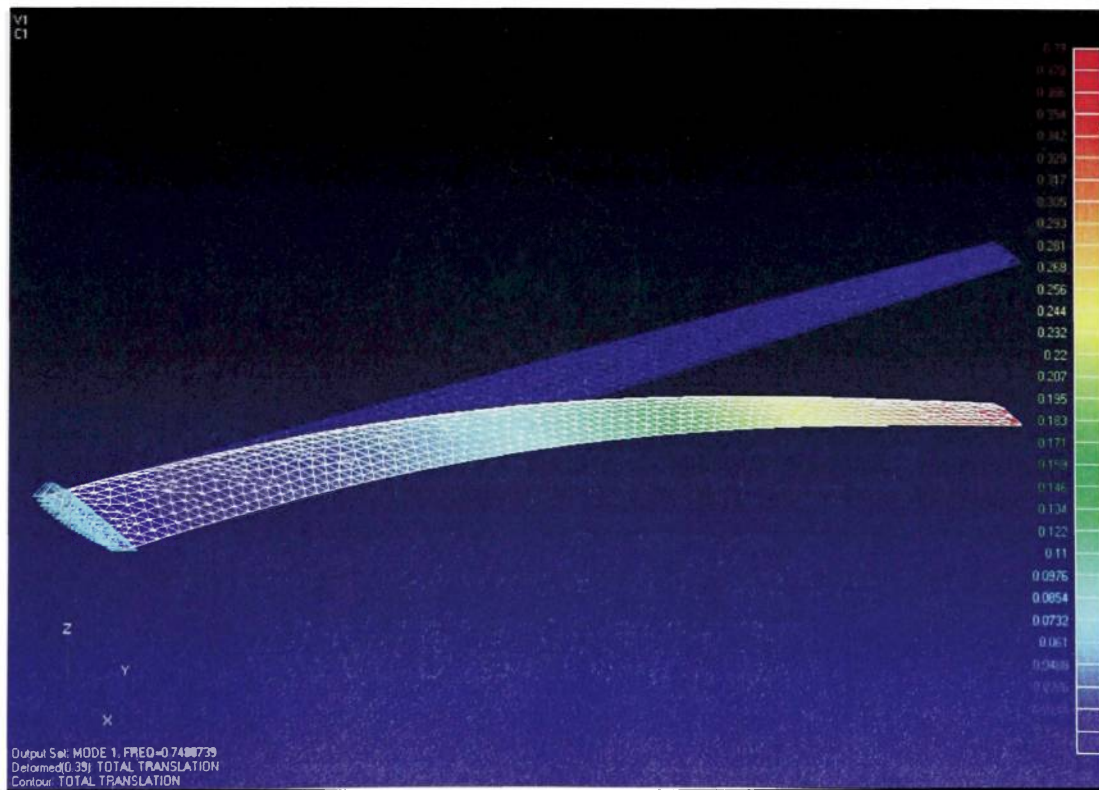


Figure A.3b: NASTRAN model first vibration mode (pure bending).

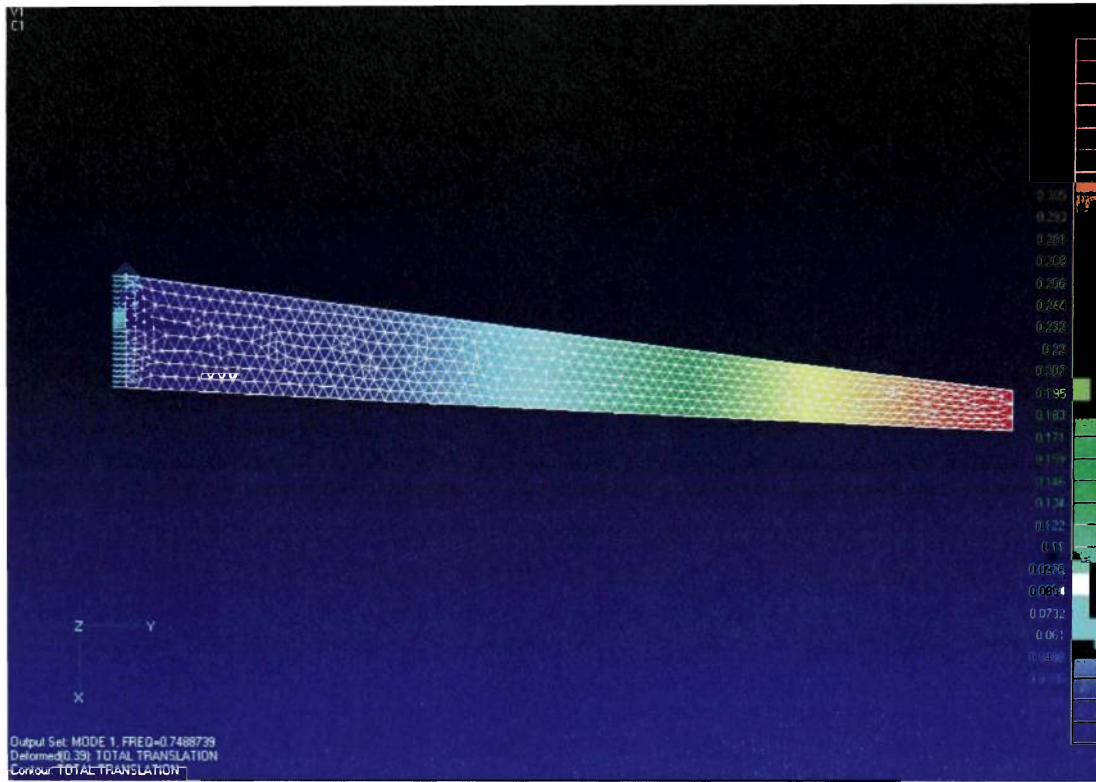


Figure A.3c: NASTRAN model first vibration mode (top view).

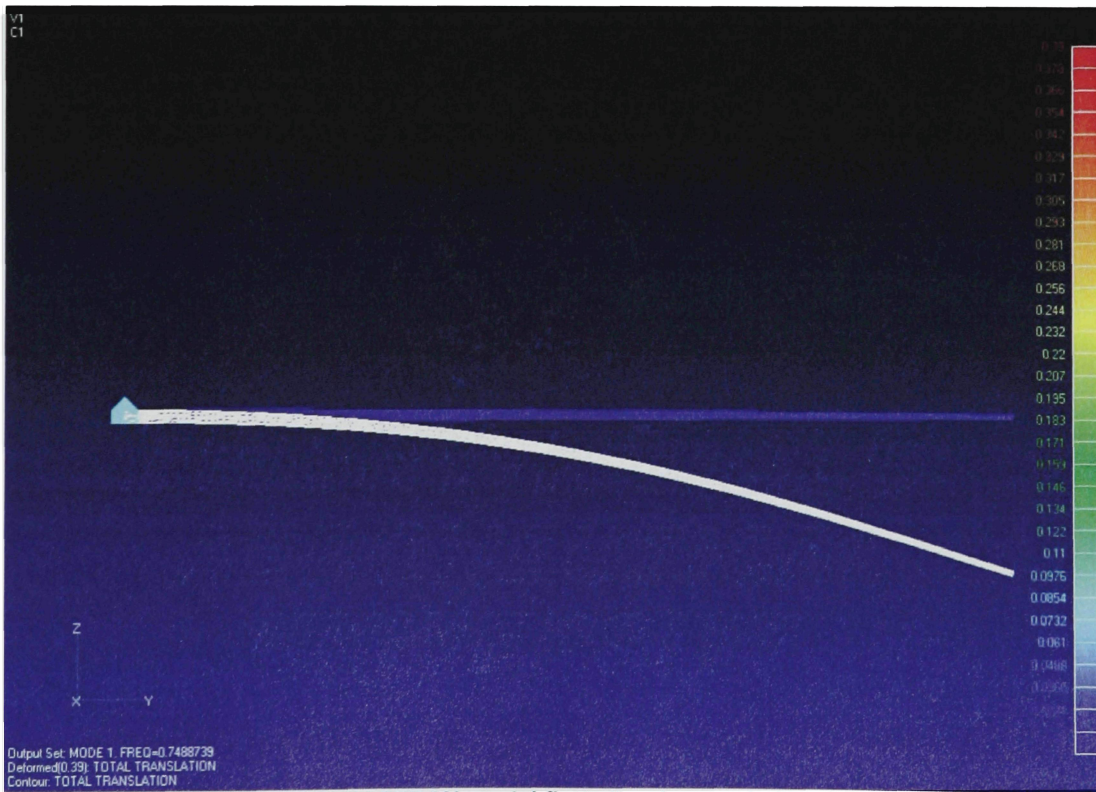


Figure A.3d: NASTRAN model first vibration mode (front view).

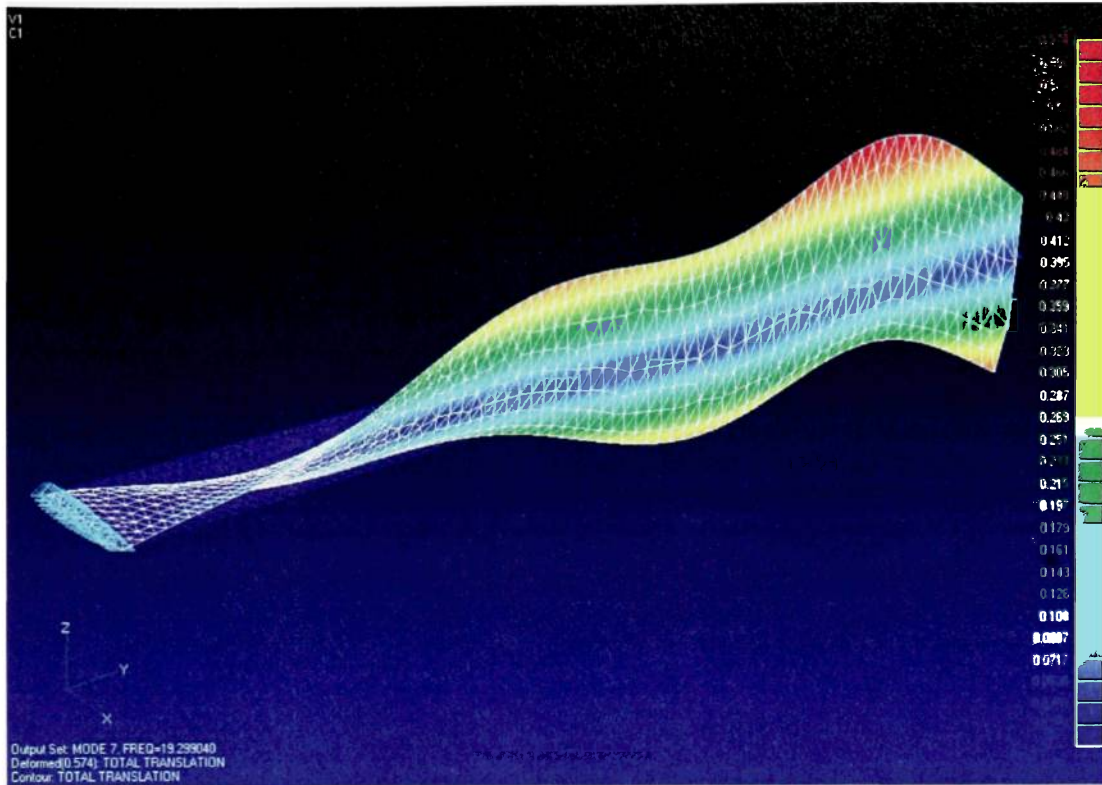


Figure A.3e: NASTRAN model first torsion mode approximation (mode 7).

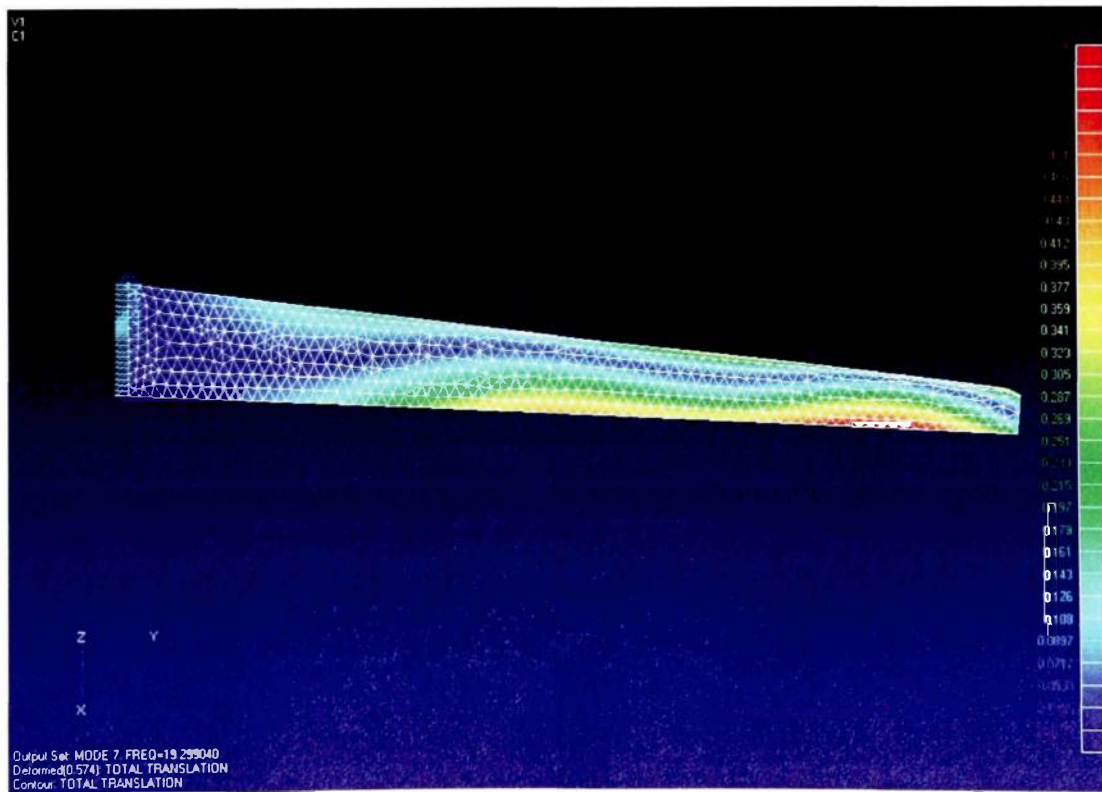


Figure A.3f: NASTRAN model first torsion mode approximation (top view).

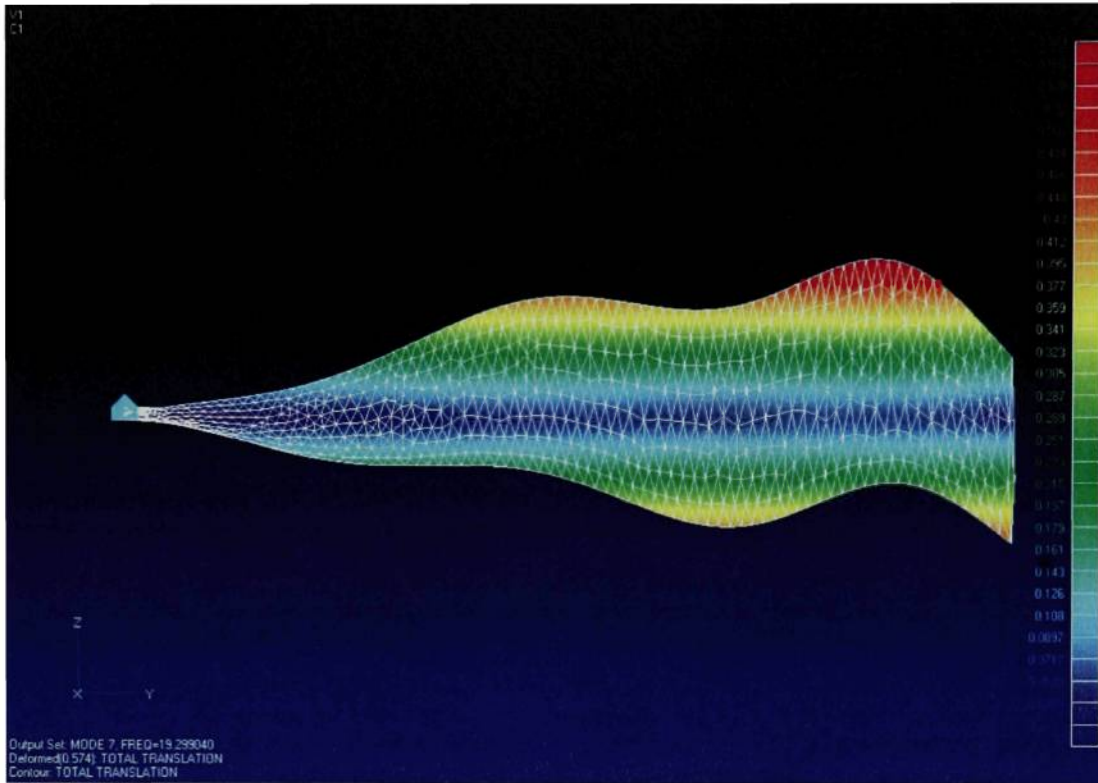


Figure A.3g: NASTRAN model first torsion mode approximation (front view).

A4. MATLAB CODE

```
*****
%-----FLUTTER ANALYSIS OF WINGS BY ENERGY METHODS-----
%*****
%-----Horacio E. Sepic Kriskovich - MSAE - October 2009-----
%*****
%-----HALE AIRCRAFT WING-----
%*****
tic
%=====
%-----FLUTTER ANALYSIS-----
%=====
%-----VARIABLE DATA-----
%=====
%.....PROGRAM PARAMETERS.....
%=====
n_max=1000;      % Maximum number of iterations for the program
                % (recommended: 1000).
n_elm=100;      % Number of elements for Bending and Torsion Free
                % Vibration Analysis by FEM (recommended: 100).
Omega_err=1.0e-5; % Precision for flutter frequency computations,
                % [Hz] (recommended: 1.0e-5).
%=====
%.....FLIGHT PARAMETERS.....
%=====
M_fl=0.85;      % Max. Mach range (recommended: 0.85)

H_fl_vctr=[10000]; % Altitude vector [m].

for n=1:1

    H_fl=H_fl_vctr(n);

    %=====
    %.....ELASTIC FOUNDATION PARAMETERS.....
    %=====
    R_kb_vctr=[1]; % Ratio elastic to clamp foundation in bending vector.

    for k=1:1

        R_kb=R_kb_vctr(k);

        R_kt_vctr=[2e-4, 6e-4]; % Ratio elastic to clamp foundation in
                                % torsion vector.

        for j=1:2

            R_kt=R_kt_vctr(j);

            K_b_ref=2.926e50; % Torsional spring to simulate a perfect
                            % clamp in bending mode, [N*m/rad]
                            % (recommended: 2.926e50).
            K_t_ref=1.743e18; % Torsional spring to simulate a perfect
                            % clamp in torsion mode, [N*m/rad]
                            % (recommended: 1.743e18).
            K_b=R_kb*K_b_ref; % Torsional spring to simulate elastic
                            % foundation in bending mode, [N*m/rad]
            K_t=R_kt*K_t_ref; % Torsional spring to simulate elastic
                            % foundation in torsion mode, [N*m/rad]

            %=====

```

```

=====FLUTTER ANALYSIS=====
=====
.....DATA INPUT.....
=====

Data_Input;

=====
.....FUNDAMENTAL UNCOUPLED NATURAL FREQUENCIES.....
=====

[Omega_b1]=BF_FEM_EF(n_elm,L_eff,m_C1,m_C2,m_C3,Ixx_C1,...
                  Ixx_C2,Ixx_C3,Ixx_C4,A_C1,A_C2,A_C3,...
                  d_1,d_2,E,K_b);

[Omega_t1]=TF_FEM_EF(n_elm,L_eff,Ip_C1,Ip_C2,Ip_C3,Ip_C4,...
                  Rho,m_C1,m_C2,m_C3,b_1,b_2,d_1,d_2,...
                  J_C1,J_C2,J_C3,J_C4,G,K_t);

Omega_h=Omega_b1*(2*pi); % Fundamental uncoupled bending shape
                        % frequency [rad/s].
Omega_a=Omega_t1*(2*pi); % " " torsion " "
                        % frequency [rad/s].

=====
-----FLUTTER SUBROUTINE-----
=====

[Omega_flutter,Q_flutter]=Flutter_Subroutine(c,b,a,bo,L_eff,...
                                           m,Iea,Phi_h,Phi_h_1,Phi_a,Omega_h,...
                                           Omega_a,Delta_ac,CL_a,Q_fl_max,n_max);

=====
-----DIVERGENCE SUBROUTINE-----
=====

[Q_divergence]=Divergence_Subroutine(c,b,a,bo,L_eff,m,Iea,...
                                     Phi_h,Phi_h_1,Phi_a,Omega_h,Omega_a,Delta_ac,...
                                     CL_a,Q_fl_max,n_max);

=====
.....OUTPUT.....
=====

fprintf('\n ----- \n')
Program Output----- \n')

fprintf('\n Uncoupled Bending Frequency: Omega_h = %g Hz \n',...
      Omega_h/(2*pi))
fprintf('\n Uncoupled Torsion Frequency: Omega_a = %g Hz \n',...
      Omega_a/(2*pi))
fprintf('\n Fundamental Frequencies Ratio: Ratio = %g \n',...
      Omega_h/Omega_a)
fprintf('\n Current Flight Altitude: H = %g m \n',...
      H_fl)

-----
fprintf('\n ----- \n')
Divergence Output----- \n')

fprintf('\n Divergence @ Q = %g Pa \n',Q_divergence)
fprintf('\n Divergence @ V = %g m/s \n',...
      sqrt(2*Q_divergence/Rho_fl))

fprintf('\n Divergence @ V = %g Km/h \n',...
      sqrt(2*Q_divergence/Rho_fl)*3.6)

```

```

fprintf('\n Divergence @ KTAS = %g \n',...
        sqrt(2*Q_divergence/Rho_fl)*3.6/1.85)
fprintf('\n Divergence @ Mach = %g \n',...
        sqrt(2*Q_divergence/Rho_fl)/(ao*sqrt(T_fl/To)))
%-----
for i=1:n_max

    Omega_diff=Omega_flutter(i,1)-Omega_flutter(i,2);

    Omega_avg=(Omega_flutter(i,1)+Omega_flutter(i,2))/2;

    if Omega_diff<Omega_err

        fprintf('\n -----
----Flutter Output----- \n')

        fprintf('\n Flutter @    Q = %g Pa \n',Q_flutter(i))

        fprintf('\n Flutter @    V = %g m/s \n',...
                sqrt(2*Q_flutter(i)/Rho_fl))
        fprintf('\n Flutter @    V = %g Km/h \n',...
                sqrt(2*Q_flutter(i)/Rho_fl)*3.6)
        fprintf('\n Flutter @ KTAS = %g \n',...
                sqrt(2*Q_flutter(i)/Rho_fl)*3.6/1.85)
        fprintf('\n Flutter @ Mach = %g \n',...
                sqrt(2*Q_flutter(i)/Rho_fl)/(ao*sqrt(T_fl/To)))
        fprintf('\n Flutter Frequency:           Omega_fl = %g
Hz \n',...
                Omega_avg)
        fprintf('\n Reduced Flutter Frequency (Strouhal): Str = %g
\n',...
                Omega_avg*2*pi*(MGC/2)/sqrt(2*Q_flutter(i)/Rho_fl))
%-----
        fprintf('\n -----Data Corrected
for Compressibility Effects by Theodorsen----- \n')

        X_f=(c_75/0.3048)*(Omega_avg*(2*pi))/(sqrt(2*...
                Q_flutter(i)/Rho_fl)*3.6/1.85);
        % Theodorsen's x-factor to enter the correction plot.
        K_f=K_f_C1*X_f^4+K_f_C2*X_f^3+K_f_C3*X_f^2+K_f_C4*X_f...
                +K_f_C5; % Theodorsen correction factor.
        V_flutter_corrected=K_f*sqrt(2*Q_flutter(i)/Rho_fl);
        % Corrected flutter speed for compressibility effects,
        % [m/s].

        fprintf('\n Theodorsen X-factor (Equivalent Strouhal):
X_f = %g \n',...
                X_f)
        fprintf('\n Theodorsen Compressibility Correction Factor:
K_f = %g \n',...
                K_f)
        fprintf('\n Corrected Flutter Speed is: V_fl_corr = %g m/s
\n',...
                V_flutter_corrected)
        fprintf('\n Corrected Flutter Speed is: V_fl_corr = %g
Km/h \n',...
                V_flutter_corrected*3.6)
        fprintf('\n Corrected Flutter Speed is: KTAS_corr = %g
\n',...
                V_flutter_corrected*3.6/1.85)
        fprintf('\n Corrected Flutter Speed is:      M_corr = %g
\n',...
                V_flutter_corrected/(ao*sqrt(T_fl/To)))

```

```

                                fprintf('\n Corrected Flutter Dynamic Pressure is:
Q_corr = %g Pa \n',...
                                1/2*Rho_fl*V_flutter_corrected^2)
                                fprintf('\n Corrected Reduced Flutter Frequency
(Strouhal): Str_corr = %g \n',...
                                Omega_avg*2*pi*(MGC/2)/V_flutter_corrected)
-----

                                fprintf('\n -----Plots
are displayed on figures 1 to 5----- \n')
                                fprintf('\n \n')

                                break

                                else

                                continue

                                end

end
-----

figure(1)
plot(Q_flutter,Omega_flutter(:,1),Q_flutter,Omega_flutter(:,2));
grid on;
xlabel('Dynamic Pressure, q [Pa]')
ylabel('Frequency, [Hz]')
hold on
title('Frequency vs. Dynamic Pressure @ Current FL')

figure(2)
V_flutter=sqrt(2*Q_flutter/Rho_fl);
plot(V_flutter,Omega_flutter(:,1),V_flutter,Omega_flutter(:,2));
grid on;
xlabel('Speed, [m/s]')
ylabel('Frequency, [Hz]')
hold on
title('Frequency vs. Speed @ Current FL')

figure(3)
V_flutter=sqrt(2*Q_flutter/Rho_fl)*3.6;
plot(V_flutter,Omega_flutter(:,1),V_flutter,Omega_flutter(:,2));
grid on;
xlabel('Speed, [Km/h]')
ylabel('Frequency, [Hz]')
hold on
title('Frequency vs. Speed @ Current FL')

figure(4)
V_flutter=sqrt(2*Q_flutter/Rho_fl)*3.6/1.85;
plot(V_flutter,Omega_flutter(:,1),V_flutter,Omega_flutter(:,2));
grid on;
xlabel('KTAS')
ylabel('Frequency, [Hz]')
hold on
title('Frequency vs. KTAS @ Current FL')

figure(5)
M_flutter=sqrt(2*Q_flutter/Rho_fl)/(ao*sqrt(T_fl/To));
plot(M_flutter,Omega_flutter(:,1),M_flutter,Omega_flutter(:,2));
grid on;
xlabel('Mach Number')

```

```

        ylabel('Frequency, [Hz]')
        hold on
        title('Frequency vs. Mach Number @ Current FL')
        %-----
        fprintf('\n ----- \n')
Program has ended----- \n')
        fprintf('\n \n')

    end

end

end

toc

%*****
%-----DATA INPUT-----
%*****
syms y
%-----
%.....MATERIAL.....
%-----
E =7.385e10; % Al 2024 T-351 Young's Modulus [Pa].
G =2.870e10; % Al 2024 T-351 Shear Modulus [Pa].
Rho=2.765e3; % Al 2024 T-351 Material's density [Kg/m^3].
%-----
%.....GEOMETRY.....
%-----
L =20.00; % Semi-span, cantilever wing's length [m].
cr=2.50; % Root's cord [m].
ct=0.90; % Root's cord [m].
%-----
Sweep_ac=6.00; % AC Sweep back angle [degrees].
%-----
c_1=-0.080; % c principal coefficient.
c_2= 2.500; % c independent term, [m].
%-----
c=c_1*y+c_2; % Chord distribution, [m].
%-----
b_1=-4.204e-3; % b principal coefficient.
b_2= 1.314e-1; % b independent term, [m].
%-----
b=b_1*y+b_2; % Distance from CG to EA, b=(Xcg-Xea) [m].
%-----
a_1=-7.233e-3; % a principal coefficient.
a_2= 2.260e-1; % a independent term, [m].
%-----
a=a_1*y+a_2; % Distance from EA to AC, a=(Xea-Xac) [m].
%-----
d_1= 0.0; % d principal coefficient.
d_2= 0.0; % d independent term, [m].
%-----
d=d_1*y+d_2; % Vertical distance from CG to EA, d=(Zcg-Zea) [m].
%-----
%.....CROSS SECTIONAL PROPERTIES.....
%-----
A_C1= 4.829e-4; % A principal coefficient.
A_C2=-3.018e-2; % A second coefficient, [m].
A_C3= 4.716e-1; % A independent term, [m^2].

```

```

A   =A_C1*y^2+A_C2*y+A_C3; % Cross sectional area distribution, A(y) [m^2].
%-----
Ixx_C1=-2.131e-7; % Ixx principal coefficient, [m].
Ixx_C2= 1.346e-5; % Ixx second coefficient, [m^2].
Ixx_C3=-3.014e-4; % Ixx third coefficient, [m^3].
Ixx_C4= 2.389e-3; % Ixx independent term, [m^4].

Ixx   =Ixx_C1*y^3+Ixx_C2*y^2+Ixx_C3*y+Ixx_C4; % Area moment of inertia
% about x-axis, Ixx(y) [m^4].
%-----
J_C1=-8.346e-7; % J principal coefficient, [m].
J_C2= 5.273e-5; % J second coefficient, [m^2].
J_C3=-1.181e-3; % J third coefficient, [m^3].
J_C4= 9.361e-3; % J independent term, [m^4].

J     =J_C1*y^3+J_C2*y^2+J_C3*y+J_C4; % Torsional constant, J(y) [m^4].
%-----
Ip_C1=-1.256e-5; % Ip principal coefficient, [m].
Ip_C2= 7.934e-4; % Ip second coefficient, [m^2].
Ip_C3=-1.777e-2; % Ip third coefficient, [m^3].
Ip_C4= 1.409e-1; % Ip independent term, [m^4].

Ip    =Ip_C1*y^3+Ip_C2*y^2+Ip_C3*y+Ip_C4; % Polar moment of inertia,
% Ip(y) [m^4].
%-----
m_C1= 1.335; % m principal coefficient, [Kg/m^3].
m_C2=-8.346e1; % m second coefficient, [Kg/m^2].
m_C3= 1.304e3; % m independent term, [Kg/m].

m     =m_C1*y^2+m_C2*y+m_C3; % Mass/unit length, m(y) [kg/m].
%-----
Iea=Ip*Rho+m*(b^2+d^2); % Mass moment of inertia about EA/unit length,
% Iea [Kg*m].

%-----
%.....FIXED PARAMETERS.....
MGC=(cr+ct)/2; % Mean Geometric Chord [m].
AR=2*L/MGC; % Aspect ratio.
Delta_ac=Sweep_ac*pi/180; % AC Sweep back angle [rad].

bo=L; % Arbitrary reference length [m].
L_eff=L/cos(Delta_ac); % Wing's effective semispan [m].
%-----
%.....AERODYNAMICS.....
CL_airfoil=6.446; % NACA 63-1-012 airfoil lift coefficient slope
% [1/rad].
CL_a=pi*(AR/(1+sqrt(1+(pi*AR/(CL_airfoil*cos(Delta_ac)))^2))); % Wing's
% lift coefficient.
%-----
%.....MODE SHAPES.....
Phi_h=1-cos(pi*y/(2*L_eff)); % Bending admissible function.
Phi_a=sin(pi*y/(2*L_eff)); % Torsion " " " "

Phi_h_1=diff(Phi_h,y); % Bending first spatial derivative.
Phi_a_1=diff(Phi_a,y); % Torsion " " " "
%-----
%.....ISA PARAMETERS.....

```

```

=====
Rho_SL=1.225; % Air density @ SL [Kg/m^3].
Rho_FL110=0.3639; % " " @ FL110 [Kg/m^3].
ao=340.26; % Speed of sound @ SL [m/s].
To=288.15; % Standard temperature @ SL [K].

if H_fl<=11000

    Rho_fl=Rho_SL*(1-0.0065*H_fl/To)^(4.2561);
    T_fl=To-6.5*H_fl/1000;

else Rho_fl=Rho_FL110*exp(-157.69*(H_fl-11000)/10^6);
    T_fl=216.65;

end

V_fl=M_fl*(ao*sqrt(T_fl/To)); % Max. speed range [m/h].
Q_fl_max=1/2*Rho_fl*V_fl^2; % Max. dynamic pressure range [Pa].

=====
.....THEODORSEN PARAMETERS.....
=====
y_75=0.75*L_eff; % 75% of wing's semi-span, [m].

c_75=c_1*y_75+c_2; % Chord for 75% semi-span, [m].

K_f_C1=-4.084e-2; % Theodorsen curve principal coefficient.
K_f_C2= 2.585e-1; % Theodorsen curve second coefficient.
K_f_C3=-6.232e-1; % Theodorsen curve third coefficient.
K_f_C4= 7.366e-1; % Theodorsen curve fourth coefficient.
K_f_C5= 9.952e-1; % Theodorsen curve independent term.
=====

-----BENDING FREQUENCY BY FINITE ELEMENTS METHOD-----
-----WITH ELASTIC FOUNDATION-----
function [Omega_b1]=BF_FEM_EF(n_elm,L_eff,m_C1,m_C2,m_C3,Ixx_C1,Ixx_C2,...
    Ixx_C3,Ixx_C4,A_C1,A_C2,A_C3,d_1,d_2,E,K_b)
=====
-----FINITE ELEMENT PARAMETERS-----
=====
n_nds=n_elm+1; % Number of nodes.
L_elm=L_eff/n_elm; % Element length, [m].

Ctr=[1]; % Constraints vector, contains the DOF's that are fixed
% (odd #: transverse DOF, even #: rotational DOF).

Ext=zeros(n_elm,2);

for i=1:n_elm

    Ext(i,1)=i;
    Ext(i,2)=i+1;

end

Ext; % Extremes vector, connects the starting and ending nodes of each

```



```

    % element.
-----
m =zeros(n_elm,1);

for i=1:n_elm

    y_sw_1=(i-1)*L_elm;
    y_sw_2=i*L_elm;
    m(i,1)=(m_C1*y_sw_1^2+m_C2*y_sw_1+m_C3)+(m_C1*y_sw_2^2+m_C2*y_sw_2+...
        m_C3))/2;

end

m; % Mass/unit length vector, contains m for each element, [Kg/m].
-----
Ixx=zeros(n_elm,1);

for i=1:n_elm

    y_sw_1=(i-1)*L_elm;
    y_sw_2=i*L_elm;
    Ixx_sw_1=(Ixx_C1*y_sw_1^3+Ixx_C2*y_sw_1^2+Ixx_C3*y_sw_1+Ixx_C4)+...
        (A_C1*y_sw_1^2+A_C2*y_sw_1+A_C3)*(d_1*y_sw_1+d_2)^2;
    Ixx_sw_2=(Ixx_C1*y_sw_2^3+Ixx_C2*y_sw_2^2+Ixx_C3*y_sw_2+Ixx_C4)+...
        (A_C1*y_sw_2^2+A_C2*y_sw_2+A_C3)*(d_1*y_sw_2+d_2)^2;
    Ixx(i,1)=(Ixx_sw_1+Ixx_sw_2)/2;

end

Ixx; % Inertia/unit length vector, contains Ixx for each element, [m^4].
-----
M_eq=m.*L_elm/420; % Equivalent mass for each element
                  % (to be assembled in M), [Kg].
K_eq=E*Ixx./L_elm^3; % Equivalent stiffness for each element
                  % (to be assembled in K), [N/m].
-----
                    -----MATRIX ASSEMBLY-----
-----
M=zeros(n_nds*2,n_nds*2);
K=zeros(n_nds*2,n_nds*2);

for i=1:n_elm

    M(Ext(i,1)*2-1,Ext(i,1)*2-1)=M(Ext(i,1)*2-1,Ext(i,1)*2-1)+M_eq(i)*...
        156;
    M(Ext(i,1)*2-1,Ext(i,1)*2) =M(Ext(i,1)*2-1,Ext(i,1)*2) +M_eq(i)*...
        22*L_elm;
    M(Ext(i,1)*2-1,Ext(i,2)*2-1)=M(Ext(i,1)*2-1,Ext(i,2)*2-1)+M_eq(i)*...
        54;
    M(Ext(i,1)*2-1,Ext(i,2)*2) =M(Ext(i,1)*2-1,Ext(i,2)*2) -M_eq(i)*...
        13*L_elm;

    M(Ext(i,1)*2,Ext(i,1)*2-1)=M(Ext(i,1)*2,Ext(i,1)*2-1)+M_eq(i)*...
        22*L_elm;
    M(Ext(i,1)*2,Ext(i,1)*2) =M(Ext(i,1)*2,Ext(i,1)*2) +M_eq(i)*...
        4*L_elm^2;
    M(Ext(i,1)*2,Ext(i,2)*2-1)=M(Ext(i,1)*2,Ext(i,2)*2-1)+M_eq(i)*...
        13*L_elm;
    M(Ext(i,1)*2,Ext(i,2)*2) =M(Ext(i,1)*2,Ext(i,2)*2) -M_eq(i)*...
        3*L_elm^2;

    M(Ext(i,2)*2-1,Ext(i,1)*2-1)=M(Ext(i,2)*2-1,Ext(i,1)*2-1)+M_eq(i)*...
        54;

```

```

M(Ext(i,2)*2-1,Ext(i,1)*2) =M(Ext(i,2)*2-1,Ext(i,1)*2) +M_eq(i)*...
13*L_elm;
M(Ext(i,2)*2-1,Ext(i,2)*2-1)=M(Ext(i,2)*2-1,Ext(i,2)*2-1)+M_eq(i)*...
156;
M(Ext(i,2)*2-1,Ext(i,2)*2) =M(Ext(i,2)*2-1,Ext(i,2)*2) -M_eq(i)*...
22*L_elm;

M(Ext(i,2)*2,Ext(i,1)*2-1)=M(Ext(i,2)*2,Ext(i,1)*2-1)-M_eq(i)*...
13*L_elm;
M(Ext(i,2)*2,Ext(i,1)*2) =M(Ext(i,2)*2,Ext(i,1)*2) -M_eq(i)*...
3*L_elm^2;
M(Ext(i,2)*2,Ext(i,2)*2-1)=M(Ext(i,2)*2,Ext(i,2)*2-1)-M_eq(i)*...
22*L_elm;
M(Ext(i,2)*2,Ext(i,2)*2) =M(Ext(i,2)*2,Ext(i,2)*2) +M_eq(i)*...
4*L_elm^2;
-----
K(Ext(i,1)*2-1,Ext(i,1)*2-1)=K(Ext(i,1)*2-1,Ext(i,1)*2-1)+K_eq(i)*...
12;
K(Ext(i,1)*2-1,Ext(i,1)*2) =K(Ext(i,1)*2-1,Ext(i,1)*2) +K_eq(i)*...
6*L_elm;
K(Ext(i,1)*2-1,Ext(i,2)*2-1)=K(Ext(i,1)*2-1,Ext(i,2)*2-1)-K_eq(i)*...
12;
K(Ext(i,1)*2-1,Ext(i,2)*2) =K(Ext(i,1)*2-1,Ext(i,2)*2) +K_eq(i)*...
6*L_elm;

K(Ext(i,1)*2,Ext(i,1)*2-1)=K(Ext(i,1)*2,Ext(i,1)*2-1)+K_eq(i)*...
6*L_elm;
K(Ext(i,1)*2,Ext(i,1)*2) =K(Ext(i,1)*2,Ext(i,1)*2) +K_eq(i)*...
4*L_elm^2;
K(Ext(i,1)*2,Ext(i,2)*2-1)=K(Ext(i,1)*2,Ext(i,2)*2-1)-K_eq(i)*...
6*L_elm;
K(Ext(i,1)*2,Ext(i,2)*2) =K(Ext(i,1)*2,Ext(i,2)*2) +K_eq(i)*...
2*L_elm^2;

K(Ext(i,2)*2-1,Ext(i,1)*2-1)=K(Ext(i,2)*2-1,Ext(i,1)*2-1)-K_eq(i)*...
12;
K(Ext(i,2)*2-1,Ext(i,1)*2) =K(Ext(i,2)*2-1,Ext(i,1)*2) -K_eq(i)*...
6*L_elm;
K(Ext(i,2)*2-1,Ext(i,2)*2-1)=K(Ext(i,2)*2-1,Ext(i,2)*2-1)+K_eq(i)*...
12;
K(Ext(i,2)*2-1,Ext(i,2)*2) =K(Ext(i,2)*2-1,Ext(i,2)*2) -K_eq(i)*...
6*L_elm;

K(Ext(i,2)*2,Ext(i,1)*2-1)=K(Ext(i,2)*2,Ext(i,1)*2-1)+K_eq(i)*...
6*L_elm;
K(Ext(i,2)*2,Ext(i,1)*2) =K(Ext(i,2)*2,Ext(i,1)*2) +K_eq(i)*...
2*L_elm^2;
K(Ext(i,2)*2,Ext(i,2)*2-1)=K(Ext(i,2)*2,Ext(i,2)*2-1)-K_eq(i)*...
6*L_elm;
K(Ext(i,2)*2,Ext(i,2)*2) =K(Ext(i,2)*2,Ext(i,2)*2) +K_eq(i)*...
4*L_elm^2;

end

K;
K(2,2)=K(2,2)+K_b/K_eq(1); % Contribution of the elastic foundation to the
% overall stiffness matrix.

M=double(M); %[Kg].
K=double(K); %[N/m].
=====
%.....SOLVER.....
=====
* Solution of the eigenvalue problem for natural frequencies

```

```

M_inv=inv(M);
H      =M_inv*K;

for i=1:length(Ctr)

    H(Ctr(i)-i+1,:)=[];
    H(:,Ctr(i)-i+1)=[];

end

E=eig(H);
=====
% .....OUTPUT.....
% =====
Omega_b1=sqrt(E)/(2*pi);          % Bending frequencies vector, w's [Hz].

Omega_b1=min(double(Omega_b1)); % Fundamental bending frequency, w1 [Hz].

fprintf('\n Uncoupled Bending Frequency:   Omega_h = %g Hz \n',Omega_b1)
%*****

%*****
%-----TORSION FREQUENCY BY FINITE ELEMENTS METHOD-----
%*****
%-----WITH ELASTIC FOUNDATION-----
%*****
function [Omega_t1]=TF_FEM_EF(n_elm,L_eff,Ip_C1,Ip_C2,Ip_C3,Ip_C4,Rho,...
    m_C1,m_C2,m_C3,b_1,b_2,d_1,d_2,J_C1,J_C2,J_C3,J_C4,...
    G,K_t)
%*****
%-----FINITE ELEMENT PARAMETERS-----
%*****
n_nds=n_elm+1;      % Number of nodes.
L_elm=L_eff/n_elm; % Element length, [m].
%*****
Ctr=[];             % Constraints vector, contains the DOF's that are fixed
%                   % (only rotational DOF's).
%*****
Ext=zeros(n_elm,2);

for i=1:n_elm

    Ext(i,1)=i;
    Ext(i,2)=i+1;

end

Ext; % Extremes vector, connects the starting and endind nodes of
%    % each element.

%-----
Iea=zeros(n_elm,1);

for i=1:n_elm

    y_sw_1=(i-1)*L_elm;
    y_sw_2=i*L_elm;
    Iea_sw_1=(Ip_C1*y_sw_1^3+Ip_C2*y_sw_1^2+Ip_C3*y_sw_1+Ip_C4)*Rho+...
        (m_C1*y_sw_1^2+m_C2*y_sw_1+m_C3)*((b_1*y_sw_1+b_2)^2+...
        (d_1*y_sw_1+d_2)^2);
    Iea_sw_2=(Ip_C1*y_sw_2^3+Ip_C2*y_sw_2^2+Ip_C3*y_sw_2+Ip_C4)*Rho+...

```

```

                (m_C1*y_sw_2^2+m_C2*y_sw_2+m_C3)*((b_1*y_sw_2+b_2)^2+...
                (d_1*y_sw_1+d_2)^2);
Iea(i,1)=(Iea_sw_1+Iea_sw_2)/2;

end

Iea; % Mass polar moment of inertia about EA vector, contains Iea for each
     % element, [Kg*m].
-----
J=zeros(n_elm,1);

for i=1:n_elm

    y_sw_1=(i-1)*L_elm;
    y_sw_2=i*L_elm;
    J(i,1)=((J_C1*y_sw_1^3+J_C2*y_sw_1^2+J_C3*y_sw_1+J_C4)+...
            (J_C1*y_sw_2^3+J_C2*y_sw_2^2+J_C3*y_sw_2+J_C4))/2;

end

J; % Torsional constant vector, contains J for each element, [m^4].
-----
I_eq=Iea.*L_elm/2; % Equivalent mass polar moment of inertia about EA for
                  % each element (to be assembled in I), [Kg*m^2].
K_eq=G*J./L_elm; % Equivalent stiffness for each element (to be
                 % assembled in K), [N*m].
-----
                    -MATRIX ASSEMBLY-
-----
I=zeros(n_nds,n_nds);
K=zeros(n_nds,n_nds);

for i=1:n_elm

    I(Ext(i,1),Ext(i,1)) =I(Ext(i,1),Ext(i,1)) +I_eq(i);
    I(Ext(i,1)+1,Ext(i,1)+1)=I(Ext(i,1)+1,Ext(i,1)+1)+I_eq(i);

    -----

    K(Ext(i,1),Ext(i,1)) =K(Ext(i,1),Ext(i,1)) +K_eq(i);
    K(Ext(i,1),Ext(i,1)+1)=K(Ext(i,1),Ext(i,1)+1)-K_eq(i);

    K(Ext(i,1)+1,Ext(i,1)) =K(Ext(i,1)+1,Ext(i,1)) -K_eq(i);
    K(Ext(i,1)+1,Ext(i,1)+1)=K(Ext(i,1)+1,Ext(i,1)+1)+K_eq(i);

end

K;
K(2,2)=K(2,2)+K_t/K_eq(1); % Contribution of the elastic foundation to the
                          % overall stiffness matrix.

I=double(I); % [Kg*m^2].
K=double(K); % [N*m].
-----
.....SOLVER.....
-----
% Solution of the eigenvalue problem for natural frequencies
I_inv=inv(I);
H =I_inv*K;

for i=1:length(Ctr)

    H(Ctr(i)-i+1,:)=[];

```

```

        H(:,Ctr(i)-i+1)=[];

end

E=eig(H);
%=====
%.....OUTPUT.....
%=====
Omega_t1=sqrt(E)/(2*pi);      % Torsion frequencies vector, w's [Hz].

Omega_t1=min(double(Omega_t1)); % Fundamental torsion frequency, w1 [Hz].

fprintf('\n Uncoupled Torsion Frequency:   Omega_a = %g Hz \n',Omega_t1)
%*****

%*****
%-----FLUTTER SUBROUTINE-----
%*****
function [Omega_flutter,Q_flutter]=Flutter_Subroutine(c,b,a,bo,L_eff,m,...
        Iea,Phi_h,Phi_h_1,Phi_a,Omega_h,...
        Omega_a,Delta_ac,CL_a,Q_fl_max,n_max)

syms y
WTB=waitbar(0,'Calculating Flutter Envelope...');
%=====
%.....MATRIX ASSEMBLY.....
%=====
% Definition of mass terms [M]:
M_hh=int(m*(Phi_h)^2,y,0,L_eff);
M_ha=int(m*b*(Phi_h)*(Phi_a),y,0,L_eff);
M_ah=M_ha;
M_aa=int(Iea*(Phi_a)^2,y,0,L_eff);

% Definition of elastic terms [K]:
K_hh=(Omega_h)^2*M_hh;
K_aa=(Omega_a)^2*M_aa;

% Definition of aerodynamic terms [A]:
A_hh=-CL_a/2*int(c*(Phi_h*Phi_h_1*sin(Delta_ac)-a*Phi_h_1^2*...
        (sin(Delta_ac))^2),y,0,L_eff);
A_ha=-CL_a/2*int(c*(Phi_h*Phi_a*cos(Delta_ac) -a*Phi_h_1*Phi_a*...
        sin(Delta_ac)*cos(Delta_ac)),y,0,L_eff);
A_ah= CL_a/2*int(c*(a*Phi_h_1*Phi_a*sin(Delta_ac)*cos(Delta_ac)),y,0,...
        L_eff);
A_aa= CL_a/2*int(c*(a*Phi_a^2*(cos(Delta_ac))^2),y,0,L_eff);

%-----
% Assembly of equations of motion in matrix form:
M_11=M_hh*bo^2;
M_12=M_ha*bo;
M_21=M_ah*bo;
M_22=M_aa;

K_11=K_hh*bo^2;
K_12=0;
K_21=0;
K_22=K_aa;

A_11=A_hh*bo^2;

```

```

A_12=A_ha*bo;
A_21=A_ah*bo;
A_22=A_aa;

M=[M_11 M_12; M_21 M_22];
K=[K_11 K_12; K_21 K_22];
A=[A_11 A_12; A_21 A_22];
=====
% .....SOLVER.....
=====
% Solving the eigenvalue problem (frequency domain):
step_q=Q_fl_max/n_max; % Step for dynamic pressure.
Q_flutter=zeros(n_max,1);
Omega_flutter=zeros(n_max,2);

for i=1:n_max

    waitbar(i/n_max,WTB)

    q=0:step_q:Q_fl_max;
    q=q(i);

    D_11=K_11-q*A_11;
    D_12=K_12-q*A_12;
    D_21=K_21-q*A_21;
    D_22=K_22-q*A_22;

    % Solving the characteristic equation:
    A=M_11*M_22-M_12*M_21;
    B=-D_11*M_22-D_22*M_11+D_21*M_12+D_12*M_21;
    C=D_11*D_22-D_12*D_21;

    A=double(A);
    B=double(B);
    C=double(C);

    root1=(-B+sqrt(B^2-4*A*C))/(2*A);
    root2=(-B-sqrt(B^2-4*A*C))/(2*A);

    Omega_flutter(i,1)=sqrt(root1)/(2*pi);
    Omega_flutter(i,2)=sqrt(root2)/(2*pi);
    Q_flutter(i)=q;

end

close(WTB)
=====
% .....DIVERGENCE SUBROUTINE.....
% .....
function [Q_divergence]=Divergence_Subroutine(c,b,a,bo,L_eff,m,Iea,...
    Phi_h,Phi_h_1,Phi_a,Omega_h,Omega_a,Delta_ac,...
    CL_a,Q_fl_max,n_max)

syms y
WTB=waitbar(0,'Calculating Divergence...');
=====
% .....MATRIX ASSEMBLY.....
=====
% Definition of mass terms [M]:
M_hh=int(m*(Phi_h)^2,y,0,L_eff);
M_ha=int(m*b*(Phi_h)*(Phi_a),y,0,L_eff);

```

```

M_ah=M_ha;
M_aa=int(Iea*(Phi_a)^2,y,0,L_eff);

% Definition of elastic terms [K]:
K_hh=(Omega_h)^2*M_hh;
K_aa=(Omega_a)^2*M_aa;

% Definition of aerodynamic terms [A]:
A_hh= CL_a/2*int(c*(Phi_h*Phi_h_1*sin(Delta_ac)+a*Phi_h_1^2*...
                (sin(Delta_ac))^2),y,0,L_eff);
A_ha=-CL_a/2*int(c*(Phi_h*Phi_a*cos(Delta_ac) +a*Phi_h_1*Phi_a*...
                sin(Delta_ac)*cos(Delta_ac)),y,0,L_eff);
A_ah=-CL_a/2*int(c*(a*Phi_h_1*Phi_a*sin(Delta_ac)*cos(Delta_ac)),y,0,...
                L_eff);
A_aa=-CL_a/2*int(c*(a*Phi_a^2*(cos(Delta_ac))^2),y,0,L_eff);
%-----
% Assembly of equations of motion in matrix form:
K_11=K_hh*bo^2;
K_12=0;
K_21=0;
K_22=K_aa;

A_11=A_hh*bo^2;
A_12=A_ha*bo;
A_21=A_ah*bo;
A_22=A_aa;

K=[K_11 K_12; K_21 K_22];
A=[A_11 A_12; A_21 A_22];
%=====
%.....SOLVER.....
%=====
% Solving the characteristic equation, [D]=[K]-q*[A]:

A=A_11*A_22-A_12*A_21;
B=-K_11*A_22-K_22*A_11;
C=K_11*K_22;

A=double(A);
B=double(B);
C=double(C);

Q_divergence_1=(-B+sqrt(B^2-4*A*C))/(2*A);
Q_divergence_2=(-B-sqrt(B^2-4*A*C))/(2*A);

Q_divergence=abs(Q_divergence_1);

close(WTB)
%*****

%*****
%-----BENDING FREQUENCY BY RAYLEIGH-RITZ METHOD-----
%*****
function [Omega_b1]=BF_RRM(L_eff,E,Ixx,m)
%=====
%.....ADMISSIBLE FUNCTIONS.....
%=====
Phi1=(y/L_eff)^2; % Admissible functions, Phi(y).
Phi2=1-cos(pi*y/(2*L_eff));

Phi1_1=diff(Phi1,y); % 1st. spatial derivatives.

```

```

Phi2_1=diff(Phi2,y);

Phi1_2=diff(Phi1_1,y);      % 2nd. spatial derivatives.
Phi2_2=diff(Phi2_1,y);
%=====
%.....SOLVER.....
%=====
% Solution of the eigenvalue problem, which is represented by the
% expression det([N]-w^2*[D])=0.

% Definition of [N] matrix:
N_11=int(E*Ixx*(Phi1_2)^2,y,0,L_eff);
N_12=int(E*Ixx*(Phi1_2)*(Phi2_2),y,0,L_eff);
N_21=N_12;
N_22=int(E*Ixx*(Phi2_2)^2,y,0,L_eff);

N=[N_11 N_12; N_21 N_22];
N=double(N);

% Definition of [D] matrix:
D_11=int(m*(Phi1)^2,y,0,L_eff);
D_12=int(m*(Phi1)*(Phi2),y,0,L_eff);
D_21=D_12;
D_22=int(m*(Phi2)^2,y,0,L_eff);

D=[D_11 D_12;D_21 D_22];
D=double(D);
%-----
% Solution of the characteristic equation;
AA=D_11*D_22-D_12^2;
BB=2*N_12*D_12-N_11*D_22-D_11*N_22;
CC=N_11*N_22-N_12^2;
DD=BB^2-4*AA*CC;
%-----
%.....OUTPUT.....
%-----
Omega_b1=sqrt((-BB-sqrt(DD))/(2*AA))/(2*pi); % 1st bending frequency, [Hz].
Omega_b2=sqrt((-BB+sqrt(DD))/(2*AA))/(2*pi); % 2nd bending frequency, [Hz].

Omega_b1=double(Omega_b1);
Omega_b2=double(Omega_b2);
%*****

%-----TORSIONAL FREQUENCY BY RAYLEIGH-RITZ METHOD-----
%*****
function [Omega_t1]=TF_RRM(L_eff,G,J,Iea)
%-----
%.....ADMISSIBLE FUNCTIONS.....
%-----
Theta1=(y/L_eff); % Admissible functions, Theta(y) [rad].
Theta2=sin(pi*y/(2*L_eff));

Theta1_1=diff(Theta1,y); % 1st. spatial derivatives.
Theta2_1=diff(Theta2,y);
%=====
%.....SOLVER.....
%=====
% Solution of the eigenvalue problem, which is represented by the

```



```

% expression det([D]^(-1)*[N]-w^2*[I])=0.

% Definition of [N] matrix:
N_11=int(G*J*(Theta1_1)^2,y,0,L_eff);
N_12=int(G*J*(Theta1_1)*(Theta2_1),y,0,L_eff);
N_21=N_12;
N_22=int(G*J*(Theta2_1)^2,y,0,L_eff);

N=[N_11 N_12; N_21 N_22];
N=double(N);

% Definition of [D] matrix:
D_11=int(Iea*(Theta1)^2,y,0,L_eff);
D_12=int(Iea*(Theta1)*(Theta2),y,0,L_eff);
D_21=D_12;
D_22=int(Iea*(Theta2)^2,y,0,L_eff);

D=[D_11 D_12;D_21 D_22];
D=double(D);
-----
% Solution of the characteristic equation;
AA=D_11*D_22-D_12^2;
BB=2*N_12*D_12-N_11*D_22-D_11*N_22;
CC=N_11*N_22-N_12^2;
DD=BB^2-4*AA*CC;
=====
% .....OUTPUT.....
% .....
Omega_t1=sqrt((-BB-sqrt(DD))/(2*AA))/(2*pi); % 1st torsion frequency, [Hz].
Omega_t2=sqrt((-BB+sqrt(DD))/(2*AA))/(2*pi); % 2nd torsion frequency, [Hz].

Omega_t1=double(Omega_t1);
Omega_t2=double(Omega_t2);
% *****

```